



Michaela Kohlová

**Desenvolvimento de novos tipos de membranas biocompatíveis  
para hemodiálise para separação de biomoléculas**

Tese do 3º Ciclo de Estudos Conducente ao Grau de Doutoramento em Ciências  
Farmacêuticas

Trabalho realizado sob a orientação da Professora Doutora Maria da Conceição  
Branco Montenegro e Professor Doutor Petr Solich e co-orientação da Professora  
Doutora Alice Santos-Silva

Setembro 2020





Michaela Kohlová

**Development of new types of biocompatible haemodialysis  
membranes for separation of biomolecules.**

Dissertation Thesis of the PhD Degree in Pharmaceutical Sciences

The work was carried out under the supervision of Professor Maria da Conceição  
Branco Montenegro and Professor Doctor Petr Solich and co-supervision of  
Professor Alice Santos-Silva

September 2020

According to the legislation, the reproduction of any part of this dissertation is not allowed.

De acordo com a legislação em vigor, não é permitida a reprodução de qualquer parte desta dissertação.

This dissertation thesis was developed in regime *Cotutelle*, based on a bilateral agreement between the Faculty of Pharmacy in Hradec Králové, Charles University and the Faculty of Pharmacy, University of Porto.

## ACKNOWLEDGEMENT

I would like to thank prof. RNDr. Petr Solich, CSc. and prof. Maria da Conceição Branco da Silva for the opportunity to study at regime *Cotutelle* and to work in parallel at the Department of Analytical Chemistry, Faculty in Pharmacy in Hradec Králové, Charles University and Department of Chemical Sciences, Faculty of Pharmacy University of Porto.

I would like to thank my consultant assoc. prof. Alice Santos-Silva for expert advices in biochemistry area.

A huge thank belongs to Célia Gomes Amorim, Ph.D., for her never-ending support, permanent motivation, enormous patience, valuable discussions, and friendly leading during my studies. To Susana Rocha, Ph.D. I want to thank for teaching me her excellent laboratory skills and for valuable advices when dealing with new experimental work. Thank belongs also to associate prof. Alberto de Nova Araújo for technical support during the project development.

I would like to thank my Czech and Portuguese co-workers and friends, Lucie Novosvětská, Ivana H. Šrámková, Burkhard Horstkotte, Martina Háková, and Ivona Lhotská for very kind and friendly environment, and for their endless long-distance assistance and technical support; Álvaro Torrinha, Renato Gil, Jaime Mendoza, Luis Zambrano, and Rosa Couto for being helpful during my experimental work and for nice out-of-work times. Big thank belongs to all my other colleagues from both faculties for their kindness and the lovely time we have spent together during my studies.

I would like to especially thank to my entire family for their never-ending patience, optimism, cheering, support and that they never let me to give up.

I would like to acknowledge the financial support of various grant agencies, listed below, which enabled me to accomplish research tasks and to present research data at national and international conferences:

- the Grant Agency of the Charles University, project 860216
- the Project of Specific Research, SVV 260412
- the Mobility fund and the Erasmus+ grant of the Charles University
- the project FCT/MCTES grant UIDB/50006/2020
- the project Dial4life (PTDC/MEC-CAR/31322/2017 - POCI-01-0145-FEDER-031322)
- the project EFSA-CDN (CZ.02.1.01/0.0/0.0/16\_019/0000841)

## ABSTRACT

This dissertation thesis was focused on the development, preparation, and optimization of flat sheet polysulfone membranes, which would meet the characteristics required for membranes used for haemodialysis treatment. The thin porous membranes were prepared by spin coating method, followed by phase inversion via immersion precipitation. The composition, as well as the preparation process of the membranes, were optimized, to obtain a membrane with good mechanical performance in flow conditions, adequate selective separation ability, and biocompatibility.

The prepared membranes with the appropriate characteristics were modified with bioactive compounds to minimize oxidative stress and/or inflammation, which are common complications in haemodialysis treated patients. Three different modification approaches were used to prepare the bioactive membranes.

The membranes with antioxidant activity were obtained by direct incorporation of  $\alpha$ -tocopherol,  $\alpha$ -lipoic acid, and of their mixture, into the membrane structure during the preparation process. The concentration of antioxidants incorporated into the membrane had to be optimized, to find an ideal amount to provide antioxidant activity, without altering membrane selective permeability. The effectiveness of antioxidant incorporation into membrane structure was proved by *in vitro* tests.

The other modification approach was superficial adsorption of newly synthesized inhibitors of human neutrophil elastase; three different inhibitors containing  $\beta$ -lactam ring were evaluated. These membranes were prepared to diminish inflammation, caused by elevated level of circulating human neutrophil elastase. The inhibition of elastase activity by these modified membranes was evaluated to select the most promising compound for further *in vitro* experiments.

The last tested membrane modification was by incorporation of molecularly imprinted polymers into the membrane structure during the preparation process, to selectively remove uremic toxins from the blood of patients with renal failure. This preliminary study proved that it will be possible to incorporate compounds of this type with adequate selectivity for different toxins, in polysulfone members.

Obtained data may contribute to future research work on polysulfone membrane modifications, since membrane preparation and modification processes, using different approaches to improve bioactivity of the membranes, were optimized; the proposed bioactive membranes have potential for haemodialysis membranes and may reduce the cardiovascular risk associated with the high morbidity and mortality in patients on haemodialysis treatment.

**Keywords:** haemodialysis, polysulfone membranes, antioxidants, inhibitors of neutrophil elastase



## RESUMO

Esta dissertação teve como objetivo o desenvolvimento, preparação e otimização de membranas planares, de polisulfona que cumprissem os requisitos necessários para poderem ser utilizadas em processos de tratamento de hemodiálise.

As membranas porosas e finas foram preparadas pelo método de “spin coating”, seguido de inversão de fase via precipitação por imersão. Foram otimizados quer a sua composição quer o processo de preparação por forma a obter membranas com boas características mecânicas para serem usadas em condições de fluxo, com capacidade de separação seletiva e biocompatibilidade. As membranas preparadas com as características apropriadas foram modificadas com compostos bioativos para minimizar o stress oxidativo e /ou a inflamação, complicações estas que são comuns em pacientes sujeitos a tratamento de hemodiálise. Foram seguidos dois tipos de estratégias para a preparação das membranas bioativas.

As membranas com atividade antioxidante foram obtidas pela incorporação direta de  $\alpha$ -tocoferol, ácido  $\alpha$ -lipóico e a mistura de ambos na estrutura da membrana, durante o processo de preparação. A concentração de antioxidantes incorporados na membrana teve que ser otimizada, por forma a encontrar uma quantidade ideal que apresentasse a maior atividade antioxidante possível, mas que a sua permeabilidade seletiva não fosse alterada. A eficácia da incorporação de antioxidantes na estrutura da membrana foi comprovada por testes *in vitro*.

A outra abordagem de modificação das membranas foi feita recorrendo à adsorção superficial de inibidores da elastase de neutrófilos humanos, recentemente sintetizados; foram avaliados três inibidores diferentes contendo um anel  $\beta$ -lactâmico. Essas membranas foram preparadas com o objetivo de diminuir a inflamação causada pelo nível elevado de elastase de neutrófilos humanos em circulação. O grau de inibição da atividade da elastase foi avaliado, *in vitro*, para as membranas que incorporavam o composto mais promissor.

Por último, testou-se a incorporação, na estrutura da membrana, de polímeros de impressão molecular, durante o seu processo de preparação. O objetivo era a preparação de membranas que pudessem remover seletivamente toxinas urémicas do sangue de pacientes com insuficiência renal. Este estudo foi apenas preliminar; no entanto, o conceito de modificação sugerida da membrana foi comprovado. Este estudo preliminar provou que será possível incorporar compostos deste tipo com seletividade adequada para diferentes toxinas, em membranas de polisulfona.

Os resultados obtidos podem contribuir para futuros trabalhos de pesquisa sobre modificações da membrana do PSf, uma vez que os processos de preparação e modificação da membrana, usando diferentes abordagens para melhorar a sua bioatividade foram otimizados; as membranas bioativas propostas têm potencial para serem usadas em hemodiálise contribuindo para reduzir o risco cardiovascular associado à alta morbidade de pacientes em tratamento.

**Palavras-chave:** hemodiálise, membranas de polisulfona, antioxidantes, inibidores da elastase de neutrófilos humanos

## TABLE OF CONTENT

<b>1.</b>	<b>INTRODUCTION .....</b>	<b>1</b>
<b>2.</b>	<b>OBJECTIVES OF THE WORK.....</b>	<b>2</b>
<b>3.</b>	<b>THEORETICAL PART .....</b>	<b>4</b>
<b>3.1.</b>	<b>Chronic kidney disease.....</b>	<b>4</b>
<b>3.2.</b>	<b>End-stage renal disease.....</b>	<b>5</b>
<b>3.3.</b>	<b>ESRD associated complications .....</b>	<b>7</b>
3.3.1.	Uraemia .....	7
3.3.2.	Oxidative stress .....	10
3.3.3.	Inflammation .....	13
3.3.4.	Neutrophil elastase .....	15
3.3.5.	Anaemia.....	16
3.3.6.	Other complications .....	17
<b>3.4.</b>	<b>Dialysis.....</b>	<b>18</b>
3.4.1.	Peritoneal dialysis .....	20
3.4.2.	Haemodialysis.....	20
3.4.2.1.	Haemodialysis system .....	21
3.4.2.2.	Principles of haemodialysis .....	24
3.4.2.3.	Side effects of haemodialysis .....	26
<b>3.5.</b>	<b>Targeting the improvement of complications associated to ESRD patients under HD treatment.....</b>	<b>28</b>
3.5.1.	OS and antioxidant defence systems .....	28
3.5.1.1.	Enzymatic antioxidant system .....	29
3.5.1.2.	Antioxidants .....	30
3.5.2.	Inflammation: inhibitors of human neutrophil elastase .....	34
3.5.3.	Future trends in haemodialysis.....	37
<b>3.6.</b>	<b>Haemodialysis membranes.....</b>	<b>38</b>
3.6.1.	Membrane characteristics for the HD processes .....	39
<b>3.7.</b>	<b>Membranes composition.....</b>	<b>43</b>
3.7.1.	Main polymer .....	43
3.7.2.	Polymeric additives .....	50
3.7.3.	Solvent.....	52

<b>3.8. Bioactive membranes .....</b>	<b>54</b>
3.8.1. Techniques for membrane modifications.....	54
3.8.2. Vitamin E-coated membrane.....	55
3.8.3. Other bioactive membranes .....	56
<b>3.9. Membranes geometries and preparation processes .....</b>	<b>57</b>
3.9.1. Hollow-fibre membranes .....	57
3.9.2. Flat sheet membranes .....	58
3.9.3. Phase inversion process.....	60
<b>3.10. Membrane characterisation methods.....</b>	<b>64</b>
3.10.1. Morphological characterization .....	64
3.10.2. Wettability, water contact angle and protein fouling .....	66
3.10.3. Membrane biocompatibility .....	68
3.10.3.1. Haemocompatibility assays .....	68
3.10.4. Mechanical properties.....	71
<b>4. EXPERIMENTAL PART.....</b>	<b>73</b>
<b>4.1. Development and characterization of flat sheet polysulfone membrane... 73</b>	
4.1.1. Introduction and main objective of the experimental work .....	73
4.1.2. Chemicals and Instrumentation.....	74
4.1.3. Microfluidic system development to study membrane separation ability. 75	
4.1.4. Composition and preparation of the casting solution .....	76
4.1.5. Statistical data analysis.....	80
4.1.6. Membrane preparation.....	80
4.1.7. Membrane characterization .....	84
4.1.7.1. Dialysis experiment.....	84
4.1.7.2. Membrane morphology .....	88
4.1.7.3. Mechanical properties.....	90
4.1.7.4. Porosity, density, and equilibrium water content .....	90
4.1.7.5. Contact angle .....	91
4.1.7.6. Protein adsorption.....	92
4.1.7.7. Biocompatibility.....	93
4.1.8. Concluding remarks .....	95
<b>4.2. Development of bioactive membranes by incorporation of antioxidants .. 97</b>	
4.2.1. Introduction and main objectives of the experimental work .....	97

4.2.2.	Chemicals and Instrumentation .....	98
4.2.3.	Statistical data analysis .....	99
4.2.4.	Preparation of modified PSf membrane with antioxidants.....	99
4.2.5.	Optimization of the amount of antioxidant in the casting solution.....	100
4.2.6.	Dialysis experiment .....	104
4.2.7.	Antioxidant stability of the modified membranes over storage time .....	105
4.2.8.	Antioxidant leaching from the modified membranes .....	106
4.2.9.	Antioxidant capacity in vitro: blood assays .....	107
4.2.10.	Morphology of the modified membranes .....	108
4.2.11.	Mechanical properties .....	109
4.2.12.	Contact angle .....	110
4.2.13.	Protein adsorption .....	111
4.2.14.	Biocompatibility .....	111
4.2.15.	Concluding remarks .....	116
<b>4.3.</b>	<b>Development of bioactive membrane enriched with neutrophil elastase inhibitors.....</b>	<b>118</b>
4.3.1.	Introduction and main objective of the experimental work .....	118
4.3.2.	Chemicals and Instrumentation .....	119
4.3.3.	Synthesized elastase inhibitors .....	119
4.3.4.	Elastase activity assay .....	120
4.3.5.	Elastase activity inhibition by new inhibitors .....	121
4.3.6.	Elastase activity inhibition by modified PSf membranes with inhibitors.....	122
4.3.7.	Adsorption of elastase inhibitors on PSf membranes .....	124
4.3.8.	Haemolysis test.....	125
4.3.9.	Concluding remarks .....	126
<b>4.4.</b>	<b>Development of membrane incorporating molecularly imprinter polymer.....</b>	<b>128</b>
4.4.1.	Introduction and objectives of the experimental work .....	128
4.4.2.	Chemicals and Instrumentation .....	129
4.4.3.	MIP synthesis.....	129
4.4.4.	MIP selectivity evaluation for p-cresol .....	131
4.4.5.	Modification of PSf membrane with MIP .....	132
4.4.6.	Concluding remarks .....	133
<b>5.</b>	<b>CONCLUSIONS .....</b>	<b>134</b>

6.	REFERENCES .....	137
7.	SUPPLEMENTARY MATERIAL .....	155

## INDEX OF FIGURES

Figure 1: Incidence of RRT per million population in 2016 among different European countries. ....	7
Figure 2: Effect of neutrophil activation on the ESRD. ....	15
Figure 3: Haemodialysis equipment. (A) The first model of haemodialysis device used by W.J. Kolff in 1945; (B) current haemodialysis machine. ....	21
Figure 4: Scheme of haemodialysis circuit. ....	22
Figure 5: Molecular structure of $\alpha$ -tocopherol. ....	31
Figure 6: Molecular structure of $\alpha$ -lipoic acid. ....	32
Figure 7: Scheme of $\alpha$ -lipoic acid and dihydrolipoic acid pathway of regenerating endogenous antioxidants such vitamins C, $\alpha$ -tocopherol, and glutathione. ....	34
Figure 8: Human neutrophil elastase inhibitor structure. (A) Structure of the inhibitor $\alpha_1$ – protease inhibitor. The P1 and P1' sites of reactive centre loop points out the location of the peptide bound cleaved by the HNE before inhibition. (B) Mechanism of the serine protease. ....	35
Figure 9: Schematic membrane module representing solute permeating across the membrane. ....	41
Figure 10: Comparison of sieving curves of low-flux, high-flux membrane with glomerular basement membrane. ....	42
Figure 11: Scanning electron microscopy image of symmetric unmodified cellulosic vs. asymmetric polysulfone hollow-fibre membranes. ....	46
Figure 12: Schematic representation of hollow-fibre dialyser design (A) and real image of commercial hollow-fibre dialyser with magnified cross-section of polysulfone hollow-fibres (B). ....	47
Figure 13: Chemical structure of polyvinylpyrrolidone (A) and polyethylene glycol (B). ....	50
Figure 14: Different membrane morphologies associated to different types of solvent demixing rate. ....	52
Figure 15: Mutual diffusivity of various polymeric solvents with water, used as a nonsolvent in the coagulation bath ....	53
Figure 16: Diagram of hollow-fibre membrane preparation via phase inversion. ....	58
Figure 17: Spin coating process ....	59
Figure 18: Schematic structure of symmetric and asymmetric membranes showing the different morphologies. ....	61
Figure 19: Process of phase inversion via immersion precipitation. ....	62
Figure 20: Example of water contact angle of materials with different hydrophilicity. ....	67
Figure 21: Oxygen plasma cleaner used to treat silicon platform in off and on state. ....	75
Figure 22: Silicon microchannel platform. ....	76
Figure 23: Image of the spin coater in closed and open positions. ....	81

Figure 24: Image of dried PSf membrane.....	81
Figure 25: Image of PSf membranes incubated in an environment with high humidity, prior phase inversion in a coagulation bath. ....	83
Figure 26: Fluidic system to evaluate membrane separation ability, composed of two closed circuits, separated by the semipermeable membrane under study .....	84
Figure 27: Schematic diagram of solutes filtration by symmetric (A) and asymmetric (B) membrane.....	85
Figure 28: Effect of different masses (wt%) of PVP K30 on membranes (M7-M9) dialysis performance.....	88
Figure 29: The SEM cross-section images of membrane M9.. ....	89
Figure 30: Optical microscopy images of Wright stained blood smears.....	94
Figure 31: Urea reduction ratio (URR [%]) of PSf membranes modified with different concentrations of $\alpha$ -TCP (A) and ALA (B). ....	100
Figure 32: Comparison of the redox capacity of modified membranes prepared with different concentrations of ALA, evaluated by FRAP assay. ....	102
Figure 33: Comparison of the redox capacity of membranes modified with ALA and $\alpha$ -TCP, evaluated by FRAP assay.....	102
Figure 34: Antioxidant activity of PSf membranes enriched with $\alpha$ -TCP, ALA and with a combination of both.....	103
Figure 35: URR values presented by unmodified and modified PSf membranes.....	104
Figure 36: Protein rejection (BSA and human lysozyme) of unmodified and modified PSf membranes, enriched with $\alpha$ -TCP, ALA and with a combination of both . ....	105
Figure 37: Cross-section images of PSf – ALA (a), PSf - $\alpha$ -TCP (b), PSf - ALA/ $\alpha$ -TCP (c), and unmodified PSf membranes (d), by scanning electron microscopy.....	109
Figure 38: Adsorption of BSA on unmodified and modified PSf membranes. ....	111
Figure 39: Optical microscopy images of Wright stained blood smears.....	112
Figure 40: Plasma concentration of free Hb after incubation of whole blood with unmodified and modified PSf membranes.....	113
Figure 41: Inhibition curve of AAN-5 used to determine $IC_{50}$ .....	122
Figure 42: Inhibitor adsorption test on the membranes surface. ....	123
Figure 43: Inhibitory activity of membranes modified with different concentrations inhibitors AAN-5, AAN-7, and AAN-8. ....	124
Figure 44: Plasma concentration of free Hb after incubation of whole blood with HNEI AAN-5 and AAN-8. ....	126
Figure 45: Molecular structure of p-cresol. ....	130
Figure 46: A set up of template molecule removal from powdered MIP.....	130
Figure 47: Effect of pH on adsorption of p-cresol by MIP. ....	131
Figure 48: SEM cross-section image of PSf membrane containing MIP incorporated in its structure.....	132



## INDEX OF TABLES

Table 1: Classification and definition of chronic kidney disease.....	5
Table 2: Three groups of uremic toxins with their the most relevant adverse effects. ....	9
Table 3: Markers of OS and their usual quantification methods.....	12
Table 4: Summary of characteristics of PD and HD and comparison of their risks and benefits. ....	19
Table 5: Comparative composition of dialysis fluid and blood plasma. ....	23
Table 6 : Exogenous therapeutic inhibitors of human neutrophil elastase.....	37
Table 7 : HD membranes: their advantages and limitations.....	48
Table 8: Summary of tested variations of casting solution composition.. ....	79
Table 9: The exact composition of the prepared PSf membranes.....	80
Table 10: Summarized conditions for PSf membranes preparation. ....	83
Table 11: Mechanical properties of membrane M9.....	90
Table 12: Summary of evaluated characteristics of membrane M9.....	93
Table 13: Lipid-peroxidation (LPO), total antioxidant status (TAS) and ascorbic acid (AA) plasma levels after incubation of whole blood with membrane samples. ....	108
Table 14: Mechanical properties values of unmodified and modified PSf membranes PSf - ALA, PSf - $\alpha$ -TCP, and PSf - ALA/ $\alpha$ -TCP. ....	110
Table 15: Water contact angle values of unmodified and modified PSf membranes PSf - ALA, PSf - $\alpha$ -TCP, and PSf - ALA/ $\alpha$ -TCP ....	110
Table 16: Data on coagulation and complement activation after incubation of blood with unmodified and modified PSf membranes. ....	115
Table 17: Summarized characteristics of the newly synthesized elastase inhibitors: AAN-5, AAN-7, and AAN-8. ....	120
Table 18: Amount of adsorbed HNEI on membrane surface in dependence on the initial concentration.....	125

## INDEX OF ABBREVIATIONS

4-HNE	4-hydroxy-2-nonenal	GC	gas chromatography
AA	ascorbic acid	GFR	glomerular filtration rate
AAT	$\alpha_1$ – antitrypsin	GPx	glutathione peroxidase
ACN	acetonitrile	GSH	glutathione (reduced form)
ADMA	asymmetric dimethylarginine	GSSG	glutathione (oxidized form)
AFM	atomic force microscopy	Hb	haemoglobin
AGEs	advanced glycation end products	HD	haemodialysis
ALA	$\alpha$ -lipoic acid	HNE	human neutrophil elastase
AN	acrylonitrile	HPLC	high performance liquid chromatography
APTT	activated partial thromboplastin time	ID	internal diameter
CAS	chemical abstracts service	IHC	immunohistochemistry
CAT	catalase	IL	interleukin
CDA	cellulose diacetate	INF	interferon
CKD	chronic kidney disease	ISO	International Organization for Standardization
CRP	C-reactive protein	KDIGO	kidney disease improving global outcomes
CTA	cellulose triacetate	LDL	low-density lipoprotein
CV	cardiovascular	LOOH	lipid hydroperoxides
CVD	cardiovascular disease	LPO	lipid peroxidation
DCM	dichloromethane	MDA	malonyldialdehyde
DMA	dimethylacetamide	MIP	molecularly imprinted polymer
DMF	dimethylformamide	MS	mass spectrometry
DMSO	dimethyl sulfoxide	MW	molecular weight
ELISA	enzyme-linked immunosorbent assay	MWCO	molecular weight cut-off
EPO	erythropoietin	NAC	N-acetylcysteine
ESA	erythropoiesis-stimulating agents	NADP	nicotinamide adenine dinucleotide phosphate
ESRD	end-stage renal disease	NCDS	National Cooperative Dialysis Study
EVAL	ethylene-vinyl alcohol copolymer	NIP	non-imprinted polymer
FRAP	ferric reduction antioxidant power	NIPS	nonsolvent induced phase separation

NMP	N-methyl-2-pyrrolidinone	TAS	total antioxidant status
NO	nitric oxide	TBARS	thiobarbituric acid reactive substances
OS	oxidative stress	TEP	triethyl phosphate
PAM	polyacrylamide	TMP	transmembrane pressure
PAN	polyacrylonitrile	TMU	tetramethylurea
PC	polycarbonate	TNF	tumour necrosis factor
PD	peritoneal dialysis	UHPLC	ultra-high performance liquid chromatography
PEG	polyethylene glycol	URR	urea reduction ratio
PEPA	polyester polymer alloy	VEM	vitamin E-coated membrane
PES	polyethersulfone	$\alpha_1$ PI	$\alpha_1$ – protease inhibitor
PLT	platelet	$\alpha_2$ M	$\alpha_2$ – macroglobulin
PMMA	poly(methyl methacrylate)	$\alpha$ -TCP	$\alpha$ -tocopherol
PMN	polymorphonuclear		
PMNL	polymorphonuclear leukocytes		
pmp	per million population		
PSf	polysulfone		
PT	prothrombin time		
PTX3	pentraxin 3		
PVC	polyvinyl chloride		
PVP	polyvinylpyrrolidone		
$Q_{B/D}$	blood/dialysate flow rate		
RBC	red blood cell		
Rd	reductase		
rhEPO	recombinant human erythropoietin		
RNS	reactive nitrogen species		
ROS	reactive oxygen species		
rpm	resolutions per minute		
RRT	renal replacement therapy		
SD	standard deviation		
SEM	scanning electron microscopy		
SEM	standard error of the mean		
SLPI	secretory leukocyte protease inhibitor		
SOD	superoxide dismutase		
TAC	total antioxidant capacity		



## 1. INTRODUCTION

End-stage renal disease is a growing health problem, with increasing prevalence worldwide, associated with high financial burden for health systems. Patients suffering from ESRD exhibit higher morbidity and mortality rates compared to the general population. For their surveillance, renal replacement therapies are usually required. Haemodialysis as a practical means of replacing kidney function started and developed in the 20<sup>th</sup> century.

From the 1960s, when the first extracorporeal dialysis technique was introduced in human therapy, several solutions have been used that contributed to improve the technical procedure. What became more evident from that period were the developments that emerged related to dialyzing membranes, especially the importance of the type of material used for their manufacture, their composition and geometry.

Despite the efforts, the improvements made over time in the materials used for dialysis membranes to achieve biocompatibility and good separation of biomolecules, patients undergoing haemodialysis treatment still suffer from oxidative stress, chronic inflammation, anaemia, malnutrition and others, mostly caused by the inadequate uremic toxins removal and by the long-term contact between blood and artificial material of the semipermeable membrane. Modifications of the membrane characteristics like pore size, pore uniformity, hydrophilicity and bioactivity, can be done by changes in membrane composition by additives and/or by adding compounds with specific biological functions, improving membrane dialysis characteristics and thereby patients' quality of life.

In this context, it is important to seek the development of biocompatible membranes for future application in haemodialysis systems, with more beneficial characteristics to health and wellbeing of these patients.

## 2. OBJECTIVES OF THE WORK

The main objective of the presented dissertation work was to develop and optimize a flat sheet, polymeric, semipermeable membrane, which could be further modified with bioactive compounds, in order to ameliorate the haemodialysis patients' quality of life. The major reason for the development of this work was the increasing number of renal disease patients worldwide; whose life is dependent on this renal replacement therapy. Despite the technical improvements in recent years, this treatment is still associated with adverse effects and high risk of cardiovascular morbidity and mortality. Therefore, there is a need for continuous innovation and improvement in this area of haemodialysis treatment.

The first objective was to develop a polysulfone membrane that presented characteristics comparable to the membranes commonly used for haemodialysis treatment, namely the selective separation for biomolecules and biocompatibility. In other words, the membrane would be permeable for accumulated blood toxins and concurrently, would not cause adverse reactions, when contacting with blood. However, the developed membranes were fabricated in smaller scale and simplified geometry, compared to commercial membranes, as they would be adequate to the conditions of laboratory testing conditions. The membrane composition and preparation procedure had to be optimized to fulfil these requirements; various physical and biological methods were used to evaluate the specific characteristics of the developed membranes.

The second objective was to modify/improve the functionality of the membrane to gain ability to diminish oxidative stress associated with chronic inflammation, which are commonly presented by patients undergoing haemodialysis treatment. For this purpose, the membrane was enriched with different antioxidant compounds. This enrichment process had to be optimized to maximize the antioxidant activity, without compromising the biocompatibility and the selective separation ability.

Another strategy was to introduce bioactivity to the membrane by enrichment with synthetic inhibitors of human neutrophil elastase. This serine protease is released by neutrophils that are activated during the haemodialysis process and that may lead to degenerative and inflammatory changes. Thus, inhibiting elastase activity and preventing these adverse effects would be important. This objective was carried out in cooperation with the Department of Pharmaceutical Chemistry, Faculty of Pharmacy, University of Lisbon, who kindly provided the newly synthesized inhibitors.

In addition, another strategy for modifying membranes was considered. The incorporation of molecularly imprinted polymers, specific for uremic toxins, which are difficult

to remove by conventional haemodialysis, was also our aim. This method is still under development and testing but seems to be promising.

### **3. THEORETICAL PART**

#### **3.1. Chronic kidney disease**

Chronic kidney disease (CKD) is a long-term progressive loss of renal function with decreased glomerular filtration rate (GFR). Its prevalence is increasing worldwide, being recognized as a growing public health risk affecting nowadays 10 – 12% of the population (1). This prevalence is expected to continue to rise, mostly in developed countries, due to general aging of the population and increasing numbers of patients with diabetes mellitus and hypertension, which are major causes of CKD (2). In developing countries, the main causes of CKD are different, since CKD may be, mainly, the result of elevated and continuous exposure to harmful toxins and drugs, and from recurrent infections. Patients with CKD present increased comorbidities that, usually, result from the disease itself. They also present high hospitalization rate, due to the higher prevalence of nutritional, infectious, hormonal, and psychological disorders, which is further associated with poor quality of life. Above that, CKD patients show a higher mortality rate, mainly due to cardiovascular disease (CVD) events, and their lifespan is considerably shorter when compared to age matched healthy population (2).

The Global Burden of Disease study reported in 2015, that an estimated 1.2 million deaths were directly associated with CKD (3). The cardiovascular mortality of CKD patients is two-fold higher, when compared to general population, and grows with declining of GFR (4, 5).

CKD is classified into 5 stages with different severity of the disease, based on the cause of the disease, GFR and albuminuria. The disease classification is summarized in Table 1. The measurement of GFR is difficult and several methods exist for its calculation. Usually, GFR is estimated by using blood levels of creatinine or of cystatin C.

Rapidly progressive CKD can lead to kidney failure within months, although it usually evolves over decades and some patients do not progress to other disease stage for many years (6).

Due to the increased prevalence of the disease, the high costs and poor outcomes of the treatment, the CKD constitutes a worldwide public health threat. Public health interventions and professional recommendations and guidelines from Kidney Disease Improving Global Outcomes (KDIGO) are available to improve the prevention, screening, and treatment to prevent disease progression into renal failure (6). When CKD remains uncontrolled it progresses to end-stage renal disease (ESRD) and patients will need renal replacement treatment (RRT) to survive.



Thanks to remarkable progress in laboratory investigation and clinical trials, current testing can detect early stages of the disease, and therefore the screening methods for populations at increased risk are nowadays more available.

*Table 1: Classification and definition of chronic kidney disease. Modified from (7).*

Stage	Description	GFR mL min <sup>-1</sup> per 1.73 m <sup>2</sup>
stage 1	normal GFR; often asymptomatic; persistent albuminuria, proteinuria, haematuria; can be reverse	≥ 90
stage 2	mild decrease in GFR; often asymptomatic; persistent albuminuria, proteinuria, haematuria; can be reverse	60 to 89
stage 3	moderate decrease in renal function; early renal insufficiency	30 to 59
stage 4	severe decrease in GFR; late renal insufficiency	15 to 29
stage 5 (end-stage renal disease)	renal failure; uraemia; dialysis	< 15

*GFR: glomerular filtration rate*

### 3.2. End-stage renal disease

ESRD is a severe pathological condition that results from a gradual and irreversible loss of kidney function with a significant reduction in the GFR and albuminuria. As shown in Table 1, according the National Kidney Foundation ESRD is classified as the gravest stage of CKD (stage 5), with GFR below 15 mL min<sup>-1</sup> 1.73 m<sup>-2</sup> for a minimal period of 3 months (7). Patients with these conditions of renal failure require renal replacement therapy (RRT) via dialysis (haemodialysis and peritoneal dialysis) or via kidney transplantation.

Although ESRD affects global population there are considerable variations in disease prevalence among countries, including those within Europe. These variations within populations seem to result from differences in the main CKD risk factors and from their dependence on several elements such as diet, smoking, physical activity, race, and socioeconomic status of the patients. Dialysis treatment has a significant socio-economic

impact causing a major financial burden on healthcare systems. It is estimated that over 3 million patients worldwide have access to RRT and that the expenses connected with HD treatment in developed countries represent approximately 5% of the health system budgets. In middle-income countries, treatment with dialysis or kidney transplantation creates a huge financial strain for the majority of the people who need it. Also, in approximately 112 countries many people cannot afford treatment at all, resulting in the death of over 1 million people annually from untreated kidney failure (8).

Despite the significant technological and pharmaceutical improvements in ESRD treatment, patients' survival rate remains low. The survival rate of ESRD patients during the first year of haemodialysis (HD) is in Europe around 84% while the 5-year survival rate drops to around 63% (9). The type of material used for HD membrane significantly affects the surveillance rate, since use of highly biocompatible membranes can reduce inflammatory response induced during contact of blood with the artificial material. The most common cause of death in ESRD patients are cardiovascular disease events, which are up to 20 times more frequent than those in the general population (10). The high cardiovascular risk is attributed to a complex interconnection of traditional risk factors including age, obesity, lifestyle, arterial hypertension, diabetes, dyslipidaemia, and additional disease-associated risk factors, such as systemic inflammation, oxidative stress, anaemia, hyperparathyroidism, left ventricular hypertrophy, endothelial dysfunction, and others (11).

The incidence of RRT in Europe is summarized on the map presented below (Figure 1). The results refer to 2016 and are related to ESRD patients starting RRT. The highest incidence of newly treated patients was reported in Greece, approximately 250 per million population (pmp), the second place belonged to the Czech Republic, with 243 pmp, and on the third position was Portugal, with 236 pmp newly treated patients (12).

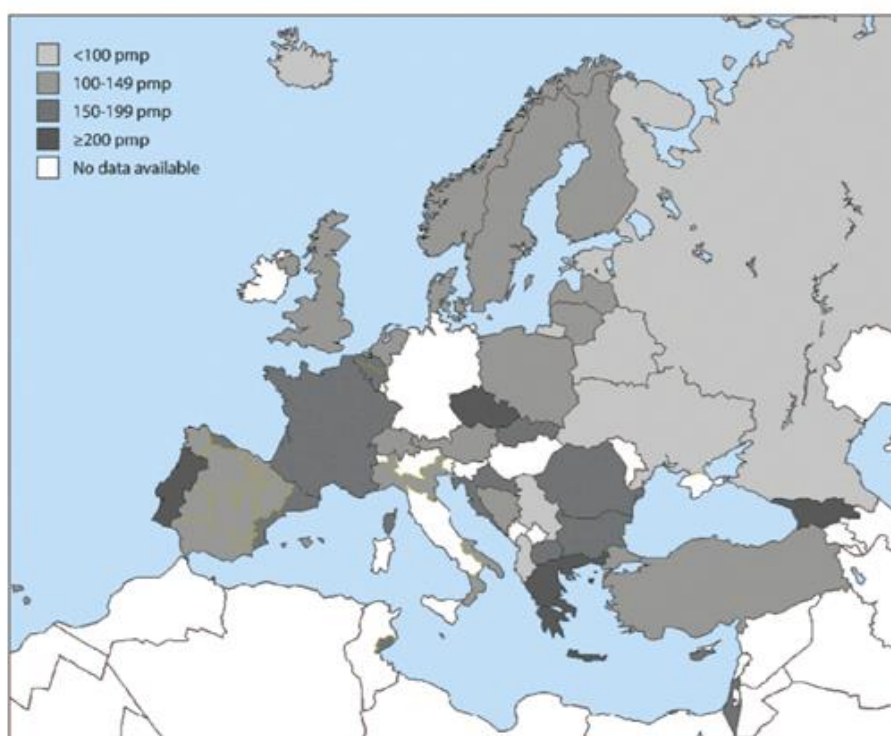


Figure 1: Incidence of RRT per million population in 2016 among different European countries. The incidence for Czech Republic, Poland, Russia, Slovakia, and Tunisia only includes patients receiving dialysis. Reproduced from (12).

### 3.3. ESRD associated complications

ESRD is associated with many disease related conditions and, unfortunately, some of them become more pronounced when the patient starts with regular HD treatment. The consistently presented complications include oxidative stress and systemic inflammation which are important mediators of atherosclerosis and of other cardiovascular diseases (CVD); moreover, they may contribute to enhance anaemia, cachexia, worsening the disease and the overall patient's quality of life and outcome.

#### 3.3.1. Uraemia

Uraemia is a clinical condition marked by elevated concentrations of urea in the blood, associated with decreased renal function. Uraemia is characterized by the retention of waste products, known as uremic toxins, which in physiological conditions are eliminated by urine. These non-excreted uremic toxins accumulate in blood and cause many adverse effects, known as the uremic syndrome. Systemic effects of uraemia are numerous and most often interrelated, as they are frequently caused by action of the combination of uremic

toxins, rather than by a single uremic toxin. Besides that, not all the retained uremic toxins have established impact or known toxic effect (13).

Among the severe uraemia related complications are the cardiovascular (CV) events, when the CVDs are leading causes of death by uremic patients (14). Hyperkalaemia, hypocalcaemia, hyperphosphatemia, hypomagnesemia, and metabolic acidosis are also manifestations of the uremic syndrome. Uraemia also negatively influences mineral bone metabolism due increasing levels of parathyroid hormone and deficit of vitamin D and calcium. Uremic encephalopathy can also result from endogenous uremic toxins in ESRD patients, although unusual, ranging from mild inattention to coma. The immune response in uremic patients is often altered, resulting in greater susceptibility to infections. Anaemia is a common feature in ESRD patients and platelet function may be disturbed (15). Together with anxiety and depression, common in these patients, all uraemia associated complications contribute significantly to patients' poor wellbeing, worsening of the disease and to the outcome of patients.

The uremic toxins, responsible for the above-mentioned complications, can be divided into three groups according to its molecular size: small molecules, middle-sized molecules, and protein-bound toxins. The first group includes solutes with a molecular mass smaller than 500 Da, with a high degree of water solubility and negligible protein binding, such as urea and creatinine. The second category of molecules, with medium size, have molecular masses that vary between 500 to 60 000 Da and contain predominantly peptides and proteins that accumulate in uraemia, such as  $\beta$ 2-microglobulin. The third group corresponds to solutes with small molecular mass (< 500 Da) but with chemical characteristics that preclude the possibility of their circulation in bound and unbound forms. These small organic molecules, such as indoxyl sulphate and *p*-cresol, have typically ionic and/or hydrophobic character and bind strongly to plasma albumin. These toxins are difficult to be removed by dialysis, but their removal can be improved by using the high-flux dialysers. (16-18). The most relevant uremic toxins and their adverse effects are summarized in Table 2.

Table 2: Three groups of uremic toxins with their the most relevant adverse effects.

Uremic toxin	Effect	References
<b>Small water-soluble molecules</b>		
urea	<ul style="list-style-type: none"> <li>involved in insulin resistance, free radical production, apoptosis</li> <li>generation of ammonia; associated with CV mortality</li> </ul>	(19)
guanidines	<ul style="list-style-type: none"> <li>suppress anti-inflammatory reaction</li> <li>ADMA inhibits the production of NO; progression of CVD</li> </ul>	(18, 20)
purines	<ul style="list-style-type: none"> <li>xanthine and hypoxanthine induce vasoconstriction</li> <li>uric acid is linked to pro-inflammatory processes</li> </ul>	(17)
oxalate	<ul style="list-style-type: none"> <li>deposition in bone, joints, skin; contributes to renal injury and myocardial fibrosis</li> </ul>	(21)
polyamines	<ul style="list-style-type: none"> <li>inhibition of erythropoiesis and platelet aggregation; neurotoxic and cytotoxic</li> <li>spermine induces oxidative stress</li> </ul>	(22)
<b>Middle size molecules</b>		
$\beta$ 2-microglobulin	<ul style="list-style-type: none"> <li>causes bone and joint amyloid deposits</li> </ul>	(23)
parathyroid hormone	<ul style="list-style-type: none"> <li>disturbs homeostasis by increasing calcium level; leads to hyperparathyroidism</li> </ul>	(18)
<b>Protein bound compounds</b>		
advanced glycation end products	<ul style="list-style-type: none"> <li>induction of oxidative stress, inflammation, and endothelial dysfunction</li> </ul>	(17)
advanced oxidation protein products	<ul style="list-style-type: none"> <li>induce production of ROS</li> </ul>	(17)
cresols	<ul style="list-style-type: none"> <li>induce production of ROS; <i>p</i>-cresol is hepatotoxic</li> </ul>	(17, 24)
hippurates	<ul style="list-style-type: none"> <li>induce production of ROS; hippuric acid is associated with kidney damage</li> </ul>	(25)
homocysteine	<ul style="list-style-type: none"> <li>contributes to atherosclerosis and other CVD; enhances thrombogenicity</li> </ul>	(18)
indoles	<ul style="list-style-type: none"> <li>deterioration of renal function; indoxyl sulphate enhances drug toxicity</li> </ul>	(18)

ADMA: asymmetric dimethylarginine; NO: nitric oxide; CV: cardiovascular; CVD: cardiovascular disease; ROS: reactive oxygen species

### 3.3.2. Oxidative stress

Generation of oxidative compounds is a physiological process, which is important in defence mechanisms against pathogens and malignant cells, as well as tissue injuries, for repairing/remodelling processes. The inflammatory cells, as neutrophils and macrophages, are important sources of reactive oxygen species (ROS), which are produced through the oxidative or respiratory burst. When inflammatory cells are activated the metabolic oxidative burst is triggered leading to the rapid production and release of ROS, such as superoxide anion ( $O_2^-$ ) and hydrogen peroxide ( $H_2O_2$ ) (26). The enzyme system nicotinamide adenine dinucleotide phosphate (NADP) oxidase, that is bound to the cellular membranes, reduces  $O_2$  to  $O_2^-$ , which is highly unstable and very rapidly converted into  $H_2O_2$ . Superoxide anion and hydrogen peroxide react with other molecules forming further powerful and highly reactive oxidants.  $O_2^-$  reacts with nitric oxide (NO) generating highly reactive nitrogen species, while  $H_2O_2$  reacts with intracellular iron and, via the Fenton reaction, forms hydroxyl radical ( $OH^\cdot$ ).  $OH^\cdot$  is strongly implicated in cell lipid peroxidation, protein modifications, and DNA damage. Hydrogen peroxide is the substrate for the enzyme myeloperoxidase that catalyses the reaction between  $H_2O_2$  and chloride ions, producing the oxidant hypochlorous acid ( $OCl^-$ ). Hypochlorous acid is a powerful oxidant able to oxidize different types of biomolecules and to react with endogenous amines, forming chloramines (27).

The oxidative burst and formation of ROS is regulated by the presence of cellular oxidant and antioxidant systems. When the balance between antioxidants and ROS is disrupted because of either impaired/insufficient antioxidant system defence or excessive production and accumulation of ROS, the oxidative stress (OS) is subsequently developed (28).

OS is common in ESRD patients and is present from the early stages of the disease; it is further enhanced with disease progression, especially when patients initiate HD treatment. The imbalance between pro-oxidants and antioxidants in ESRD patients may have various contributing factors.

As mentioned in Section 3.3.1, several retained uremic toxins are pro-oxidants and can stimulate the activation of polymorphonuclear cells, enhancing the production and release of ROS (29). Malnutrition and/or dietary restriction causing depletion of antioxidants, such as vitamin C, vitamin E and selenium naturally consumed in diet, may also contribute to OS in ESRD patients. Besides that, the majority of the vitamins is water soluble, and thus as they can be removed from blood during the HD treatment and their reserves are rapidly depleted (30).

The progression of inflammation and OS following the kidney injuries, underlying the development of CKD, leads to further changes in the kidney tissue contributing to the progression of kidney damage. The linkage between inflammation and OS with kidney damage has been reported in several studies, showing a strong inverse association between the decline of GFR and the increase in OS biomarkers (31).

The aforementioned antioxidants are very unstable with half-life times of a few seconds. Therefore, their *in vivo* evaluation is generally not feasible. In contrast, the end-products of macromolecules (lipids, proteins, DNA) with oxidative modifications are stable for hours or weeks and accumulate in patient's blood, which makes them ideal markers of OS (27). However, the inadequate removal of waste products from the blood in ESRD patients may interfere in the evaluation of the OS status of these patients, leading to misinterpretation. For this reason, the use of biomarkers from early steps of the oxidative chain rather than its end-products is more appropriate in ESRD patients (32).

There is variety of OS biomarkers that can be classified into two groups:

- a) Biomolecules that are modified by interactions with ROS, measuring the direct chemical impact of ROS in biological systems. DNA/RNA, lipids (including phospholipids), proteins and carbohydrates are molecules that can be modified *in vivo* by excessive ROS. The OS modified products of these molecules are used as biomarkers. They are listed, together with the method for their quantification, in Table 3.
- b) Molecules that are generated in response to increased redox stress, such as xanthine oxidase and myeloperoxidase, and can be used as markers of ROS generation. Protein thiol-disulphide oxidoreductases (thioredoxin, peroxiredoxin) are used as markers of antioxidant defence. The concentration of these enzymes can be evaluated in plasma samples by enzyme-linked immunosorbent assay (ELISA) (33).

During the lipidic peroxidation, the reaction of ROS (hydroxyl and peroxy radicals) with unsaturated fatty acids initiates the autocatalytic chain reaction, during which the fatty acid (linoleic and arachidonic acid) is broken to smaller and more stable products. Among them, aldehyde acrolein, 4-hydroxy-2-nonenal (4-HNE) and malondialdehyde (MDA), are the most evaluated biomarkers of lipid peroxidation. MDA can be evaluated by different techniques (Table 3), such as high performance liquid chromatography (HPLC) or the thiobarbituric acid reactive substances (TBARS) assay; the thiobarbituric acid reacts with MDA to form a coloured product which can be easily detected spectrophotometrically. To measure the presence of 4-HNE in biological samples, including protein-bound aldehydes, protein immunodetection is the most common, either by immunohistochemistry or by ELISA (Table 3). The specificity of the monoclonal antibodies against HNE-His adducts allows the

quantification of 4-HNE in human tissues, tissue homogenates, and in plasma and serum samples (27, 33, 34).

It is important to notice that the activated inflammatory cells release ROS, together with pro-inflammatory cytokines, which may further amplify the OS and inflammation by triggering the activation of other inflammatory cells.

Table 3: Markers of OS and their usual quantification methods. Modified from (33).

Markers of oxidative stress	Quantification methods
<b>Lipid peroxidation</b>	
MDA	<ul style="list-style-type: none"> <li>• spectrophotometrically using TBARS assay</li> <li>• in plasma using HPLC or ELISA</li> </ul>
4-HNE	<ul style="list-style-type: none"> <li>• in tissues by IHC</li> <li>• in plasma by HPLC or ELISA</li> </ul>
F <sub>2</sub> -isopropanes	<ul style="list-style-type: none"> <li>• in plasma by HPLC, GC-MS or ELISA</li> <li>• in urine by GC-MS, HPLC-MS/MS or ELISA</li> </ul>
Acrolein	<ul style="list-style-type: none"> <li>• in tissues by IHC</li> </ul>
Oxidized LDL	<ul style="list-style-type: none"> <li>• in plasma or isolated LDL by ELISA</li> </ul>
<b>Protein oxidation</b>	
Advanced oxidation protein products	<ul style="list-style-type: none"> <li>• in plasma protein carbonyls are detected after derivatization with 2,4-dinitrophenylhydrazine by ELISA or HPLC</li> </ul>
<b>Carbohydrate oxidation</b>	
Advance glycation end-products (AGEs)	<ul style="list-style-type: none"> <li>• in skin by IHC</li> <li>• in plasma or serum by ELISA</li> <li>• specific AGEs such as pentosidine by HPLC</li> </ul>
<b>Nucleic acid oxidation</b>	
8-oxo-2-deoxyguanosine	<ul style="list-style-type: none"> <li>• in urine by UHPLC-MS/MS or by ELISA</li> </ul>

TBARS: thiobarbituric acid reactive substances; HPLC: high performance liquid chromatography; IHC: immunohistochemistry; ELISA: enzyme-linked immunosorbent assay; GC: gas chromatography; MS: mass spectrometry; LDL: low-density lipoprotein; UHPLC: ultra-high performance liquid chromatography



### 3.3.3. Inflammation

The aetiology of inflammation in ESRD patients is multifactorial and may be associated to intercurrent clinical events, comorbidities (e.g. OS, uraemia, hypoxia, fluid and sodium overload, immune dysfunction, diabetes, CVD), renal disease and dialysis. As already referred, when renal tissue injuries occur, the inflammatory cells as macrophages and neutrophils, get activated and release different inflammatory mediators. Activated neutrophils release pro-inflammatory cytokines, such as interleukin (IL)-1 and tumour necrosis factor- $\alpha$  (TNF- $\alpha$ ), ROS/RNS and the content of their granules, which include several constituents such as serine proteases. In response to these mediators the vascular permeability is increased, enabling fast migration of more neutrophils and macrophages into the site of injury, further propagating and perpetuating inflammation by activating other inflammatory cells that will produce more pro-inflammatory cytokines and ROS (35).

The chronic pro-inflammatory conditions in ESRD, with excessive inflammatory cell activation, may lead to dysfunction of innate immune system further worsening the inflammation presented by these patients. The macrophages, which normally play an important role in host defence against microbial infections and in tissue healing process, in patients with ESRD their functions may be impaired, increasing the susceptibility of these patients for bacterial infections (36). The contribution of monocytes/macrophages to the systemic inflammation is also given by the spontaneous activation of these cells and the expansion of circulating monocytes, which are able to upregulate the basal production of inflammatory cytokines and ROS (37). The circulating macrophages, that increase after the HD procedures, may contribute to the development and progression of atherosclerotic plaque and therefore, to increase the risk for CV events (36). Polymorphonuclear leukocytes (PMNL) are part of the first line of defence against invading microbes and play an important role in inflammation. The PMNLs are phagocytic cells with many intracellular granules containing different types of constituents, such as bactericidal proteins, proteolytic enzymes (neutrophil elastase), lysozyme, NADP oxidase generating ROS, myeloperoxidase, and lactoferrin. Disturbances in any of these essential microbicidal functions may lead to an increased risk for bacterial infections. Like the monocytes and macrophages, the functionality of PMNLs in ESRD patients may be impaired. Due to the presence of the uremic toxins, the PMNLs can be spontaneously activated, which leads to degranulation of the cytoplasmic granules into extracellular space. The released bactericidal substances, together with excessive ROS generation, contribute to the systemic OS, inflammation and tissue damage presented in these patients (36, 38). The adaptive immune system may be also affected by uraemia. The number of the antigen-presenting cells and their antigen-

presenting capacity is decreased. The depletion of T-lymphocytes due to increased cell turnover and apoptosis also occurs, leading to increased susceptibility of ESRD patients to infections (36).

In the ESRD patients the persistent systemic inflammation contributes to a large number of complications including atherosclerosis, cardiovascular disease, cachexia, protein energy wasting, and anaemia, whereas immune deficiency leads to impaired response to vaccination, and increased incidence of microbial infections. Together, these abnormalities account for the large proportion of morbidities and CVD mortality in patients suffering with ESRD (36).

As inflammation is associated with many complications, the evaluation of the inflammatory state and its progression is very important in ESRD patients. The measurement of inflammatory biomarkers in blood is commonly used in clinical practice. The most used biomarkers of inflammation are C-reactive protein (CRP), an acute-phase protein; a pro-inflammatory mediator TNF- $\alpha$  (39); an independent predictors of CVD cytokine IL-6, and pentraxin-3 (PTX3), which is produced in response to inflammatory signals by immune cells at the local of inflammation. PTX3 levels are increased in HD patients, and an association between PTX3 and cardiovascular morbidity has been reported, suggesting a linkage with CVD risk in ESRD patients on dialysis (40, 41).

Both, enhanced OS and inflammation are known to be tightly interrelated with ESRD, with general mechanism of renal endothelial dysfunction, and with kidney disease progression (Figure 2). Since they are also associated with a variety of other diseases such as CVD, atherosclerosis, hypertension, cancer, diabetes, arthritis, neurodegenerative diseases and others, OS and inflammation might have an important predictive value for the outcome of ESRD patients (42).

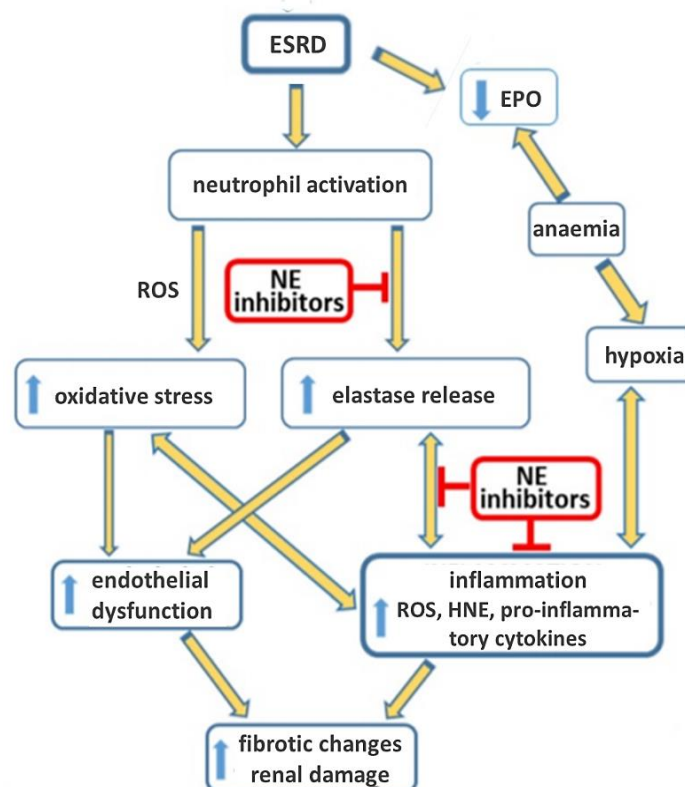


Figure 2: Effect of neutrophil activation on the ESRD. Schematic representation of interconnection between single complications. The activation of neutrophils with release of ROS and NE leads to oxidative stress contributing to endothelial dysfunction and to inflammation with further release of pro-inflammatory cytokines. These changes lead to fibrotic alterations resulting in deepened renal damage. Anaemia, resulting from the reduced production of EPO by failure kidney, leads to hypoxia, promoting inflammation. Modified from (43).

ESRD: end-stage renal disease; EPO: erythropoietin; NE: neutrophil elastase

### 3.3.4. Neutrophil elastase

Human neutrophil elastase (HNE) is an enzyme with molecular weight of 30 kDa, which belongs to the family of chymotrypsin-like serine proteases. It is able to degrade almost all extracellular matrix proteins, as well as a variety of blood proteins and plays an important role in the regulation of the immune response (44). In neutrophils the elastase is stored in the azurophilic (primary) granules that contain other serine proteases, and is released into the extracellular space by cell degranulation (45, 46). Its active site is formed by a catalytic triad of histidine–serine–aspartic acid, which binds to the substrate and cleave the peptide bond.

Under the physiological conditions, released HNE is responsible for host defence mechanism, when the main role is intercellular degradation of foreign organic molecules phagocytosed by neutrophils. Extracellularly is responsible for tissue remodelling, degrading elastin fibres (47). Besides elastin, HNE is also able to cleave coagulation and complement factors, leading to their activation, and several pro-inflammatory cytokines

which in contrary causes their inactivation (48, 49). In addition to the proteolytic activity, neutrophil elastase is known to induce the production and release of pro-inflammatory cytokines (IL-6 and IL-8) from the activated leukocytes.

The daily amount of elastase released from neutrophils is approximately 50 mg and, since it occurs without any clinical evidence of tissue degradation (50), the proteolytic activity of HNE must be tightly regulated by endogenous protease inhibitors.

In HD patients with chronic inflammation, elastase levels are likely to be increased, altering the above-mentioned favourable function of elastase to a potentially harmful role. The HNE might remain active due to imbalance between (elevated) elastase and the (inadequate) endogenous elastase inhibitors. In such conditions, the unregulated excessive proteolytic activity of elastase may lead to a variety of degenerative changes, including lung tissue damage and kidney tissue damage that may contribute to organ failure, making elevated HNE levels a major health concern (46).

The HNE is also an important mediator of acute and chronic inflammatory response. It perpetuates the cycle of inflammation by promoting the generation of chemoattractants (IL-8, TNF- $\alpha$ ) for recruitment of more neutrophils into the tissue, with further activation and release of their granule content locally, creating a milieu with a high concentration of neutrophil elastase that might exceed the availability of endogenous elastase inhibitors (51).

This evidence of insufficient activity of endogenous inhibitors towards proteolytic activity of HNE in presence of inflammation and oxidative stress emphasizes the need for synthetic HNE inhibitors and therefore, new antiprotease treatment strategies to effectively inhibit HNE are being developed. Moreover, several studies reported that after dialysis procedures the blood levels of elastase increase (52, 53), further strengthening the need for the development of bioactive dialysis membranes that could inhibit excessive elastase and thereby, its adverse effects.

### **3.3.5. Anaemia**

Anaemia is very common in HD patients and is associated with fatigue, reduced exercise tolerance, dyspnoea, poor wellbeing, increased risk of hospitalization and elevated morbidity and mortality, related to CVD. According to KDIGO, the anaemia is diagnosed when haemoglobin (Hb) concentration is  $<13.0 \text{ g dL}^{-1}$  in males, and  $<12.0 \text{ g dL}^{-1}$  in females (54).

The anaemia of ESRD patients may arise from several different causes, namely iron deficiency, inflammation, and uremic toxins; however, the major cause is the decreased production of erythropoietin (EPO) hormone. EPO is almost exclusively produced by the

kidneys and is responsible for stimulating erythropoiesis. Due to kidney damage, EPO is not sufficiently produced to compensate the removal of senescent red blood cells (RBC) (55). The lifespan of circulating erythrocytes is shortened due to a decrease of cell deformability, which increases susceptibility of RBCs to lysis. This aberration is probably caused by the uremic toxins incorporation into membrane lipids or/and by oxidative alteration of membrane structure, as a consequence of the increase of oxidative stress (56, 57). These membrane changes lead to RBC shape perturbations that may negatively influence blood rheology (58).

The systemic inflammation presented by ESRD patients also contribute to the anaemia, namely via increased level of hepcidin, an iron-regulatory hormone. (59). The pro-inflammatory cytokine IL-6, released from activated inflammatory cells, induces hepcidin production in the liver. The increased hepcidin leads to a reduction in dietary iron absorption and to an elevated sequestration of circulating iron by macrophages. The reduced iron absorption and mobilization from iron storages results in insufficient iron availability for erythropoiesis (59, 60). Moreover, in ESRD patients an absolute iron deficiency is also common and may be due to dietary restrictions, poor intestinal absorption, gastrointestinal bleeding, blood loss due to frequent laboratory blood sampling, and blood loss in fluids and dialysis equipment (55, 61). Inflammation may also contribute to anaemia via inhibition of the proliferation and differentiation of erythroid progenitor cells by inflammatory cytokines (TNF- $\alpha$ , IL-1 and interferon- $\gamma$ ) (62, 63).

When the ESRD patients develop symptomatic anaemia, they should undergo treatment by iron supplementation and/or administration of erythropoiesis stimulating agents (ESAs), such as recombinant human EPO (rhEPO). The administration of high doses of ESAs has been associated with increased risk for CV events and therefore, the actual guidelines for treatment of anaemia with ESAs are more conservative (64). ESAs also induce proliferation of cancer cells and thus, may induce progression of malignancy, which may lead to further deterioration of renal function, and lower survival rate (65, 66). The majority of ESRD patients respond adequately to ESAs, although 5-10% of them do not respond properly to this therapy (64, 67).

### **3.3.6. Other complications**

When the kidneys are not working properly, its dysfunction may alter acid-base homeostasis, fluid and electrolyte regulation, hormone production and secretion and elimination of waste products. Altogether, these abnormalities can result in metabolic disturbances and finally, conditions such as anaemia, hypothyroidism, hypertension,

acidaemia, hyperkalaemia, protein–energy wasting, and malnutrition. Mineral and bone disorders in ESRD are characterised by abnormalities in serum concentrations of calcium, phosphorus, 1,25-dihydroxycholecalciferol, and parathyroid hormone. These patients may also present signs of peripheral nervous system and central nervous system disorders including peripheral neuropathy, restless leg syndrome, sleep disorders, and cognitive impairment (2).

Other ESRD associated complications are dyslipidaemia, malnutrition, and cachexia, which are associated to increased risk for CVD events, protein energy wasting and dietary restrictions, respectively. Metabolic acidosis is a frequent complication of kidney disease due to retention of acids, phosphates, and sulphates, and decreased generation of ammonia. Acidosis has been shown to have deleterious effects upon bone health, nutritional parameters, and protein metabolism (68). Fatigue, weakness, frailty, and decreased health-related quality of life are common but non-specific and might be caused by other comorbid disorders (6).

### **3.4. Dialysis**

Dialysis is defined as the diffusion of molecules in solution across semipermeable membrane along the concentration gradient, when the main goal of dialysis is to restore body fluid environment, that is provided by normal kidney function. This is accomplished by the exchange of waste products from the blood into dialysate fluid and by the transport of deficient solutes from dialysate into blood (69). When renal replacement by kidney transplant is not possible, dialysis is a lifesaving procedure for most ESRD patients, increasing their life expectancy for years or even decades. There are two main types of dialysis, known as haemodialysis (HD) and peritoneal dialysis (PD). The sort description and comparison of these two treatment methods are summarized in Table 4.

Table 4: Summary of characteristics of PD and HD and comparison of their risks and benefits.

	Characteristics	Advantages	Disadvantages
<b>Peritoneal dialysis</b>	<ul style="list-style-type: none"> <li>Carried out at home, using patient's peritoneal membrane</li> <li>2-3 litres of PD fluid exchanged daily every 4-6 hours or automatically overnight</li> <li>Mostly used for treatment of children</li> </ul>	<ul style="list-style-type: none"> <li>Portable equipment</li> <li>Better patient's quality of life</li> <li>Better survival during the first two years</li> <li>Similar to kidney function</li> <li>No need for vascular access</li> <li>Less CV risks</li> <li>Lower cost</li> </ul>	<ul style="list-style-type: none"> <li>Requires education of patient/family</li> <li>Possibility of excessive fluid loss/retention</li> <li>Risk of peritonitis; peritonea fibrosis and systemic infection</li> <li>Frequent weight gain</li> <li>Risk of hypotension; hernia</li> <li>Risk of abdominal bleeding; membrane failure or clogged catheter</li> </ul>
<b>Conventional haemodialysis</b>	<ul style="list-style-type: none"> <li>Carried out in hospital/HD centres</li> <li>Duration of treatment 3-5 hours 3x per week</li> </ul>	<ul style="list-style-type: none"> <li>Majority of toxins and excess fluid are removed from blood</li> <li>Possibility of home treatment</li> <li>Less patient's responsibility</li> <li>Contact with caregivers and community of patients</li> </ul>	<ul style="list-style-type: none"> <li>Requires dietary restrictions</li> <li>Risk of infection of vascular access or dialysate</li> <li>Causes low blood pressure</li> <li>High risk of CV events</li> <li>Chronic inflammation and OS</li> </ul>

PD: peritoneal dialysis; HD: haemodialysis

### **3.4.1. Peritoneal dialysis**

Peritoneal dialysis (PD) is a type of RRT by which the peritoneal membrane in patient's abdomen is used as the HD membrane, allowing the removal of uremic toxins and waste products from the body into the peritoneal cavity containing up to three litres of sterile dialysate fluid (70). The dialysate solution is composed by sodium, potassium, calcium, magnesium and chloride, osmotic agent (glucose) and buffer with low pH 5.2 (acetate, lactate, bicarbonate) to control acidosis. This dialysate fluid is introduced through a permanent catheter in the lower abdomen and removed after a specific time. The exchange of the dialysate fluid may be either at regular intervals throughout the day (after 4 - 6 hours), known as continuous ambulatory dialysis, or continuously overnight with the assistance of the automated cycler, which exchanges up to 15 liters of dialysate fluid during the night (71).

Substitution of the kidney function by PD allows ESRD patients to have a more flexible treatment schedule, as it can be carried out at any clean place. PD treatment is frequently preferred for pediatric patients, since their blood volume is smaller, and this type of dialysis avoids the technical complications associated with the vascular access used for conventional HD procedure. Besides that, due to treatment flexibility, school attendance as well as the psychological, emotional, and social development and the quality of child's family life is improved (72). In addition, less food and fluid intake restrictions are applied to patients on PD treatment, as compared to conventional HD. PD has been associated with a lower mortality rate, especially in the first three years of treatment, compared to HD, probably due to the better preservation of the residual renal function. Another benefit of this type of dialysis is related to the lower costs of the treatment (70). However, DP has been associated with some complications including peritonitis and/or sepsis, sudden death, CV events, fluid overload, malnutrition and dialysis infectivity; in the first two years about 70% of PD patients are switched to conventional HD or home HD. The main causes that determine this change are peritonitis and CV events experienced by patients (73).

### **3.4.2. Haemodialysis**

Haemodialysis is the most common type of RRT using extracorporeal removal of waste products and excessive fluids from the patient's body. The selective blood clearance is carried out by a semipermeable membrane placed in a dialyser, through which the blood is continuously driven by systems of pumps and tubes in a form of sophisticated equipment.

The first successful clinical use of an artificial kidney for treatment of renal failure was performed by the physician W.J. Kolff in 1945. He developed a dialyzer composed of few



meters of membrane made of cellophane, wound around a rotating drum (Figure 3A). This successful attempt to treat a patient with acute kidney failure confirmed the effectiveness of this therapeutic method based on the use of an artificial kidney for RRT (74).



A



B

Figure 3: Haemodialysis equipment. (A) The first model of haemodialysis device used by W.J. Kolff in 1945; (B) current haemodialysis machine. Accepted from (75) and (76), respectively.

Since then, the HD treatment has undergone significant improvements, not only in terms of the equipment design (Figure 3B), performance, and biocompatibility of the equipment, but also by improving the treatment modality. The conventional HD treatment, which used to be carried out exclusively in hospitals or specialised clinics, can be nowadays performed at home, where the patients use their own HD equipment. These patients can use the options of short daily HD treatment (6 times/week for 90-180 minutes) or the slow nocturnal HD performed during patient's sleep (6 times/week for 8-10 hours) (77).

#### 3.4.2.1. Haemodialysis system

The aim of the HD system is to deliver blood in a safe manner from the patient to the dialyzer, to efficiently remove uremic toxins and excess fluids, and to deliver the cleaned blood back to the patient. The main components of HD system (Figure 3B) are: extracorporeal circuits for blood circulation, dialyser, blood and dialysate pump, device for mixing and degassing dialysate, pump for injecting anticoagulant heparin into blood, heating system, and monitoring and safety system. A scheme of the HD circuit and blood flow direction inside the system is shown in Figure 4.

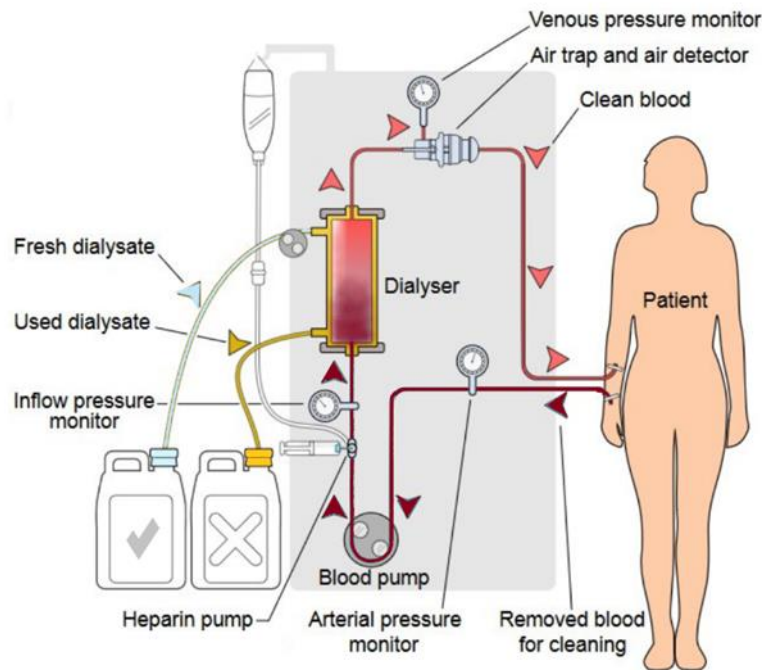


Figure 4: Scheme of haemodialysis circuit. Modified from (78).

The system of detectors, controllers and monitors allow the management of important parameters, such as blood and dialysate flow rate, dialysate composition, and circuit's pressure. Blood tubing is made of biocompatible and nontoxic material, usually PVC or silicon, which causes less blood clotting. The peristaltic pump is responsible for blood flow rate ( $Q_B$ ) in the circuit from 200 to 600 mL min<sup>-1</sup>, while the flow rate of dialysate fluid ( $Q_D$ ) is higher, from 500 to 800 mL min<sup>-1</sup>. The fluxes are in counter current, to maximize diffusive solute transfer and are usually in set ratio:  $Q_D : Q_B = 1.2 : 1.0$  (79, 80).

An inherent part of HD equipment is the dialysate system. The dialysate is a proportional mixture of ultrapure pre-heated water (35 - 42 °C) with dialysate concentrate. The dialysate composition is a key element for an effective and safe HD, since it influences the exchanges of electrolytes between blood and dialysate, restoring corporal electrolytes and acid–base equilibrium, and strongly affects intradialytic CV stability. The dialysate should normalize plasma electrolyte and mineral concentrations and ensure adequate toxins and phosphate removal (79, 81). The composition of dialysate is summarized in Table 5.

Table 5: Comparative composition of dialysis fluid and blood plasma. The arrows indicate the direction of solutes movement. Modified from (81).

Components	Effect	Dialysate fluid [mmol L <sup>-1</sup> ]	Blood plasma [mmol L <sup>-1</sup> ]
Na <sup>+</sup>	to obtain Na <sup>+</sup> zero balance and to normalize body water	135 - 145	136 - 140
K <sup>+</sup>	maintains normal cardiac and skeletal muscle function	0.0 - 4.0	← 3.5 - 5.0
Ca <sup>2+</sup>	To maintain CV stability and normal bone turnover	0.0 - 2.5	2.0 - 2.6
Mg <sup>2+</sup>	To prevent hypomagnesemia associated CV mortality	0.5 - 1.0	← 0.8 - 1.2
Cl <sup>-</sup>	control of metabolic acidosis	99 - 110	98 - 106
acetate/citrate	improves pH	2.5 - 5.0	/
bicarbonate	to maintain acid–base balance	27 - 39 →	21 - 28
glucose	to generate osmotic pressure, protect from intradialytic hypoglycaemia	0.0 - 11.1	44.4 - 66.6
pH	To minimize the risk of bicarbonate and calcium precipitates formation.	7.1 - 7.3	7.4

The main part of the HD system is the dialyser (hereinafter also referred to as dialysis membranes), which acts as an artificial kidney and replaces the vital functions of the non-functioning kidney. The membrane inside the dialyser is a key determinant of overall dialyzer function. The dialyser has a tubular shape with length of 16 – 26 cm, containing in average 7 – 17 thousand hollow-fibres that allow solutes and fluid transfer between blood and dialysate. Typical fibres have an internal diameter of 180–200 µm and a wall thickness of about 25 – 45 µm, yielding 1.0 –2.5 m<sup>2</sup> of surface area. Inside the dialyser the fibres are covered with spacer yarns, which are filaments designed to create optimal spacing between them. The bundle of hollow-fibre membranes is then encapsulated at both ends with silicone rubber and enclosed in polyurethane outer housing that forms the dialysate compartment. Before being used, the entire dialyser must be sterilized, usually by heat (steam), by

radiation ( $\beta$  or  $\gamma$  radiation) or by chemicals (ethylene oxide). The sterilization techniques by steam and radiation are more favourable, since ethylene oxide has propensity to attach to the potting material of the dialyzer and cause allergic reactions (82).

A dialyzer can be classified in one of two ways, either according to the membrane composition, especially according to the used polymer for membrane fabrication, or according to its ability to remove solutes from blood (83). Since the polymeric membrane is the essential part of the dialyzer and is responsible for blood purification, its most important characteristics that influence its performance will be described in detail in Section 3.6.

In general, the geometry of the dialyser varies according to the polymer used for membrane fabrication, intended application and mainly, according to the total volume of blood that needs to be purified, indicated by body mass index of the patient.

### 3.4.2.2. Principles of haemodialysis

As referred, the aim of HD treatment is to remove uremic toxins and extra water from ESRD patient's blood. The solute removal from bloodstream is performed by combination of three mechanisms: diffusion, convection, and adsorption. If the solute removal is carried out predominantly by convection, the RRT is referred as hemofiltration; when the solute removal is mediated through diffusion simultaneously with convection, the RRT method is commonly referred as hemodiafiltration.

The uremic toxins removed by HD can be divided into three main categories: 1) small water-soluble compounds with molecular weight (MW) < 500 Da, that can be removed by diffusion with any dialysis membrane; 2) middle-sized molecules with MW in range 500 – 15 000 Da, which can only be removed through dialyzer membranes with pores large enough (high-flux membrane); and 3) protein-bound molecules, mostly with a MW of 500 Da or larger, very difficult to remove due to their protein binding (84).

The primary mode for removal of small solutes with MW less than 500 Da (e.g., urea) by HD is diffusion, due to the concentration gradient between plasma and dialysate. This diffusive process occurs in both directions for solutes whose concentration in the dialysate is higher than internally. This solute transport across the membrane is due to concentration gradient in accordance with the Fick's 1<sup>st</sup> law of diffusion (Equation 1), where  $J$  is the flux of the solute which measures the amount of solute that will flow through the membrane area during a specific time interval;  $D$  represents diffusion coefficient [ $\text{cm}^2 \text{s}^{-1}$ ];  $A$  is the area of membrane surface;  $dc$  is the difference of solute concentration across the membrane, and  $dx$  means the thickness of the membrane.

$$J = -D \times A \times \frac{dc}{dx} \quad (\text{Equation 1})$$

The rate of diffusion depends on the solute molecular size, but thickness and porosity of the membrane also plays an important role. The rate of diffusion is greatest for small molecules and decreases logarithmically as solute size increases. The diffusion rate also decreases with increasing membrane thickness and with reducing porosity. The diffusive transport is a specific characteristic of a dialyser and is expressed by mass transfer area coefficient KoA [ $\text{mL min}^{-1}$ ], where Ko is the permeability coefficient of the membrane for the given solvent, and A the total effective surface area. KoA represents theoretical maximal clearance of the particular dialyser for a given solute, at infinite  $Q_B$  and  $Q_D$ , and this KoA value is provided by the dialyser manufacturer (85, 86). KoA is a purely diffusive parameter, therefore can be estimated for small MW solutes, but for larger solutes, such as  $\beta$ 2-microglobulin, cannot be reliably estimated as their removal is not achieved by diffusion (87).

The removal of middle-sized and large solutes through the membrane is possible by convection process. Convective transport in HD uses a pressure gradient (rather than concentration gradient) and by increasing the transmembrane pressure, the water is pushed down through the membrane according to the pressure gradient. The dissolved solvents are then passively removed across the membrane together with the water movement. For this reason, the convection clearance is sometimes referred as a solvent drag. When the convective clearance is applied, the removal of small solutes is nearly the same as with diffusion, while the clearance of middle-sized molecules and fluid removal are much higher. However, the ultrafiltration rate and thus, the solute removal, is determined by the pressure gradient across the membrane, referred as transmembrane pressure (TMP), by the hydraulic permeability, and by the pore size of the membrane (86, 88).

Adsorption also belongs between the principles of solutes removal. The adhesion of macromolecules and proteins on the membrane surface primarily depends on the pore diameter and on the hydrophilicity of the membrane material. Membranes highly adsorptive for molecules with a MW greater than  $\beta$ 2-microglobuline (11.6 kDa) can play an important role in the removal of pro-inflammatory mediators (TNF- $\alpha$ , IL-1 $\beta$ , IL-6). Unfortunately, adsorption also contributes to the removal of anti-inflammatory mediators and proteins, such as plasminogen and albumin (89). High protein adsorption on the membrane surface can reduce its diffusive and convective capacities and therefore, negatively affect the membrane permeation ability. For this reason, the membrane protein adsorption capacity should be only of moderate level, providing the ability of the membrane to bind protein-bound uremic toxins, without compromising the diffusive and convective removal capacity (90).

A priority criterion to assess the efficacy of HD treatment, is the evaluation of urea removal capacity. This is expressed as  $KtV$ , where  $K$  is the urea clearance by the dialyzer [ $\text{m}^3 \text{s}^{-1}$ ],  $t$  is the time of dialysis session [s], and  $V$  is the patient's volume distribution of urea [ $\text{m}^3$ ] (83). This measure of adequacy of dialysis is based on the National Cooperative Dialysis Study (NCDS) that examines the effects of the prescribed dialysis on the clinical outcome of the patients. Through a 12-month morbidity data, determined in four HD treatment groups, with different dialysis prescriptions, the NCDS observed that the hospitalization decreased for patients with a  $KtV > 0.9$  (91). The results of subsequent studies, suggesting that higher  $KtV$  levels are associated with lower mortality (92, 93), led to the general recommendation of the Kidney Disease Outcome Quality Initiatives, that the single  $KtV$  value for HD performed three times a week should be targeted to 1.4 (94). To achieve this  $KtV$  value, the  $Q_B$  should be between 350 - 450  $\text{mL min}^{-1}$  and treatment time in the range 3.5 - 4.5 hours, using dialyzers with a membrane surface area of approximately 1.4  $\text{m}^2$  (83, 95).

#### **3.4.2.3. Side effects of haemodialysis**

Although the HD is lifesaving method, it is also associated with acute and chronic side effects, based on its action timeframe. Both types may be either life-threatening or mild, but still will have significant contribution to worsening of patients' wellbeing and to diminishing their quality of life. Given the high complexity of the dialysis treatment and frail health conditions of the patients with ESRD, the spectrum of HD related complications is broad.

Many of these complications are associated with the rate of solute exchange, change of osmolarity and ultrafiltration rate. Significant side effects may also occur from the interaction between blood and artificial material of HD membrane or any other components of HD system. Despite the high professional training of the medical and nurse staff, some complications may arise from human error (96). The effects associated solely to the membrane will be discussed in separated sections.

#### **Acute complications**

Acute complications may occur in routine treatments and soon after HD treatment begins. Intradialytic hypotension occurs in approximately 25-50% of treated patients, and the associated ischemia may cause organ damage and increase CV risk mortality. The intradialytic hypotension may cause several symptoms, such as muscle cramps, due to decreased blood osmolarity, nausea, vomiting, dizziness, and fainting. Headache, fatigue, and anxiety are also quite common side effects of HD treatment. A severe drop in blood

pressure also increases the risk of blood clots. If blood coagulation is not properly controlled, stroke, seizures, and heart damage may occur (97, 98).

Acute complications can also arise from dialysate impurities or inadequate dialysate water treatment. Bacterial contamination of dialysate may cause pyrogenic reactions. Frequently used disinfectants may cause allergic reactions if they are not adequately rinsed out before the dialysis session, and hydrogen peroxide, chloramine and chlorine can cause haemolysis (99). Among the less frequent causes are venous air embolism, venous needle dislodgement with haemorrhage and allergic reaction to HD related medication (96).

### **Chronic complications**

Some complications persist for a long time after termination of HD procedure, mostly due to their complex and systemic effect. Electrolyte imbalance is an example of these complications and is caused by the uncontrolled removal of chemical elements, essential for body function, into the dialysate fluid (96). Other common long-lasting complications are the infections at the site of vascular access for HD procedure – central venous catheter or arteriovenous fistulas (100).

Amyloidosis is another very common complication among HD treated patients, associated predominantly with the inability of HD membrane to remove uremic toxin  $\beta$ 2-microglobulin. Deposition of amyloid mainly affects joints, generating a clinical picture of stiffness, pain and swelling of joints; causes spondyloarthropathy; carpal tunnel syndrome, and deposits beneath the skin. This makes amyloidosis a major cause of the physical disabilities that affect patients 'quality of life' (101).

Another relevant complication of HD treatment results from the chronically elevated OS (details of OS-associated complications are described in Section 3.3.2) which is more pronounced in ESRD patients on long-lasting dialysis treatment. The Increased OS in HD patients is mainly due to the repeated interaction of inflammatory blood cells with the HD membrane (which is not perfectly biocompatible), followed by an increase of free radicals production, and/or to reduced antioxidants, required to counterbalance the overproduction of ROS (42).

As previously stated, the bio-incompatibility is a reaction that results from the direct contact of blood with and artificial material of HD membranes. The blood interaction with HD membrane results in activation of circulating leukocytes with release of their activation products. The activation of complement system by the alternative pathway also contributes to the enhanced pro-inflammatory reaction, with further release of cytokines and other activation products. It was reported that the level of ROS was up to 14 times higher after a single HD treatment, when compared to the plasma level before the procedure (102). The

activation and degranulation of leukocytes results also in the release of HNE into the extracellular matrix (the complications associated with the increase of HNE levels were previously detailed in the Section 3.3.4).

It is important to highlight, that elevated OS together with chronic inflammation contribute to increase the risk for CV events and are therefore, considered as independent predictors of morbidity and mortality in ESRD patients, particularly enhanced in patients on regular HD treatment (103-105).

To decrease this patient's burden, the improvement of HD membrane biocompatibility, reducing ROS generation and leukocyte activation after contact of blood with membrane surface, is still a topic of current interest. The research conducted to improve this unfavourable situation for HD patients is trying to come up with new approaches to meliorate the outcome of these patients.

### **3.5. Targeting the improvement of complications associated to ESRD patients under HD treatment**

Due to the strong interconnection between renal damage/reduced glomerular filtration rate – uraemia – OS – inflammation – CV risk events, the amelioration of one factor in this “chain” will be reflected in the others. Several interventions have been proposed to target the improvement in ESRD associated complications, reaching from lifestyle modifications, through pharmacological interventions, to optimization of dialysis. Therefore, the following Sections will focus on improving OS by effects of antioxidants and on chronic inflammation via HNE inhibition.

#### **3.5.1. OS and antioxidant defence systems**

As already mentioned, ROS production is a physiological process that triggers a set of defence systems, to protect the body against the adverse effects of OS. There are two main defence systems, including enzymatic and non-enzymatic antioxidants, but besides these two, there are also universal unspecific systems to prevent the generation of free radicals, such as metal chelation by metal-binding proteins (28).

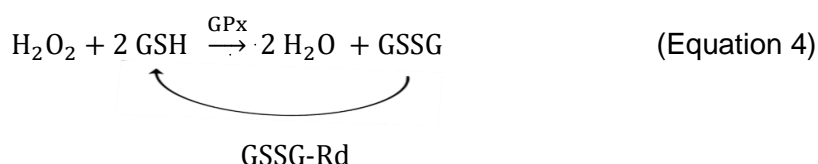
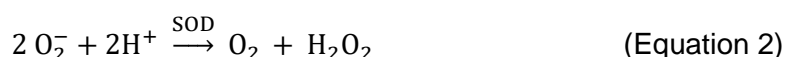
The power of the antioxidant defence system is usually evaluated by total antioxidant capacity (TAC) test, which measures the amount of free radicals scavenged by a test solution. The assays measuring TAC can be either direct, based on the ability of the solution to inhibit the oxidation of a substance, or indirect assays, which are based on determination of the ability of a sample to reduce a metal complex. Among the direct methods, Trolox



equivalent antioxidant capacity is one of them; in what concerns to indirect assays, the ferric reducing ability of plasma (FRAP), and the cupric reducing antioxidant capacity are described. The mentioned methods are based on spectrophotometric measurement, that makes them simple and low-cost procedures. However, these methods present some limitations. One of them, the TAC assay can provide limited information about the antioxidant status since they do not measure all antioxidant components. Another drawback of these assays is their inability to evaluate the role of enzymatic antioxidants (106). The ideal approach would be a determination of plasma levels of all individual antioxidants and the erythrocyte content of enzymatic antioxidants. However, this approach implies several time-consuming assays.

### 3.5.1.1. Enzymatic antioxidant system

The enzymatic antioxidant system is present in all cells, which makes it powerful primary defence system against reactive species and OS. These enzymes are classified into three main groups: superoxide dismutase (SOD), catalase (CAT) and glutathione peroxidase (GPx). SOD accelerates the dismutation rate of superoxide anion into molecular oxygen and hydrogen peroxide (Equation 2), as the first line of enzymatic antioxidant defence (30, 107). CAT is one of the most efficient redox enzymes, present in all cells, responsible for reduction of hydrogen peroxide to water and oxygen (Equation 3). The main function of GPx is to reduce lipid hydroperoxides to their corresponding alcohols and to protect cells and tissues from oxidative damage by removing hydrogen peroxide with the oxidization of glutathione (GSH). Oxidized glutathione disulphide (GSSG) is converted back to its reduced form by glutathione reductase (GSSG-Rd) (Equation 4) (108).



To overcome the harmful effect of the free radicals and thereby to contribute to reduce the high mortality rate of ESRD patients, exogenous antioxidants are commonly administered to reduce OS and/or to supplement their loss (109). Antioxidants such as vitamin C and E, lipoic acid, N-acetylcysteine (NAC) and GSH have been used as oral

supplements in order to correct the progressive decrease of blood antioxidants and to alleviate the exacerbated generation of ROS in HD patients (110).

### **3.5.1.2. Antioxidants**

#### **Glutathione**

GSH is the major thiol compound participating in cellular redox reactions. Under the OS, GSH is oxidized to GSSG and this oxidized form is regenerated by GSSG-Rd (Equation 4). As an enzymatic antioxidant, GSH is capable to scavenge  $\text{H}_2\text{O}_2$ ,  $\text{OH}^-$  and chlorinate oxidants (27). Besides its antioxidant activity, glutathione has many physiological, including detoxification of xenobiotics, and regulation of immune response (111).

#### **N-acetylcysteine**

NAC is another well-known thiol free radical scavenger that induce glutathione production by replenishing glutathione stores. NAC exerts great anti-inflammatory activity and is widely used as a pharmacologic antioxidant (112). Oral administration of NAC ( $\geq 600$  mg per day) decreased circulating levels of renal injury and OS markers (ADMA, MDA) (113). NAC supplementation was also associated with a significant improvement in GPx activity in RBCs and significant increase in serum TAC levels (114). The administration of higher daily doses successfully suppressed chronic inflammation, and OS status in HD treated patients. Moreover, NAC has demonstrated protective effect against nephropathy, by suppression of the OS-derived injury of renal tubular cells (115). Overall, it was shown, that oral or intravenous administration of antioxidant NAC has positive therapeutic effect and can significantly reduce dialysis-induced OS (103).

#### **Vitamin E ( $\alpha$ -tocopherol)**

Vitamin E is a group of eight liposoluble compounds which can be divided into two classes, called tocopherols and tocotrienols, with different biological effect. The most potent compound is  $\alpha$ -tocopherol ( $\alpha$ -TCP) (Figure 5). The other isoforms  $\beta$ -,  $\gamma$ -,  $\delta$ -tocopherol present lower biological activity, when compared to  $\alpha$  isoform [132]. Besides that, it is the only form of vitamin E that is abundantly found in a diet (116). The chiral molecule of  $\alpha$ -TCP has eight stereoisomers, all of them have equal antioxidant activities, but only those in the 2R-configuration have high biologic activity (117).

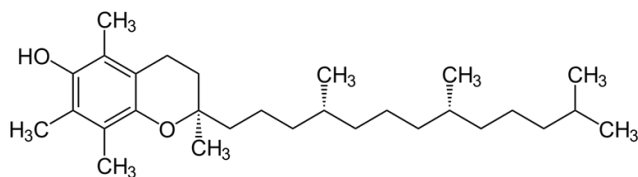
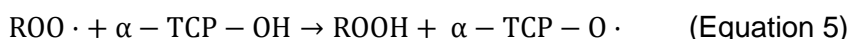


Figure 5: Molecular structure of  $\alpha$ -tocopherol.

The most important biological function of  $\alpha$ -TCP is its antioxidant activity. Its antioxidant function is strongly related to the reactive peroxyl radical scavenging, that terminates chain reactions of oxidation of polyunsaturated fatty acids, and thereby preserves the stability of biological membranes and protects them from ROS induced injury. In the presence of ROS, lipid hydroperoxides (ROOH) are oxidized to peroxyl radicals (ROO $\cdot$ ) giving rise to tocopheroxyl radical ( $\alpha$ -TCP-O $\cdot$ ) (Equation 5). The advantageous effect of the  $\alpha$ -TCP is that ROO $\cdot$  react much faster with it than with polyunsaturated fatty acids. In this way,  $\alpha$ -TCP acts as a chain-breaking antioxidant, preventing the further auto-oxidation of polyunsaturated fatty acids in the biological membranes or lipoproteins (118).



$\alpha$ -TCP is the most powerful antioxidant in biological membranes of white blood cells and RBC, where bonds tightly in membrane lipoproteins and protects them against oxidation (110, 116). Oral administration of 600 mg  $\alpha$ -TCP per day significantly improved anaemia and led to increased  $\alpha$ -TCP levels in plasma and in RBC (119). Significant reduction of OS markers plasma levels, in association with increased plasma levels of GSH, GPx and SOD, were observed after oral supplementation with  $\alpha$ -TCP doses in range 200 – 800 mg per day (120). Most of the carried-out studies with  $\alpha$ -TCP supplementation show a decrease in oxidative stress, reduction of pro-inflammatory cytokines circulating level and therefore, may have a beneficial effect on CV events. Moreover,  $\alpha$ -TCP may exert an antiatherogenic effect, since it reduces the oxidation of LDL (121). One clinical outcome trial with 196 ESRD patients found that  $\alpha$ -TCP administration was associated with reduced risk of the CV events (122)

However, some studies showed that the above mentioned beneficial effect of antioxidant  $\alpha$ -TCP is dose dependent, and it seems that in excessive doses may act as pro-oxidant (123, 124).

## Vitamin C (ascorbic acid)

Vitamin C, also known as ascorbic acid, is a water-soluble vitamin, required for many biosynthetic pathways. During HD therapy, a significant amount of vitamin C is lost from blood into dialysate. Vitamin C has ability to protect lipids against peroxidation by acting as a scavenger of ROS and by reduction of lipid hydroperoxyl radicals via the  $\alpha$ -TCP redox cycle. The tocopheroxyl radical reacts with vitamin C or other hydrogen donors (e.g. glutathione) and  $\alpha$ -TCP returns to its reduced state (Equation 6) (118).



Since HD patients have a high vitamin C deficit, its supplementation might help them reducing OS. Several studies have showed positive outcome in the decrease of OS markers after administration of water-soluble antioxidant vitamin C. Daily oral administration of this vitamin (250 mg) decreased significantly the plasma OS biomarkers among HD treated patients, while only a single high dose of vitamin C (2 000 mg) successfully reduced OS markers during the HD procedure (125, 126).

Due to the interaction of vitamin C and  $\alpha$ -TCP in “vitamin E recycling” effect, the oral supplementation of combination of these two antioxidants can lead to decreased OS, thus providing a useful therapeutic option (127)

## $\alpha$ -Lipoic acid

$\alpha$ -Lipoic acid (ALA) is a naturally occurring fatty acid that can be synthesized by humans; in the body ALA functions as a cofactor in several mitochondrial enzymatic complexes involved in cells energy metabolism. ALA (Figure 6) exists as two enantiomers: (R)-isomer, which is biologically active, and (S)-isomer. Commercially produced ALA is, usually, a racemic mixture of R- and S-form. ALA is soluble in both water and lipids and is, therefore, widely distributed in cellular membranes and also in cytosol and extracellular matrix (128).

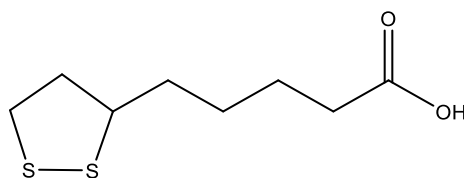


Figure 6: Molecular structure of  $\alpha$ -lipoic acid.

Both forms of ALA, the oxidized form (containing disulphide) and the reduced form dihydro-lipoic acid (DHLA) (containing dithiol) show antioxidant properties. The mechanism

of ALA reduction is highly tissue specific when substantial part of the ALA is converted to DHLA by lipoamide hydrogenase. These two forms (ALA and DHLA) create a potent redox couple, able to regenerate several antioxidants (GSH, vitamins E and C), since DHLA can be, by quenching the free radicals, recycled to oxidized ALA form (128). The pathway of this regeneration process is schematically shown in Figure 7. ALA and DHLA are able to scavenge hydroxyl radicals, hypochlorous acid and singlet oxygen, but seem ineffective against hydrogen peroxide. ALA is also able to chelate divalent metal ions and forms stable complexes (129).

ALA is a natural inhibitor of cellular membrane oxidation by directly scavenging ROS. Moreover, it is involved in lipid and glucose metabolism and inhibits vascular calcification (129). Due to these great OS protective properties, ALA has been studied as a therapeutic substance for tissue injury caused by ROS, as in the case of patients with ESRD undergoing HD treatment. Several studies were carried out to test the effect of ALA supplementation (600 mg per day) on OS, inflammation, and erythropoiesis, in HD patients. The results showed that although ALA intake caused a significant decrease in CRP serum levels, there was no effect on TAC and OS biomarkers concentrations (130). A study with HD patients treated with rhEPO did not show improvements in OS and inflammation biomarkers after oral administration of the dose above described; however, a significant reduction of rhEPO doses was observed (131). Combined daily administration of ALA (600 mg) and vitamin E (360 mg) led to the improvement of nutritional and inflammatory status, but, as in previous studies, no effect on lipid peroxidation status was observed (132).

Although the administration of the ALA/ $\alpha$ -TCP mixture has not shown protection against tissue damage related to oxidation, its administration has been well tolerated by patients. Since these antioxidants are inexpensive, their administration can be recommended to patients suffering from diseases associated with OS complications, such as diabetes, hypertension, and cardiac ischemia (133).

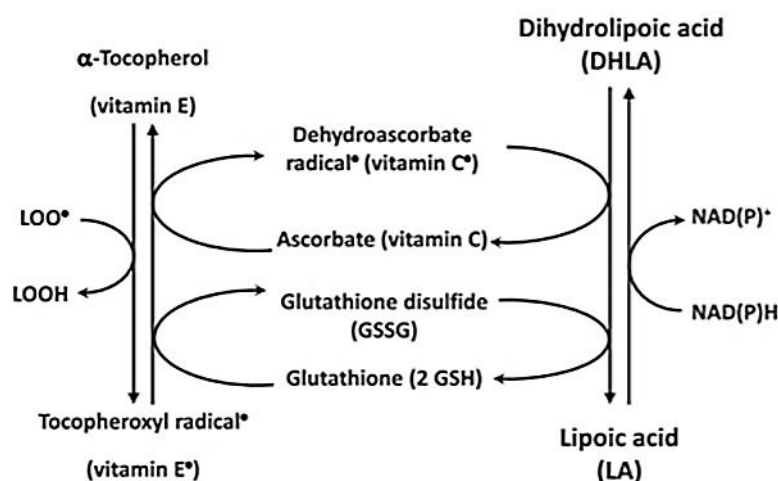


Figure 7: Scheme of  $\alpha$ -lipoic acid and dihydrolipoic acid pathway of regenerating endogenous antioxidants such as vitamins C,  $\alpha$ -tocopherol, and glutathione. Modified from (128).

*LOO•*: peroxyl radical; *LOOH*: lipid hydroperoxides; *NAD(P)•*: nicotinamide adenine dinucleotide (phosphate) radical; *NAD(P)H*: Nicotinamide adenine dinucleotide phosphate

### 3.5.2. Inflammation: inhibitors of human neutrophil elastase

#### Endogenous HNE inhibitors

As already noticed above, the proteolytic activity of HNE is regulated by endogenous protease inhibitors, frequently referred as serpins (abbreviation from serine protease inhibitors), which play an important role in the regulation of the immune response. These are present in body fluids and can protect against excessive proteolysis by neutrophil elastase in both manners, in circulation and locally. The inhibitor inactivates HNE by mimicking the substrate sequence of amino acids recognized at the active site of the proteinase, to facilitate an initial interaction with elastase. The second step in inactivation is the formation of a tight complex, which is then rapidly cleared from circulation by endocytosis (50, 134).

These endogenous inhibitors include  $\alpha_1$  – protease inhibitor ( $\alpha_1$ PI), also known as  $\alpha_1$  – antitrypsin (AAT),  $\alpha_2$  – macroglobulin ( $\alpha_2$ M), secretory leukocyte protease inhibitor (SLPI), elafin and monocyte neutrophil elastase inhibitor, known as SerpinB1. They inhibit the neutrophil elastase activity by creating complexes;  $\alpha_1$ PI and SLPI form complexes with neutrophil elastase in molar ratio 1:1, and with  $\alpha_2$ M at 1:2 ratio.

The  $\alpha_1$ PI (55 kDa) is a major endogenous elastase inhibitor, which accounts for approximately 92% of all elastase inhibition.  $\alpha_1$ PI is produced in liver and circulates in plasma in high concentration ( $54 \mu\text{mol L}^{-1}$ ) (135). The inhibition of neutrophil elastase by  $\alpha_1$ PI is irreversible; the inhibitor, through its catalytic site, forms a stable complex with the

enzyme (Figure 8). The  $\alpha_2M$  in a large protein (725 kDa), which stereochemically entraps elastase inside its structure, and thereby restrict the access to its substrate (136). Due to this unspecific way of inhibition  $\alpha_2M$  inactivates a large variety of proteinases. SLPI and elafin are produced at the sites of inflammation, as a response to inflammatory stimuli, such as neutrophil elastase and TNF- $\alpha$ . SLPI is a smaller protease inhibitor (10.5 kDa), localized in bronchial secretion. SerpinB1 is an elastase inhibitor produced by neutrophils and macrophages and is not secreted into the extracellular space but neutralizes the elastase proteolytic activity inside the cell cytoplasm (137).

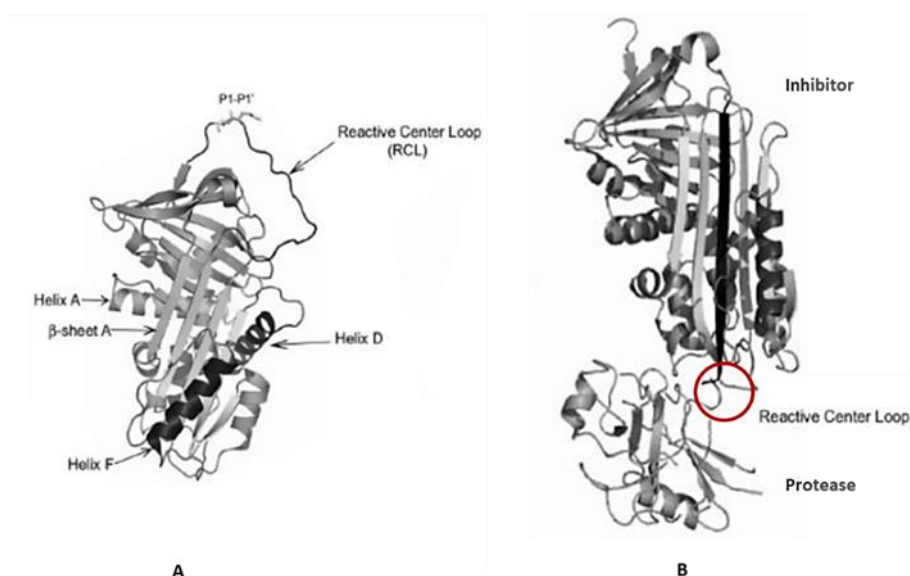


Figure 8: Human neutrophil elastase inhibitor structure. (A) Structure of the inhibitor  $\alpha_1$  – protease inhibitor. The P1 and P1' sites of reactive centre loop points out the location of the peptide bound cleaved by the HNE before inhibition. (B) Mechanism of the serine protease. Modified from (138).

## Exogenous and therapeutic HNE inhibitors

As already noticed, under the condition of chronic inflammation commonly presented by ESRD patients treated with HD, the amount of released elastase from activated neutrophils may overwhelm the inhibitory capacity of the endogenous inhibitors. To prevent the excessive proteolytic activity, further worsening renal damage and amplifying the immune reaction, complementary inhibitors have been administrated to ESRD patients as therapeutic agents. This treatment strategy may involve isolated natural or synthetic inhibitors (43, 139).

To substitute efficiently the endogenous inhibitors, the ideal therapeutic HNE inhibitors should be resistant to oxidation, to proteolysis and to *in vivo* degradation, to maintain their activity for the longer time period. They should have small size, to promote a better access to HNE when it is bound to extracellular matrices and to molecular or cellular components (140).

The HNE inhibitors used in clinical practice are classified into five groups. The 1<sup>st</sup> generation of inhibitors are of biological origin and some present low stability. This group includes  $\alpha_1$ PI that is isolated from human plasma, purified and lyophilized for the intravenous administration (commercial name Zemaira<sup>®</sup>); and, elafin (Tiprelestat<sup>®</sup>) (43). The 2<sup>nd</sup> generation inhibitors use a small molecule, forming an irreversible complex; these inhibitors are able to inhibit HNE bound to the neutrophil membrane (141). This group of 2<sup>nd</sup> generation inhibitors includes compounds known as ONO-6818 (Freselestat) (142) and ONO-5046, also known as Sivelestat. Its sodium hydrate is until now the only clinically registered synthetic HNE inhibitor (Elaspol<sup>®</sup>), which is used to treat pneumonia and acute lung injury. However, because its administration is exclusively intravenous, and due to poor pharmacokinetics and low specificity, this inhibitor can potentiate several adverse effects and, therefore, its use is limited (143, 144). The 3<sup>rd</sup> and 4<sup>th</sup> generation inhibitors are small molecules originated from pyridine structure, causing reversible HNE inhibition. To date, only two optimized, potent and orally bioavailable inhibitors have been clinically tested: AZD9668 (Alvelestat) and BAY-678 (145, 146). The best-in-class 5<sup>th</sup> generation of HNE inhibitors includes compounds that are very selective towards HNE and with very good potency (picomolar concentration) (141). The inhibitor BAY 85-8501 showed excellent potency of inhibition, already comparable to the endogenous inhibitors. The classification of the inhibitors and their action are summarized in Table 6.

The inhibitors with  $\beta$ -lactam structure are well-known acylating agents of serine proteases. The first irreversible inhibitors of HNE based on the  $\beta$ -lactam scaffold were the cephalosporin sulfones derivatives. Further simplification of the  $\beta$ -lactam template led to the development of azetidine-2-ones, potent, orally available, and a more stable inhibitor of HNE. The 4-oxo- $\beta$ -lactams were found to be time dependent inhibitors, which inhibit HNE in irreversible manner and have been proposed as potent non-competitive inhibitors, with very low half maximal inhibitory concentration ( $IC_{50}$ ). In order to obtain additional improvement of the inhibitory function of these inhibitors with  $\beta$ -lactam motif, the strategy is to enhance the rate of acylation of the catalytic serine residue and thereby improve inhibitory properties (147, 148).

Natural compounds are a potential source of HNE inhibitors, and some of them were already reported to inhibit HNE activity *in vitro* (149). Phenolic compounds, such as flavonoids, tannins and further cinnamic and caffeic acid derivatives have been reported as direct HNE inhibitors. Unfortunately, flavonoids are highly metabolized during oral application, which decreases their potency to micromolar concentrations (150). Terpenoids (151), long chain fatty acids (152), coumarins (153) and many other natural compounds were also found to inactivate HNE (154).



Besides all above mentioned benefits of treatment with exogenous HNE inhibitors, there is no sound guidance to the degree of elastase that has to be inhibited, in order to show beneficial clinical effects of inhibitors administration. In general, the aim might be a 50–90% inhibition range of elastase to reach (presumably) beneficial clinical effects without compromising the innate immune response function of the patient (141).

*Table 6 : Exogenous therapeutic inhibitors of human neutrophil elastase.*

<b>Inhibitor</b>	<b>Classification</b>	<b>Action</b>
Sivelestat	2 <sup>nd</sup> generation	Inhibition of released and membrane bound HNE
Freselestat	2 <sup>nd</sup> generation	Inhibition of released and membrane bound HNE
Alvestat	3 <sup>rd</sup> generation	Selective reversible inhibition of HNE
BAY-678	4 <sup>th</sup> generation	Selective reversible inhibition of HNE
BAY-85-8501	5 <sup>th</sup> generation	Improved potency and inhibitory capacity for HNE reversible inhibition
4-oxo- $\beta$ -lactams	5 <sup>th</sup> generation	Selective irreversible HNE inhibition

*HNE: human neutrophil elastase*

### **3.5.3. Future trends in haemodialysis**

Other trends in HD treatment are heading towards improvement of patients' quality of life. Since the patients usually undergo the treatment, on average three times per week, their regular personal and professional activities are entirely adapted to the treatment, and some ordinary activities, such as travelling, becomes very difficult. For that reason, the innovations of current HD machines are orientated to miniaturization, portability, flexibility, nanofabrication, microfluidics, and wearable technology. The possibility of distance treatment also requires developments in the area of long-distance patients monitoring and device control, data transfer and communication with professional staff (155).

Currently, an automated wearable artificial kidney is tested in aim to change dialysis treatment from intermittent to continuous, by using small portable machines that can be worn throughout the day. Wearable devices can bring great options for patients who work or wish to travel. The automated wearable artificial kidney is a battery-operated device,

weighing only 2 kg and requires approximately 2 L of dialysate per treatment. It contains cleaning cartridges with series of layers to process fluid. The single layers have different functions and subsequent positions in the blood clearance process. Nevertheless, the drawback of such a small device is the frequent exchange of cleaning cartridges, every 7 hours (156).

Another area of innovation is orientated to the development of bio-hybrid devices, combining microchip filters and active cells, which are powered by the heart of the patient. The goal of using this bio-hybrid device is to use the cells to imitate natural everyday activity of the kidney, such as clearance of waste products, salt, and water, to provide more complete renal function replacement, and to keep a patient off dialysis (157).

The current research is also orientated towards the development of HD membranes from environmentally friendly materials, to reduce disposal impact of the discardable dialysers on the environment (158).

### **3.6. Haemodialysis membranes**

In the HD system the membrane, that acts as a semipermeable barrier separating blood from dialysate, plays an essential role. The first membrane representing an artificial kidney was introduced in 1944 in Nederland, but it took almost two decades until the procedure could be used for clinical therapy (159).

To fulfill the requirements for efficient and safe HD, membranes with very specific characterizations have been developed. The permeability and biocompatibility are the key elements of the HD membranes. To ensure the effective HD treatment, the membranes should have the following characteristics: an excellent biocompatibility, an appropriate ultrafiltration rate, and an effective clearance of target solutes with sharp molecular weight cut-off (MWCO) (160).

As already mentioned, the commercial membranes currently used have a tubular shape. The internal part of the hollow-fibre is the compartment that, due to its high surface area, allows blood clearance with low resistance. Adjustments in the membrane fibre geometry, by increasing the internal filtration, can improve the clearance of the middle molecules. According to the characteristics mentioned above, dialysis membranes can have different classifications. Section 3.7.1.1 discusses in detail the different types of membranes, according to the polymer used in their preparation.

### 3.6.1. Membrane characteristics for the HD processes

The membrane acts as renal glomerulus and every good membrane should have the ability to remove urea molecules of about 60 Da but should concurrently retain protein molecules like albumin with a MW of 66 kDa. For achieving this property, the mean pore size of the membrane is an important characteristic, which should be considered. Based on the solute removal characteristics, the membranes are commonly classified as low-efficiency or high-efficiency according its ability to remove urea. High-efficiency membranes have large surface area and very effective clearance of urea, which can be further improved by increasing the fluxes ( $Q_B$  and  $Q_D$ ).

Based on the pore size, the dialysis membrane can be divided into two types: low-flux (with small average pore size) and high-flux (with large average pore size). In comparison to low-flux, high-flux membranes have good removal characteristics for middle size uremic toxins, mainly  $\beta$ 2-microglobuline (83). The membranes that allows  $\beta$ 2-microglobulin clearance  $<10 \text{ mL min}^{-1}$  are defined as low-flux, while the membranes with clearance for the same solute  $>20 \text{ mL min}^{-1}$  are defined as high-flux (83). Low-flux membranes are characterized by high diffusive permeability, where small solutes move easily across them as a result of their concentration gradient. Because the low-flux membranes present poor water flow across the membrane, the transport of medium-sized and large solutes by convective transport is minor; thus, the reduction of these molecules is only negligible.

Due to the great efficiency of high-flux membranes to remove  $\beta$ 2-microglobulin from the blood circulation, this kind of membranes are nowadays widely used, and their application for HD treatment is recommended, in order to delay long-term complications of haemodialysis therapy. The use of high-flux membranes is usually also associated with removal of pro-inflammatory cytokines. The clearance of  $\beta$ 2-microglobulin reduces the probability of the amyloidosis development. Furthermore, some studies demonstrated, that patients treated with high-flux dialysers showed improved survival rate (161, 162).

The second generation of high-flux membranes (high MWCO or super-flux membranes), introduced in clinical use, are highly permeable and are characterized by MWCO close to 65 kDa. The use of these membranes enables to increase the clearance of cytokines, free light chains, and  $\beta$ 2-microglobulin. However, the non-uniformity of the pore size of these highly permeable membranes leads to increased loss of albumin and non-selective removal of important vitamins, trace elements, and hormones, which may have a negative impact in longer treatments with these membranes. Therefore, the clinical use for the super-flux dialyzers may be limited to acute short-term use (163, 164). Moreover, the use of high-flux membrane has some disadvantages, mainly due to large pore size. The

endotoxins, produced by bacterial in dialysate, can cross the HD membrane into the blood circulation. The usage of dialyser with this type of membranes requires application of ultrafiltration monitors to HD machines, otherwise the patient would suffer from large water loss by the ultrafiltration process during the treatment.

The most relevant characteristics for the membranes used in HD treatments are defined below.

### Water permeability

The membrane flow can also be related to the ultrafiltration coefficient ( $K_{UF}$ ) value, which is defined through the water permeability and as a rate at which water crosses the membrane at a given TMP.  $K_{UF}$  is usually determined according to Equation 7, where  $Q_{UF}$  is the ultrafiltration flow [ $\text{mL h}^{-1}$ ] and TMP represents the transmembrane pressure [ $\text{mmHg}$ ]:

$$K_{UF} = \frac{Q_{UF}}{TMP} \text{ [mL h}^{-1} \text{ mmHg}^{-1}] \quad (\text{Equation 7})$$

### Diffusion

Diffusion is another important feature of the membrane as it represents one of the main mechanisms of mass transfer during the HD process. It can be characterized by solute flux ( $\phi$ ), which is defined as the mass removal rate per unit of membrane area. The solute flux can be expressed by Equation 8, where  $\lambda$  is the solute partition coefficient;  $D$  is solute diffusivity;  $\rho$  represents membrane porosity as a function of pore size and pore number;  $\Delta c$  is transmembrane concentration gradient, and  $t$  represents membrane thickness (165).

$$\phi = \lambda D \rho \Delta c / t \quad (\text{Equation 8})$$

The diffusive transport is more favourable to small solutes, not only because of the inverse relationship between solute MW and diffusivity, but also because of the greater access of small solutes to the membrane porous structure. For all types of HD membrane, the small solutes (urea and creatinine) have free access into pores, therefore their partition coefficient is equal to 1. In these cases, the solutes transport depends on the porosity of the membrane and the pore radius. From the Equation 8 can be deduced that the diffusive transport is greater with smaller membrane thickness (165).

## Solute rejection

Solute retention is one of the most important membrane-performance indicators. The solute retention, referred as rejection ( $R$ ), is defined as the concentration difference across the membrane, divided by the solute concentration on the feed (donor) solution (Figure 9).

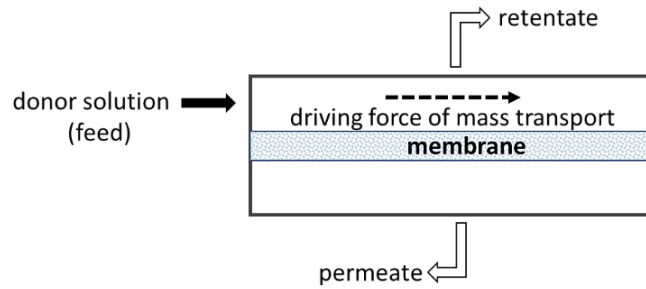


Figure 9: Schematic membrane module representing solute permeating across the membrane.

The retention of solute can be expressed according Equation 9, where  $c_1$  represents concentration of the solute of interest in the feed solution and  $c_2$  is the concentration of the solute in the permeate on the opposite side of the membrane (166).

$$R = \frac{c_1 - c_2}{c_1} = 1 - \frac{c_2}{c_1} \quad (\text{Equation 9})$$

Many factors contribute to membrane solute rejection, however solute sieving is one of the major mechanisms of rejection; solutes larger than the membrane MWCO are rejected. Rejection is controlled by several factors: molecular size, shape, and flexibility; solute diffusional in the feed solution; membrane pores; electrostatic and van der Waals forces between membrane and solutes (167). The rejection can have values within the range 0 – 1, wherein 1 signifies 100% rejection of the solute and the membrane is practically impermeable for this solute size and cannot be found in the permeate solution. Theoretically, all molecules larger than the MWCO of a membrane should be rejected.

## Molecular weight cut-off

MWCO is defined as a MW (in Da) limit, beyond which the molecules cannot pass through the membrane, and this solute is from minimum of 90% retained (commonly referred as rejected) by the membrane. Theoretically, all molecules larger than the given MWCO of a membrane, should be rejected. However, the MWCO is seldomly “sharp”, even for the large molecules (166). The MWCO of commonly used membranes may range from 3 000 Da to more than 15 000 Da. The new generation of super high-flux membranes have

cut-offs significantly higher, closer to 65 000 Da, which is almost identical to healthy kidney (168).

The MWCO can be calculate as diffusion of solvent through the membrane, according Equation 10, where  $A_w$  is solvent permeability, which it's a constant given by a membrane property;  $\Delta P$  is hydrostatic pressure difference between both sides of the membrane.

$$N_w = A_w(\Delta P) \quad (\text{Equation 10})$$

## Sieving coefficient

The ability of a solute to pass through the pores of a membrane is characterized as the sieving coefficient for a given solute. A solute with a sieving coefficient of 1.0 passes freely through the membrane, while the membrane is impermeable to a solute with a sieving coefficient of 0. The examples of sieving coefficients for low/high-flux membranes are shown in Figure 10. As can be seen from the image, high-flux membranes have sieving coefficients for albumin very close to healthy kidney.

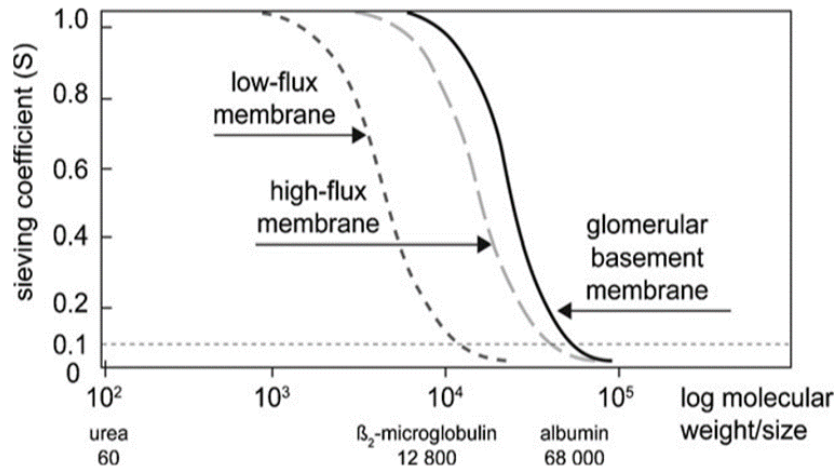


Figure 10: Comparison of sieving curves of low-flux, high-flux membrane with glomerular basement membrane. The molecular weight of the solutes is shown in Da. Accepted from (86).

Convection provides better removal of large solutes than diffusion because the decrease in sieving coefficient with increasing solute size is less marked than the decrease in diffusion coefficient. The sieving coefficient is determined by the size of the pores in the membrane and is characterized by MWCO. Dialyzer manufacturers usually provide the information about the sieving coefficients of albumin,  $\beta_2$ -microglobulin, myoglobin, and lysozyme (86). It can be calculated according Equation 11, where  $c_r$  is concentration of

solute in dialysate (receiving solution) and  $c_d$  is concentration of solute in feed (donor solution).

$$S = c_r / c_d \quad \text{(Equation 11)}$$

### **3.7. Membranes composition**

Morphological characteristics, mechanical properties, biocompatibility, and functionality of the membranes depend, especially, on the casting solution composition, the type of polymer and additive and their ratio. Therefore, choosing the appropriate polymer, solvent and the hydrophilic/lipophilic characteristics of the additive is a crucial moment in membrane development; its composition must be optimized in order to obtain a membrane with the desirable characteristics, such as excellent biocompatibility and adequate permeability.

#### **3.7.1. Main polymer**

Since the polymer is the component forming the membrane structure, its concentration in the casting solution will influence the final membrane morphology, porosity and, therefore, the water flux. Typically, the higher the concentration of the polymer, the lower the porosity of the membrane. This implies that increasing the polymer concentration will increase the probability of instantaneous demixing. When the polymer concentration exceeds certain values, there is not enough solvent and nonsolvent exchange in the casted polymer solution to form the pores during the phase separation and solidification process and, therefore, the membrane permeability is diminished. The amount of main polymer in the polymeric solution is usually in the range from 10 to 20 wt% (169).

Besides the membrane structure, the type of used main polymer influences the overall biocompatibility. The requirement of high biocompatibility during HD treatment has led to a continuous development of polymeric material for the membrane fabrication. There is a demand for membranes with a high degree of biocompatibility that create low impact on inflammatory cell activation/oxidative stress and provide good separation of biomolecules. These membranes should have a great capacity for rejection of albumin and the ability to remove medium-sized uremic toxins, mainly  $\beta_2$ -microglobulin.

This means that the type of polymer, as well as its concentration, must be taken in account and must be optimized and then selected, based on the intended membrane structure and according to the intended application.

### 3.7.1.1. Types of polymers for membrane preparation

The material used for membrane fabrication also underwent remarkable evolution, in order to improve the key characteristics: selective permeability and biocompatibility. Below, the characteristics of those that have been usually referred in the literature, are described in detail.

#### Cellulose based membranes

The first HD membranes, with the commercial name Cuprophane®, were made of cuprammonium rayon based on cotton derived polymer cellulose, dissolved in cuprammonium solution followed by other cellulosic membranes, commercially known as Bemberg®. These firstly developed membranes were commonly called regenerated cellulosic membranes since they were cast from cellulose or cotton fibres. These membranes had a homogeneous, symmetric structure and their advantage was to have thin-walled structure, with membrane thickness ranging, generally, from 5 to 15 µm. Other advantage was the good removal of small solutes from blood (170). However, the cellulosic membranes removal ability of middle-sized solutes was inadequate, resulting in accumulation of several uremic toxins, including  $\beta$ 2-microglobuline, in the blood stream (171). Besides this ineffective toxins removal, cellulosic membrane presented very low biocompatibility, which contributed to poor outcomes of patients treated with Cuprophane®. The reduced biocompatibility of cellulosic membranes was related to the presence of free hydroxyl groups in its polymeric structure, which causes the complement activation via the alternative pathway (172, 173), and the activation of leukocytes, followed by the release of pro-inflammatory cytokines (174). Therefore, the use of this type of membrane was discontinued (175, 176).

Membrane, commercially known as Hemophane®, is a type of improved cellulosic membrane. The hydroxyl groups of the membrane surface are modified with positively charged diethylaminomethyl bulky groups, which sterically inhibit the contact between the membrane and the blood cells, improving, therefore, the membrane biocompatibility (165, 177). Unfortunately, Hemophane® had ability to adsorb negatively charged heparin, which led to induction to blood coagulation and, therefore, its use was discontinued.

The poor outcomes observed by kidney disease patients treated by Cuprophane® and Hemophane® membranes triggered further research aimed to improvement of biocompatibility of membrane material (165, 178). Cellulose membranes were improved through the chemical masking of the hydroxyl groups by the acetate groups. Among them are included cellulose acetate, cellulose diacetate (CDA), and cellulose triacetate (CTA)



membranes, in accordance with the number of acetate groups introduced in the individual monomeric cellulose units. Due to these chemical modifications, up to 80% of free hydroxyl groups presented on the membrane surface, able to activate complement cascade, was eliminated (165). The CDA and CTA membranes remain in widespread clinical use. CTA shows low rate of complement activation and increased solute permeability, especially for  $\beta$ 2-microglobuline (179). The replacement of hydroxyl groups by acetates leads to an increase in membrane pore size and has the most pronounced impact on water and small solute molecule permeability (165).

### **Synthetic membranes**

To improve solutes permeability, as well as biocompatibility, many synthetic polymeric membranes have been introduced to the market and they are currently the most prevalent. The first synthetic membrane was fabricated in 1969 from acrylonitrile (AN) and was commercially known as AN-69®. Worth to notice, that dialyzers with this membrane are still used for treatment. Since then, many other synthetic membranes have been used clinically for HD treatment; nowadays, the most used synthetic membranes are, usually, recognized by the name of the polymer used for their manufacture. However, most synthetic membranes are a mixture of co-polymers, that may substantially alter the physical and chemical properties of the primary polymer, and consequently the entire membrane structure (180).

The most common synthetic membranes are: polysulfone (PSf), offering good biocompatibility and protection from endotoxins; polyethersulfone (PES) which is a blend of hydrophobic base polymers, with good biocompatibility and less albumin loss; poly(methyl methacrylate) (PMMA) with increased adsorption properties to enhance removal of some inflammatory molecules; polyester polymer alloy (PEPA); polyacrylonitrile (PAN) with good biocompatibility and enhanced fluid removal due to hydrophilic properties; polycarbonate (PC); polyamide (PAM), and ethylene-vinyl alcohol copolymer (EVAL), which has low inflammatory impact (181).

Compared to cellulosic membranes, synthetic membranes are thicker (>35  $\mu$ m) with asymmetric cross-sectional structures. The Figure 11 shows different structures of symmetric and asymmetric hollow-fibre membranes. The asymmetry refers to a two-layer structure, with an inner dense thin layer that regulates solute removal and is responsible for membrane selectivity, and a thick supporting spongy layer containing large pores (macrovoids), that works as a mechanical support, defining the membrane mechanical strength (182).

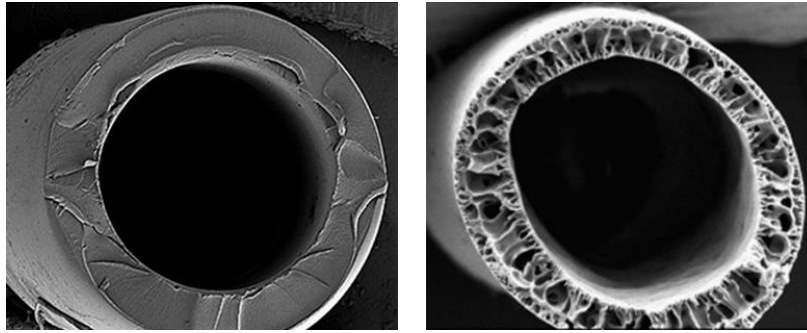


Figure 11: Scanning electron microscopy image of symmetric unmodified cellulosic vs. asymmetric polysulfone hollow-fibre membranes. Accepted from (183) and (184), respectively.

Compared to cellulosic membranes, the synthetic polymer types present more physical-chemical advantages in their structure, namely larger pore size, better hydraulic permeability, and higher filtration capacity, thus, a greater ability to remove solutes (165). The improved performance of these membranes is also due to their asymmetric structure, consisting of a denser surface layer responsible for the MWCO and for their mechanical strength compared to symmetric cellulose membranes.

The synthetic polymer membranes used in dialyzers are almost exclusively hollow-fibres (185), which tremendously increase the surface area available for blood purification. Figure 12 shows the design of a hollow-fibre dialyzer. Since the introduction of these membranes in dialyzers, a vast number of studies have been focused on evaluating their biocompatibility and separation ability, as well as their impact on the mortality and morbidity of patients undergoing HD treatment (170). It was reported that the risk of mortality of the patients dialyzed with modified cellulose and synthetic polymer membranes was at least 25% lower than that of patients treated with unsubstituted cellulose membranes (186). Moreover, the use of synthetic polymer membranes led to a decrease in the loss of serum albumin and a higher reduction of  $\beta$ 2-microglobulin, leading to overall improved mortality of the patients (187). Those membranes also showed positive effect on the inflammatory state of HD patients, by diminishment of neutrophil priming and activation (188, 189). The types of synthetic membranes with their advantages and limitation are summarized in Table 7.

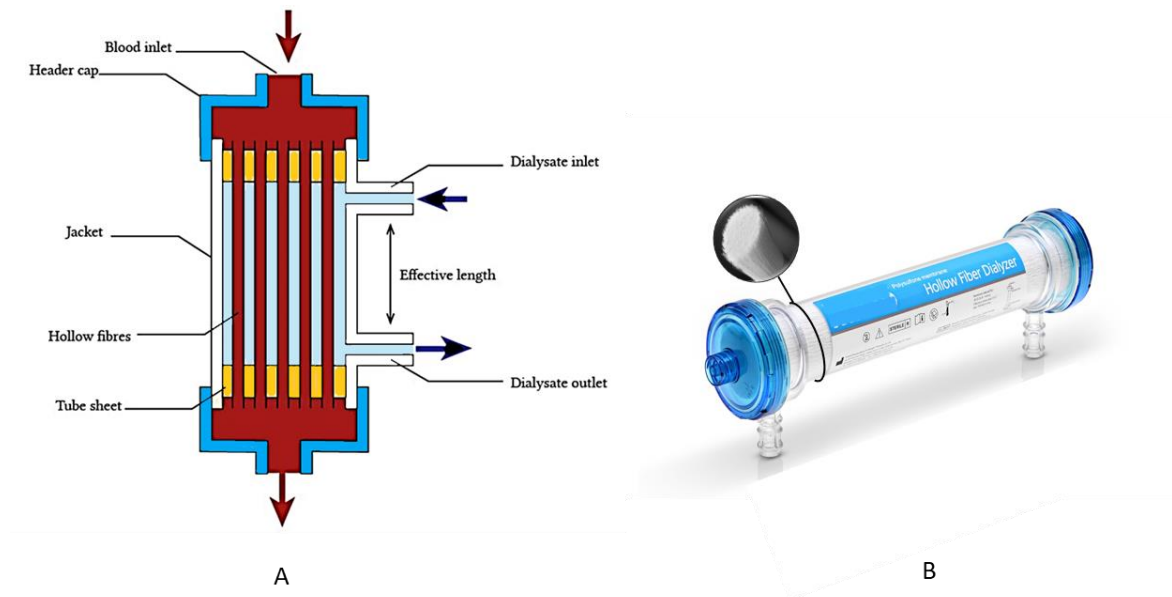


Figure 12: Schematic representation of hollow-fibre dialyser design (A) and real image of commercial hollow-fibre dialyser with magnified cross-section of polysulfone hollow-fibres (B). Adapted and modified from (190) and (191), respectively.

EVAL is a type of polymer for membrane fabrication that displays hydrophilic characteristics, reduced protein adsorption, and decreased complement and blood cell activation, compared to other synthetic materials (192, 193). Despite all these biological advantages, no further studies focusing on its potential value for clinical HD treatment have been reported. This is likely due to the fact, that the mechanical strength of EVAL is not sufficient to withstand the pressures experienced during HD procedure.

PMMA and PAN membranes have been used to produce protein-leaking dialysers with additional mechanism of protein adsorption. Owing to their hydrophobic character, the membranes exhibit increased ability for removal of some large solutes, cytokines, and middle-MW molecules, such as  $\beta$ 2-microglobulin (90, 194).

Table 7 : HD membranes: their advantages and limitations. Modified from (195).

Type of membrane	Membrane designation	Advantages	Limitations
Cellulosic	Regenerated cellulose (Cuprophane®)	<ul style="list-style-type: none"> <li>· Good small solute removal</li> <li>· Higher HD treatment adequacy compared to PSf membranes (m.)</li> </ul>	<ul style="list-style-type: none"> <li>· Higher complement activation compared to synthetic m.</li> <li>· Poor removal of middle-sized molecules</li> </ul>
Modified cellulose	Cellulose acetate (CA)	<ul style="list-style-type: none"> <li>· Lower complement activation compared to cellulosic m.</li> </ul>	<ul style="list-style-type: none"> <li>· Higher neutrophils apoptosis compared to PSf m.</li> <li>· Higher complement activation compared to synthetic m.</li> </ul>
	Hemophane®	<ul style="list-style-type: none"> <li>· Lower complement activation compared to cellulosic m.</li> </ul>	<ul style="list-style-type: none"> <li>· Higher pro-inflam. cytokine production compared to PAM</li> </ul>
Synthetic	Polycarbonate (PC)	<ul style="list-style-type: none"> <li>· Naturally hydrophilic character</li> <li>· Lower complement activation compared to cellulosic m.</li> </ul>	<ul style="list-style-type: none"> <li>· Higher inflammatory markers production compared to PAM</li> <li>· Higher complement activation compared to PAN and PSf</li> </ul>
	Polysulfone (PSf)	<ul style="list-style-type: none"> <li>· Good removal of <math>\beta</math>2-microglobulin</li> <li>· Lower mortality rate compared to cellulose m.</li> </ul>	<ul style="list-style-type: none"> <li>· Causes neutrophil activation</li> <li>· Increased pro-inflammatory cytokine production</li> </ul>
	Polyamide (PAM)	<ul style="list-style-type: none"> <li>· Good removal of <math>\beta</math>2-microglobulin</li> </ul>	<ul style="list-style-type: none"> <li>· Risk of anaphylactic reaction</li> <li>· Slight complement activation</li> </ul>
	Polyethersulfone (PES)	<ul style="list-style-type: none"> <li>· Great removal of middle MW molecules</li> </ul>	<ul style="list-style-type: none"> <li>· Protein adsorption on its surface</li> <li>· Immune system activation</li> </ul>
	Polyacrylonitrile (PAN)	<ul style="list-style-type: none"> <li>· Adsorption of pro-inflammatory cytokines and proteins</li> <li>· Lower PMN activation compared to PMMA m.</li> </ul>	<ul style="list-style-type: none"> <li>· High risk of anaphylactic reaction</li> <li>· Low complement activation</li> </ul>
	Poly(methyl methacrylate) (PMMA)	<ul style="list-style-type: none"> <li>· Good removal of <math>\beta</math>2-microglobulin by adsorption</li> <li>· Lower pro-inflam. cytokine production compared to PSf</li> </ul>	<ul style="list-style-type: none"> <li>· Slight complement activation</li> <li>· Causes mild leukopenia</li> </ul>
	Polyester polymer alloy (PEPA)	<ul style="list-style-type: none"> <li>· Low albumin permeation</li> <li>· Good <math>\beta</math>2-microglobulin removal</li> </ul>	<ul style="list-style-type: none"> <li>· Low level of complement activation</li> </ul>
	Ethylene-vinyl alcohol copolymer (EVAL)	<ul style="list-style-type: none"> <li>· Naturally hydrophilic with low protein adsorption</li> <li>· Removes high MW solutes</li> <li>· Lower neutrophil activation compared to PSf m.</li> </ul>	<ul style="list-style-type: none"> <li>· Not reported</li> </ul>
Bioactive membrane	Vitamin E coated synthetic polymer	<ul style="list-style-type: none"> <li>· Decreases oxidative stress</li> <li>· Improves inflammatory status and anaemia</li> </ul>	<ul style="list-style-type: none"> <li>· Slight complement activation</li> </ul>

Polymer PSf offers a unique combination of features that are ideal for membrane with HD applications. They can withstand a variety of sterilization techniques, including steam, gamma, electron beam, and ethylene oxide, and they can be readily formed into hollow-fibre and flat sheet membranes with highly controllable pore size distribution. In addition, PSf membranes exhibit very high mechanical strength and resistance; stability at wide range of pH 2–13; thermal stability (150–170 °C); outstanding hydrolytic stability and chemical inertness and good resistance to moderate concentrations of chlorine. The great advantage of PSf membranes for HD treatment is its outstanding biocompatibility combined with a low cytotoxicity, which leads to low levels of adverse clinical effects. These characteristics make PSf as globally proved polymer for membrane fabrication.

The first PSf-based membrane became available for routine dialysis already in 1984 (196), and nowadays, polysulfone is the most frequently used polymer for HD membrane fabrication. PSf is an ideal polymer for the manufacture of membranes with variable pore size, resulting in large pore size high-flux membranes, facilitating the efficient removal of large uremic toxins from the blood (197).

Despite these important characteristics, PSf membrane faces some limitations, when it is in contact with blood during the HD treatment. These limitations are mainly given by the hydrophobic nature of the polymer. The hydrophobic surface is prone to the adsorption of serum proteins onto its surface, which may lead to severe complications, due to activation of the complement system, platelets (PLT) and coagulation cascade. Besides the poor biocompatibility, the hydrophobic PSf membrane used for filtration in dialysis, would require very high transmembrane pressures to achieve an adequate ultrafiltration rate. Therefore, it is desirable that the PSf dialysis membrane is partially hydrophilic (197). To overcome this problem, PSf must be blended with a hydrophilic compound, which improves its biocompatibility. When compared with cellulosic membranes, these PSf membranes stand out for their better biocompatibility, their improved clearance of medium-sized molecules and for their larger surface area. They allow a higher and more rapid reduction of uremia (197) and the enhanced biocompatibility of PSf membranes also reduces oxidative stress in HD patients (198). Overall, the long-term use of PSf membranes brings an important improvement in the outcome of HD patients (198).

However, even the most biocompatible membranes were not able to exclude an inflammatory response linked to release of pro-inflammatory cytokines and ROS, during the long-term intradialytic contact with blood. Thus, new approaches are desired for developing advanced production of bioactive membranes (199).

### 3.7.2. Polymeric additives

Contrary to regenerated cellulose, which is naturally hydrophilic, synthetic polymeric membranes, including PSf membrane, are generally hydrophobic (180). The hydrophobicity is an undesirable characteristic contributing to low biocompatibility, since the hydrophobic surface is prone to protein adsorption and thus, very likely activates coagulation cascade and platelets that are known to be thrombogenic. Besides, the formed layer of adhered proteins on the membrane surface may deteriorate its permeability, which will shorten membrane lifetime and notably reduce biocompatibility. For that reason, the majority of the synthetic membranes contain hydrophilic additives (200). Biocompatible hydrophilic polymers, such as polyvinylpyrrolidone (PVP) and polyethylene glycol (PEG), are the most commonly used additives to improve hydrophilicity of the HD membrane, due to its good miscibility with PSf and high solubility in water. Their molecular structure is shown in Figure 13 (201).

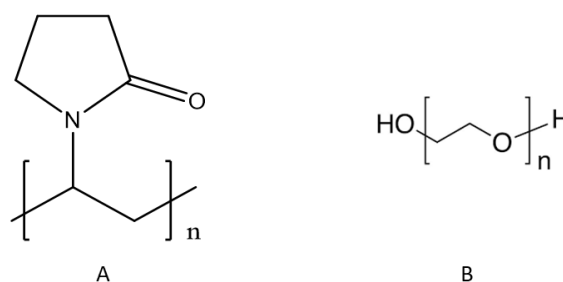


Figure 13: Chemical structure of polyvinylpyrrolidone (A) and polyethylene glycol (B).

In the past, during the Second World War, PVP was used as a plasma substitute and U.S. Food and Drug Administration and European Medicine Agency considered it as a safe polymer. PVP is also known as a pore-forming agent; the leakage of PVP from the membrane into coagulation bath, forms pores for the further solute and water transport during the phase inversion. Besides, thanks to good solubility of PVP in water, the excess amount of PVP may be rinsed out from the membrane, after the casting process. Both molecular weight and the amount of PVP are important parameters, as they influence the membrane structure and performance. The MW of PVP used in the polymer solution can range from 10 000 to 360 000 g mol<sup>-1</sup>.

The effect of adding a second polymer with hydrophilic characteristics to the casting solution was extensively studied, in order to understand the changes caused in the membrane structure. It was reported that adding a second polymer to PSf solutions, such as PVP, gives rise to membranes with higher porosity, well interconnected pores, and surface properties that are different when compared with membranes containing only PSf.

However, the amount of PVP added to the casting solution has a limit value (about 20% by weight), from which an additional increase in the concentration of PVP causes a decrease in pore size. This decrease in pore size could be attributed to the increase of the entanglement in polymer chains, which is typical for large MW polymers and it is referred as spherical structure formed by the cross-linking between the polymer chains. During the membrane formation process, the entangled chains of polymers (PSf and PVP) act as a physical cross-linked chain network, restraining the growth of the polymer-lean phase. As a consequence, the membrane pores are not allowed to grow, resulting in the formation of small pores. The small pore size at a high PVP concentration causes more resistance to fluid flow, raising TMP and thus lowering the membrane water permeability (202, 203).

PEG is a hydrophilic water-soluble polymer with application in many areas, from industry, through cosmetics, to medicine. PEG is generally considered as non-toxic, biologically inert, and safe. It can be added to the casting solution in a wide range of concentration and is available with different MW, ranging from 200 to 35 000 g mol<sup>-1</sup>. It was reported that higher PEG concentration leads to larger membrane surface pores and higher porosity. The impact of MW of PEG on membrane structure was also studied and it was shown that increasing the MW of PEG enhanced the pore number, as well as the porosity and, therefore, improve the water flux during the preparation process (204).

Surfactants, such as 1,4-dioxane, diethylene glycol dimethyl ether, acetone,  $\gamma$ -butyrolactone, Tween 20 and sorbitan monooleate series (Span-20, Span-80), have been also used as additives to the polymer solution. These additives showed ability to increase the affinity between the solvent and nonsolvent, changing the precipitation path during membrane fabrication. Furthermore, smaller surfactant molecules in the casting solution can produce larger pores on the top surface and a more porous structure in the sub-layer, leading to thicker membranes (169).

The approach of using nanoparticles as additives in the polymeric composite membrane fabrication is a new area of research. Nanoparticles, such as carbon nanotubes, multi-walled carbon nanotubes, silica, silver, titanium oxide and zinc oxide nanoparticles, have been used as fillers in polymer composite membranes. A significant increase in the ratio of surface area and volume provided by those compounds are the result of strong interfacial interactions between the nanoparticles and the surrounding polymer (169).

The final membrane morphology could be tailored by the concentration of these additives leading to optimized membrane properties, such as improved hydrophilicity, enhanced mechanical properties, and increased gravimetric porosity. However, the adverse effects of excessive additives content, such as shrinkage, tearing or other defects in the membrane formation, should be considered.

### 3.7.3. Solvent

The Solvent plays an important role in the final membrane structure. The rate of miscibility between solvent and nonsolvent, during the membrane precipitation within the phase inversion process (will be discussed in more detail in Section 3.9.3), defines the membrane morphology (Figure 14). Besides the solvent type, its amount in the polymer solution does change the viscosity of the solution, affecting the speed of solvent-nonsolvent demixing process. The increase in viscosity subsequently reduces the exchange rate of the solvent and the nonsolvent and, thus, a smaller amount of nonsolvent can penetrate into the casted polymer solution, slowing down the membrane precipitation process. It has been described that slowed-down demixing process, commonly referred as delayed demixing, leads to formation of dense sponge-like structure, whereas the fast demixing, known as instantaneous demixing, leads to finger-like structure of the membrane, with a porous thin top layer, as is schematically shown in Figure 14, together with the structures of these two types of membranes. The sponge-like membranes have small water flux, while the membranes with finger-like morphology have low salt rejections and high water fluxes (205, 206).

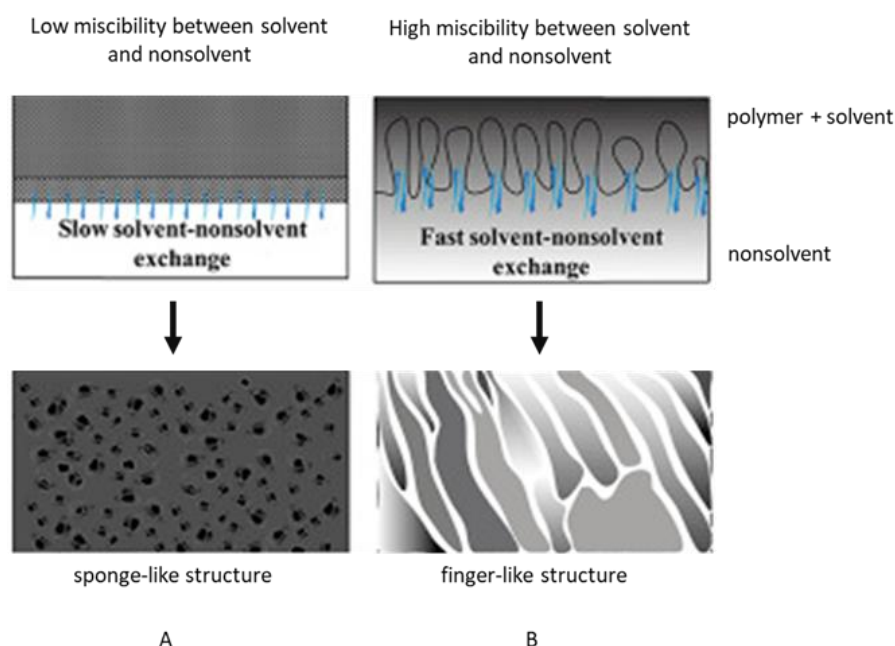


Figure 14: Different membrane morphologies associated to different types of solvent demixing rate. Modified from (206).



The choice of solvent-nonsolvent system in a membrane formation process has a great influence on membrane morphology, mechanical properties, interfacial characteristics, and separation performance. The polymer must be soluble in the selected solvent, and the solvent and nonsolvent must be miscible. Frequently, the higher the mutual affinity (or miscibility) between the solvent and nonsolvent is, the more likely instantaneous demixing will occur, which means that the polymer precipitates and a solid film is formed very rapidly ( $t < 1$  s) after immersion in the coagulation bath, and more porous membrane with finger-like morphology are obtained. There are usually several solvents that are compatible with a chosen polymer. Specifically, the PSf is soluble in aprotic polar solvents, namely in N,N-dimethylacetamide (DMA), N,N-dimethylformamide (DMF) and N-methyl-2-pyrrolidone (NMP), which are the most frequently used. For each solvent, there are a large number of compatible solvent-nonsolvent pairs, each with specific thermodynamic behaviour and miscibility (206). The examples of mutual diffusivity between different solvents and water as a nonsolvent, are shown in Figure 15.

Following the current trend of green chemistry, research has been oriented towards the use of non-toxic solvents in the membrane preparation (e.g. methyl and ethyl lactate, triethyl phosphate,  $\gamma$ -butyrolactone) and application of supercritical CO<sub>2</sub> and ionic liquids (158).

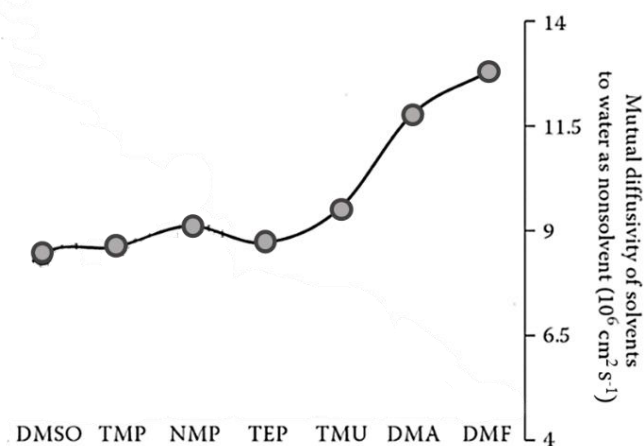


Figure 15: Mutual diffusivity of various polymeric solvents with water, used as a nonsolvent in the coagulation bath. Modified from (207).

*DMSO: dimethyl sulfoxide; TMP: trimethyl phosphate; NMP: N-methyl-2-pyrrolidone; TEP: triethyl phosphate; TMU: tetramethylurea; DMA: N,N-dimethylacetamide; DMF: N,N-dimethylformamide*

### **3.8. Bioactive membranes**

The endeavor to overcome the previously discussed complications associated to HD treatments and the requirements for increasing membrane biocompatibility, has led to new treatment strategies and continuous development/improvement in PSf membranes. One of those strategies was to obtain a membrane providing good performance and antioxidant protection to blood cells and circulating proteins and lipoproteins, during the HD treatment (82, 112). To achieve this membrane improvement, ongoing for three decades, the researchers were focused on developing enriched HD membranes with antioxidant capacity, to suppress HD-induced oxidative stress. The most commonly used approach is to immobilize antioxidants and bioactive compounds on the blood contacting surfaces of the membranes. Besides the antioxidants that have already proved positive effect on OS status, such as vitamin E (208), other types of bioactive compounds have been tested for immobilization, such as catalase, superoxide dismutase and soybean-derived phytochemical genistein (209, 210). Nevertheless, the progression of analytic methods for isolation and analysis of natural antioxidants may bring new opportunities for membrane modifications.

Moreover, other active compounds, besides antioxidants, have been considered for membrane modification, as they could potentially help to reduce OS related CVD morbidity and mortality.

#### **3.8.1. Techniques for membrane modifications**

To enhance membrane biocompatibility, modifications with bioactive compounds have been performed, using two main approaches: membrane blending and surface coating.

Blending is the simplest way for modifications of HD membrane. The compound used for blending, and the solvent used for polymer dissolution, must have similar polarity, to avoid the formation of insoluble precipitates. By this approach, the bioactive compound is incorporated into membrane structure during the preparation process. This compound is evenly distributed on the membrane surface and within the matrix, and the membrane does not need any further post-fabrication modification (211, 212).

The membrane modification by surface coating is carried out after its formation. The surface can be modified by chemical method, where covalent bonds are formed with the bioactive molecules, or by physical methods, where weaker interactions with the biomolecules are involved. In chemical immobilization, biomolecules are attached to the

membrane by strong covalent bonding, which disables easy desorption of the bonded molecules. However, this chemical modification method is usually complicated and relatively expensive. The physical method has the advantage of allowing a greater diversity of applications, especially for molecules with a high charge. With this method, biomolecules attach to the support using Van Der Waals forces and, although the binding force is weaker, the preparation of the membranes is easier. Thus, this method has been the most used, even in the preparation of membranes modified with vitamin E (213).

### **3.8.2. Vitamin E-coated membrane**

The antioxidant activity of vitamin E, a well-known scavenger of the lipid hydroperoxides involved in lipid oxidation, may reduce the oxidative stress in HD patients, and its negative consequences. For this reason, vitamin E is routinely orally administered to HD patients, to prevent the negative oxidative effects of HD treatment (121). As the interaction of blood with dialyser triggers the production of pro-oxidants, the use of vitamin E to enrich HD membrane was a good strategy for the development of a new bioactive membrane with additively provided antioxidant properties. The first clinically used vitamin E-coated membrane (VEM) was based on regenerated cellulose and was introduced in the market in 1990, under the commercial name Excebrane™. The vitamin E, particularly  $\alpha$ -TCP, was bound to the cellulose membrane via chemical interactions. Later, PSf-based VEMs were introduced in the market for clinical use, showing good biocompatibility. Nowadays, several types of modified cellulose/PSf/PES based membranes coated with vitamin E are commercially available, such as VitabranE®, CL-13, EE12 Terumo, and Clirans®E (120, 214). The vitamin E bound on the surface of these membranes can directly reduce the OS by reducing the harmful effect of the free radicals released by activated neutrophils; by this manner, the bioactive membrane can provide antioxidant protection rapidly and locally, close to the membrane. Moreover, VEM dialyzer showed to provide more effective antioxidant defence against ROS than the oral administration of vitamin E in HD patients (208). The antioxidant activity of VEM can be complemented with the oral administration of vitamin C (213).

Since the introduction of VEM into clinical dialysis practice, many clinical studies have been carried out. The antioxidant activity of VEM was confirmed by the decrease in lipid peroxidation, with further positive impact on prolonged RBC lifespan. The use of these membranes showed improved biocompatibility, as showed by the decrease in the circulating levels of pro-inflammatory markers (CRP, IL-6) (215-217). The HD treatment with VEM membranes, showed other improvements, such as, reduction of platelet adhesion,

protein adsorption and blood clotting time. Another positive effect of VEM was the reduction of neutrophil activation, as shown by the reduction in HNE circulating levels (218). A recent meta-analysis including sixty studies, compared the effect of VEM and conventional HD membranes on anemia, inflammation, OS, and dialysis adequacy, as the main endpoints of interest. The findings of these studies were consistent, confirming the positive effect of the use of VEM on HD treatment, reducing oxidative stress and inflammatory biomarkers, namely IL-6 levels. However, the beneficial effect of VEM on HD associated parameters, such as dialysis adequacy, lipid profile, and serum albumin were not confirmed (219).

Overall, the use of VEM, by reducing oxidative stress and inflammation, could contribute to reduce the risk for CVD events, the major causes associated to the high morbidity and mortality in ERDS patients on HD.

### **3.8.3. Other bioactive membranes**

Based on the use of other known therapeutic antioxidants, several bioactive membranes have been developed. However, none of those membranes, listed below, have been used for clinical treatment.

ALA was chemically immobilized into two layers of sulfonated PSf membranes. This method of immobilization showed great stability and antioxidant activity, when evaluated *in vitro* (220). Conjugated linoleic acids are known to possess biological activity, such as scavenging of free radicals, improving immune function, inhibiting of growing tumors, and others. Based on these positive effects, conjugated linoleic acids were covalently bound to CA and PAN membranes, in order to improve their biocompatibility. These bioactive membranes were studied and the results suggested a protective effect against oxidative stress in HD treated patients (221).

Another type of bioactive membrane presenting antioxidant activity, include membranes enriched with the enzymes SOD, CAT, or with both enzymes. These enzymes were covalently and ionically bound to polyethyleneimine deposited PSf membrane (210).

Even natural compounds of plant origin can be used for bioactive membranes development. The natural antioxidant, soybean-derived phytochemical genistein (4',5,7-trihydroxy isoflavone), isolated from soybean, was used to modify PES or PAM membranes. The introduction of genistein to the membrane showed positive effects, not only on decreasing of OS and inflammation, but also in the adhesion of platelets to the membrane material (222, 223).

Another approach is to reduce the negative effect of high levels of neutrophil elastase, by enriching the HD membrane with a human neutrophil elastase inhibitor (HNEI). Although

oral HNEI therapy has not been tested in HD patients, its ability to improve the negative proteolytic effects of neutrophil elastase has been studied in patients with various lung disorders, showing positive results (224, 225). Hence, an Italian research group aimed to diminish neutrophil elastase level by immobilization of the endogenous inhibitor  $\alpha_1$ -PI, isolated from human plasma, on glycidyl methacrylate crafted nylon or PES membrane. The  $\alpha_1$ -PI was anchored on the membrane via chemical immobilization. The *in vitro* tests using HNEI-coated membranes proved to be effective against the proteolytic activity of neutrophil elastase (226, 227). However, this type of enriched membrane did not undergo further development and has never been evaluated *in vivo*. This brings new perspectives for the development of this type of bioactive membrane.

### **3.9. Membranes geometries and preparation processes**

Synthetic membranes are fabricated in two geometries: hollow-fibre or flat-sheet. Both geometries can be classified as symmetric or asymmetric membrane. The most commonly used technique for polymeric membrane preparation is phase inversion, although the spinning method varies according to the membrane geometry (228).

#### **3.9.1. Hollow-fibre membranes**

Hollow-fibre membranes with cylindrical design are of great commercial interest, especially for bioseparations. They are fabricated by extruding or pumping a dope solution through a spinneret, following different methods, such as melt, dry, wet, dry-wet spinning or electrospinning. The spinneret has a tube-in-orifice structure, with about 0.5–1 mm inner diameter and 0.9–2 mm outer diameter (229). The polymeric solution is spun through the spinneret to form a fibre, which is solidified via phase inversion process. Hollow-fibre fabrication involves two coagulants (internal and external coagulants). The internal coagulant controls the inner skin morphology, while the external coagulant controls the outer skin morphology, unlike to flat sheet membrane, where the phase inversion usually starts from the top surface, after immersion in one coagulation bath (230). The diagram of hollow-fibre membrane preparation via immersion precipitation is described in Figure 16.

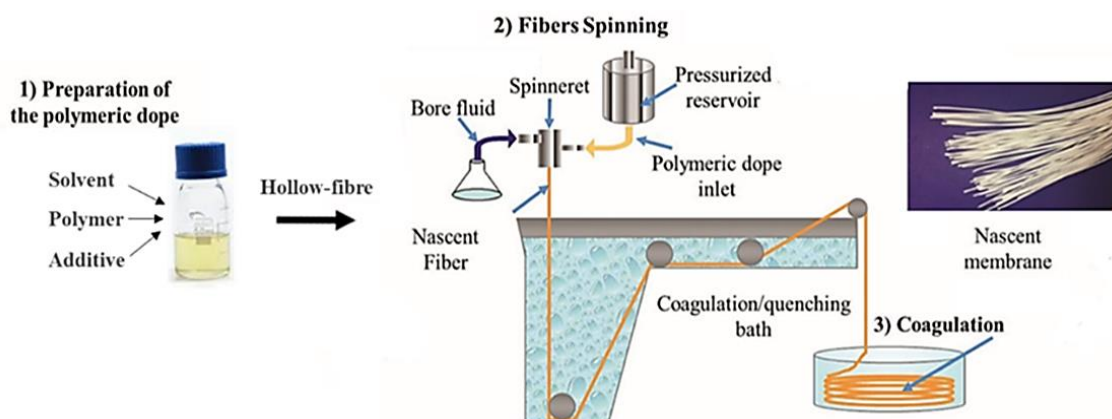


Figure 16: Diagram of hollow-fibre membrane preparation via phase inversion. Firstly, the polymeric solution is dissolved. Then, dissolved polymer is fed out of the spinneret on an air gap to evaporate the solvent (dry-wet spinning) and then goes into a coagulation bath, where the phase inversion takes place and the fibre membrane solidifies. Modified from (158).

Electrospinning is the method for fabricating ultrafine fibres, ranging from micron to nanoscale, using electrical charge to draw the fibres from a liquid and does not require the use of a coagulation bath or high temperatures to produce solid fibres from the polymer solution (231). Melt spinning is the most convenient and economic method for polymer fibre manufacturing at large industrial scales. In melt spinning, the fibre-forming substance is melted for extrusion through the spinneret and then directly solidified by cooling. Dry spinning is the method used when the fibre formation process is under controlled solvent evaporation, by stream of hot air. In wet spinning method, the spinneret is immersed in a coagulation bath and the fibre is directly spun into this bath containing nonsolvent. This spinning method is used for cellulose based hollow-fibre membranes. The dry--wet spinning method is the most commonly used for the production of hollow-fibre membranes used for HD applications, where an air gap is present between the spinneret and the coagulation bath. In this method, a partial evaporation of the solvent or phase inversion in the coagulation bath fed into the spinneret are possible in the air gap. However, the final solidification of the polymeric membrane occurs in the coagulation bath. The process of evaporation, in case of using less volatile solvents, may be accelerated by heating the spinning system (thermally assisted evaporative phase-separation process) (230).

### 3.9.2. Flat sheet membranes

As mentioned above, the commercial HD membranes are fabricated with hollow-fibre geometry. However, flat sheet membrane geometry has some advantages for experiments in a laboratory scale since their fabrication and further manipulation are easy. Flat sheet

membranes are commonly casted using a knife-like tool to disperse a polymeric casting solution equally and to control the thickness of the casted membrane, or by using the spin coating technique.

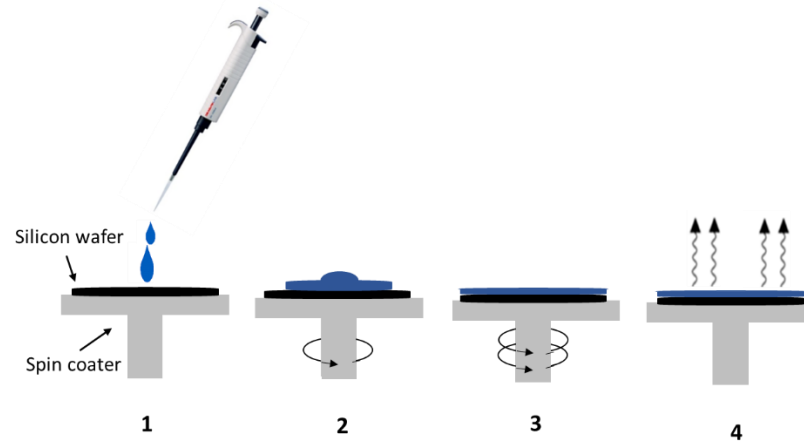


Figure 17: Spin coating process. 1) deposition of casting solution, 2) spin up, 3) spin off; rotational spreading out and thinning, 4) conditioning and solvent evaporation.

Spin coating is a common technique used to obtain uniform and thin films. Spin coating is used in a wide variety of industries and technology sectors. With this technique a polymer solution is spun on a mechanical support at high speed and the centrifugal force, together with the surface tension of the liquid, create a uniform coverage. Using this technique, a thin film ranging from a few nanometres to a few microns in thickness, can be obtained (232). As it is shown in Figure 17, this spinning process can be divided into the following 4 main steps:

- 1) Deposition: the initial step of casting the polymer solution, typically using a pipette, on the mechanical support, such as glass or silicon wafer. After the deposition, the mechanical support is spun and the centrifugal motion together with surface tension are primarily responsible for the spreading the solution across the mechanical support.
- 2) Spin up: The support reaches the desired rotation speed, either immediately or gradually, spreading the deposited (casted) solution.
- 3) Spin off: The cast polymeric solution begins to get thin, governed by viscous forces. At this spinning stage, the excessive solution flung off from the support.
- 4) Evaporation: The spinning process stops and the solvent from casted thin film starts to evaporate. The rate of the solvent evaporation is dependent on the solvent volatility and ambient conditions. Inconsistency in evaporation rate, namely at the edges of the film, will cause less uniformity in those areas of the casted film (233).

In general, the final thickness of a spin coated film is proportional to the inverse of the spin speed squared, and can be expressed by Equation 12, where  $h_f$  is final film thickness and  $\omega$  is angular velocity/spin speed.

$$h_f \propto \frac{1}{\sqrt{\omega}} \quad (\text{Equation 12})$$

As mentioned, the advantage of spin coating over other methods is its ability to produce uniform films, quickly and easily, with the desired thickness. Another benefit of this technique is that it needs easy-to-use and low-price equipment. The disadvantage of spin coating, compared with the casting knife method, is its low production rate. The fast solvent evaporation may also be a drawback; thus, to avoid an unfavourable solvent evaporation, the mechanical support has to be instantly removed from the spin coated and placed in the coagulation bath. Finally, in the spin coating process, the effective use of the material is generally very low (around 10% or less) and much of it is wasted during centrifugation (232).

Despite these drawbacks, spin coating is usually the starting point and benchmark for most academic and industrial processes that require a thin and uniform coating.

### **3.9.3. Phase inversion process**

Regardless of the membrane geometry, phase inversion is the most common process of preparing membranes. The phase inversion process in membrane technology was firstly introduced by Loeb and Sourirajan in 1960, and since then it is the most commonly used technique for membrane fabrication. This technique has gained the leadership, due to simple processing, adjustable production scale, low cost, and the possibility of adjustments to obtain a variety of membranes morphologies. The Figure 18 represents different membrane morphologies obtained by this technique. Although the actual execution of membrane preparation is a simple procedure, the basis of the phase inversion process involves both thermodynamic and kinetic aspects, making it a complicated process, difficult to be fully understood (234).



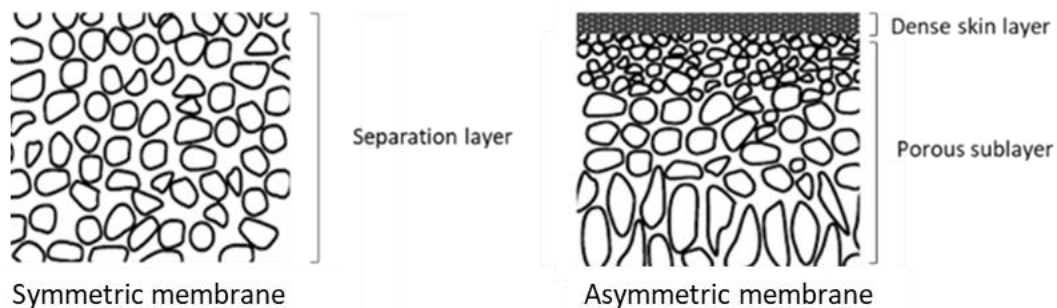


Figure 18: Schematic structure of symmetric and asymmetric membranes showing the different morphologies.

During the phase inversion process, the thin film of homogenous polymer changes from the liquid state to the solid state, after contact with another liquid, which is a nonsolvent for the polymer, but is fully miscible with the polymer solvent. Water is frequently used as the nonsolvent, although acetone and lower aliphatic alcohols are also used (206). The phase change occurs due to the exchange between polymer solvent and the nonsolvent, leading to phase separation in the polymer film, further forming the membrane structure. In more detail, the homogenous polymer solution, casted on the mechanical support gets into contact with the nonsolvent. Then, the diffusional exchange of the solvent with the nonsolvent, causes a thermodynamically unstable state of the polymer, leading to the formation of a two-phase system: polymer-rich and polymer-lean phase. This phase separation can be caused, either by liquid-liquid or by liquid-solid demixing, depending on the used phase inversion technique. Further, the phase separation occurs by nucleation and growth of polymer-lean phase. The polymer-lean phase forms the pore, while the polymer-rich phase forms the membrane matrix. The solidification process starts at the phase with the highest polymer concentration, through processes like gelation, vitrification, or crystallisation.

The phase inversion process can lead to the formation of pores with various morphologies, including open and closed pores, finger-like pores or macrovoids, contributing to a variety of membranes with different morphologies.

By phase inversion can be obtained either asymmetric membrane, composed of a dense top layer, supported by a layer of interconnected type of pores and; large elongated voids – macrovoids; or symmetric membrane with interconnected pore structure, with uniform pores all over the membrane thickness (Figure 18) (234-236). As already noticed above, the demixing process may be induced by various actions and therefore, the phase inversion covers four different techniques (235, 237).

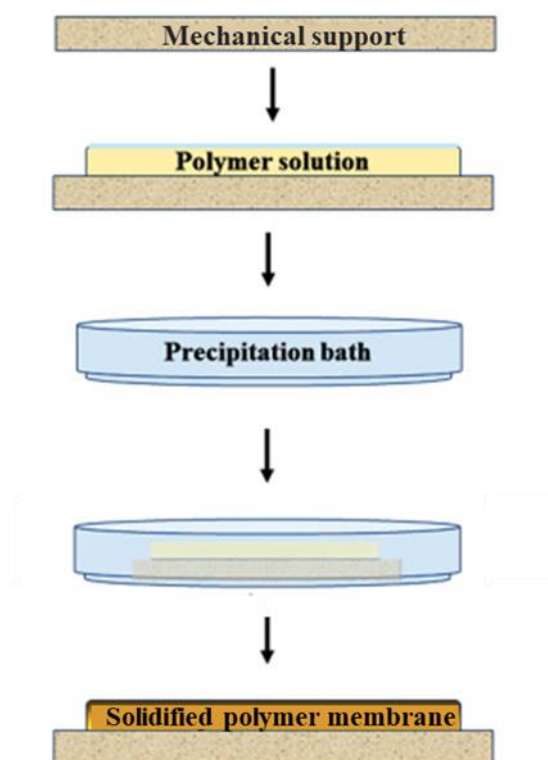


Figure 19: Process of phase inversion via immersion precipitation. The polymer solution is casted on the mechanical support and directly immersed in the coagulation bath, where the phase inversion takes place. The nonsolvent in the coagulation bath is exchanged with solvent in the polymeric film. The solidified film on the support is removed from the coagulation bath and is easily peeled off from the support.

### **Nonsolvent induced phase separation (Immersion precipitation)**

Nonsolvent induced phase separation (NIPS), commonly referred as immersion precipitation, is the most commercially available and the most frequently used technique for membrane fabrication, including membranes for HD application. NIPS reaction system uses a ternary composition, usually including a polymer, a solvent, and a nonsolvent. The process of NIPS is described, step by step, in Figure 19. This process starts by mixing a polymer and a solvent, forming an initial homogeneous solution; then, the polymer solution is casted as a thin film on a mechanical support, to obtain the required membrane shape (flat sheets or hollow-fibres); next, the thin film, together with the support, is immersed into a coagulation bath containing a nonsolvent; the phase separation takes place when the solvent exchanges with the nonsolvent, occurring the precipitation of the polymeric solution.

The final membrane structure results from a combination of mass transfer and phase separation processes (235, 238).

### **Solvent evaporation-induced phase separation**

In the phase inversion induced by vapor phase precipitation, the membrane formation occurs due to the penetration of the nonsolvent from the vapor atmosphere into the polymer film. To enable this type of phase inversion, the mechanical support with the casting film containing the main polymer and the solvent is placed into nonsolvent vapor atmosphere saturated with solvent, when the high solvent concentration in the vapour phase prevents the solvent evaporation from the cast film. This process leads to formation of a porous membrane without selective top layer (235).

### **Vapor-induced phase separation**

In this method, the polymer is dissolved in a mixture of solvent and nonsolvent, where the solvent is more volatile than the nonsolvent. Due to the volatile solvent evaporation, the solution composition changes to a higher nonsolvent and polymer content. This leads to polymer precipitation, resulting in the formation of a skinned membrane (235).

### **Thermally Induced Phase Separation**

The polymer solution containing one or more solvents is cooled down to enable the phase separation. Evaporation of the solvent induces the formation of a skinned membrane. This method is frequently used to prepare microfiltration membranes (235).

### **3.10. Membrane characterisation methods**

Commonly, there are two important aspects to consider, when selecting the ideal membrane for application in HD procedures. On one hand, it is essential to know the permeation and selective separation characteristics of the membrane, and on the other hand, the membrane must have good biocompatibility and have great inertness towards blood components.

There are many specific methods and techniques for characterizing an HD membrane, that usually require special instrumentation, and highly trained operators; the techniques that were used in the works that are part of this dissertation, are presented and described below, in detail.

#### **3.10.1. Morphological characterization**

In general, the most important membrane morphological parameters are the porosity, pore size, pore size distribution, surface roughness, MWCO, and thickness. Therefore, morphology control is the key factor in membrane fabrication. To characterize the morphological parameters, several techniques are available (239).

#### **Microscopy**

The biomolecules separation mechanism of the membrane does not depend only on chemical interactions, but also on physical interactions between the membrane and the components to be separated. The membrane morphology characteristics, such as pore size, pore distribution, and thickness, can be investigated directly by microscopy methods. These methods include scanning electron microscopy (SEM), atomic force microscopy (AFM), confocal scanning laser microscopy, and transmission electron microscopy. The main limitations of these methods are the time-consuming sample preparation and only 2D imaging analysis, either of a membrane surface, or of membrane cross-section. Today, faster and more complex techniques can give a 3D image analysis, such as X-ray computed microtomography and nuclear magnetic resonance (203, 239).

#### **Porosity**

Gravimetric porosity is a measure of the total amount of void volume in the membrane. It represents the ratio between the membrane density and the density of the matrix (203). Porosity ( $\epsilon$ ) is calculated as a function of the membrane weight using the Equation 13, where

$W_s$  and  $W_d$  is weight of the saturated and dry membrane specimen, respectively,  $\rho$  is density of the liquid (water), and  $V$  represents volume of the membrane.

$$\varepsilon [\%] = \frac{W_s - W_d}{\rho_w \times V} \times 100 \quad (\text{Equation 13})$$

### **Pore size**

Pore size and pore size distribution are important parameters to determine the characteristics and performances of porous membranes. Pore size represents the dimensions of the pores, which are channels of a variable cross-section. In general, it is assumed that the pore has a spherical shape, although other irregular shapes may exist on the membrane; therefore, for the evaluation of the pore size, this factor should be considered. The pores can be classified, according to their diameter size, into three categories: micropores ( $d < 2 \text{ nm}$ ), mesopores ( $2 < d < 50 \text{ nm}$ ) and macropores ( $d > 50 \text{ nm}$ ) (240). Membranes with a homogeneous pore size and a narrow pore size distribution have a sharper cut-off in the sieving coefficient, thus leading to improved passage of low molecular weight proteins, while reducing the loss of albumin (181).

### **Surface roughness**

Surface roughness is quantified by the deviations in the direction of the normal vector of an actual surface from its ideal geometric flat shape and dimensions (241). The smoothness of the fibre surface is evaluated by AFM; changes in surface roughness are quantified by  $R_a$  value, which is the mean distance between the surface and the centre of the reference plane of the measurement. The roughness of the internal surface of the fibre can influence several membrane properties, including protein interactions and blood coagulability (87).

### **Molecular weight cut-off**

The MWCO refers to the lowest molecular weight solute (in Da), for which 90% is retained by the membrane, or the molecular weight of the molecule that is 90% retained by the membrane (242).

### **Thickness**

The thickness represents the distance between both surfaces (top and bottom or front and back) of a membrane, depending on the geometry of the membrane - flat sheet or hollow-fibre (169).

### 3.10.2. Wettability, water contact angle and protein fouling

Wetting can be defined as the ability of liquids to keep in contact with solid surfaces and it is a direct result of intermolecular interactions, which occur when two media (liquid and solid) are brought together. Wettability is the result of the balance between three forces: the surface tension of the solid material, the surface tension of the liquid, and the interfacial tension between phases. The higher the surface tension of the liquid, the less it spreads on the solid and, therefore, the less it is wettable (243). Surface wettability is correlated with hydrophilicity or hydrophobicity of the solid surface and it is one of the most important characteristics of biomaterials. Once they are in long-term contact with blood, this feature affects the biological response of the body to the material, and therefore wettability plays a major role in material biocompatibility. Based on the wettability of a material, protein adsorption, platelet adhesion/activation, blood coagulation and cell and bacterial adhesion could be influenced (244). The material with bound plasma proteins may become thrombogenic, due to the interaction of platelets with the plasma proteins on the material surface. The adsorbed proteins, by leading to adhesion and activation of platelets (fibrinogen) or to activation of the intrinsic pathway of the blood coagulation cascade, increases the risk for a thrombotic event (244).

The wettability studies usually involve the measurements of contact angle ( $\theta$ ), which indicates the degree of wetting, when a solid and liquid interact. Contact angle has been an important parameter to determine the wetting ability of the polymer membrane surface. To evaluate the wettability of a material, the measurement of the water contact angle, a rapid and convenient technique, is used to describe hydrophilicity or hydrophobicity of the material. The contact angle is measured between the solid-liquid interface and liquid-vapour interface.

The relation between the surface wettability and the value of the contact angle, is shown in Figure 20. When the water droplet poorly spreads out on the material surface, and the water contact angle  $\theta$  is  $> 90^\circ$ , the surface is hydrophobic, with low wettability. On the contrary, when the water droplet spreads out easily on the surface of the material surface and the water contact angle  $\theta$  is  $< 90^\circ$ , the material is hydrophilic, showing good wettability. Although it may seem that there is a strongly well-defined border between hydrophilicity and hydrophobicity of a material, defined by  $\theta$  of  $90^\circ$ , based on practical experiments. Vogler proposed  $\theta \approx 65^\circ$  as the cut off  $\theta$  value, between hydrophilic and hydrophobic material, that is between a protein non-adherent and adherent material (245). Xu et al. (244) also confirmed in their study, that by increasing the water contact angle of the material, from  $60^\circ$

to 65°, the adhesion of bovine serum albumin, fibrinogen and human Factor XII to the surface, was increased.

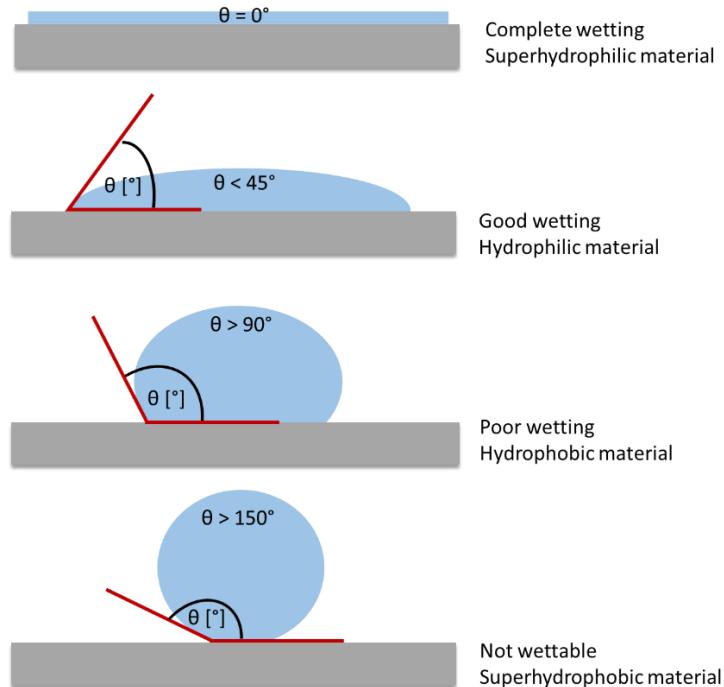


Figure 20: Example of water contact angle of material surfaces with different hydrophilicity.

## Protein fouling

The wettability of the membrane surface can influence the adsorption of proteins to the material surface by several forces, including electrostatic and hydrophobic interactions. The hydrophobic domain of the proteins binds more easily to the hydrophobic membrane surface. To enable this bond, the protein conformation must change, which can lead to protein denaturation or to loss of function/activity; the conformational change can be, however, beneficial, by enhancing the activity or the stability of the proteins. Electrostatic interactions depend on the charges of both, material surface and protein charge, which are usually a function of the pH and of the ionic strength of the solution. At low pH, the proteins are positively charged, whereas at high pH they are charged negatively (246). The electrostatic interactions are more frequent in the presence of hydrophilic material, once the protein is less susceptible to structural changes, retaining its original conformation (hydrophobic domain is inside the protein structure) (247). The protein adsorption on the material surface is a very fast process. In general, small proteins adhere to the surface firstly, due to their rapid transport to the surface, but along the time they are replaced by

larger proteins, with higher affinity towards the material (248). The bound proteins form a monolayer on the material surface, with protein mass density ranging from 1-5 mg per m<sup>2</sup> of membrane area. This dense monolayer can contribute to clogging of the material pores and, in the case of semipermeable membranes, this phenomenon can diminish its permeability. The degree of deposition depends on protein concentration, protein charge, size, structure, and their spherical orientation also plays a very important role (249).

In general, the hydrophobic material is more prone to protein adsorption; therefore, the material with higher wettability is more biocompatible and vice versa. The ideal membrane surface should have appropriate balance between hydrophilicity and hydrophobicity.

### **3.10.3. Membrane biocompatibility**

Since HD membranes are in contact with blood for long periods of time, they must meet strict criteria of biocompatibility and the interaction of its artificial material with blood cells and proteins, should be as negligible as possible. Nevertheless, all dialysis membranes activate PLT, coagulation factors, complement and leukocytes to some extent, which may eventually increase the risk for thrombotic events, chronic systemic inflammation, leukocyte dysfunction and, therefore, the evaluation of membrane biocompatibility is very important and must be assessed.

The *in vitro* evaluation of material biocompatibility commonly involves several different tests, to study, mainly, the characteristics of the membrane surface, which is in direct contact with blood, interacting with blood cells and plasma constituents. The techniques used for biocompatibility evaluation of the developed membranes will be described in this chapter, including the main principle and the relevance of each evaluation, for the biocompatibility in general.

It is important to note that not only the type of polymer used, but also the sterilization medium used, can play an important role in the biocompatibility of the membrane. In the past, sterilization methods using aldehyde or ethylene oxide were associated with a higher prevalence of adverse reactions and, therefore, they have been largely replaced by other sterilization methods, such as steam and gamma ray irradiation (250).

#### **3.10.3.1. Haemocompatibility assays**

All the materials intended for medical devices must be tested for haemocompatibility. This evaluation is carried out in accordance with the regulations described by the



International Organization for Standardization (ISO), specifically according to ISO 10993-4, Biological evaluation of medical devices — Part 4: Selection of tests for interactions with blood (251).

### **Membrane-induced activation of complement**

Membranes for HD activate the complement system, primarily via the alternative pathway. The activation is initiated by covalent binding of the component C3b to the membrane surface, predominantly to hydroxyl groups. Through several proteolytic reactions, the complement system gets further propagated, resulting in the formation of two protein fragments, C5a and C5b. In general, the “a” fragments are involved in the inflammatory response, while the “b” fragments contribute to the further enzymatic activity in the cascade. The final complement components form the membrane attack complex that may cause damage to the cells, namely RBC lysis, decreasing their lifespan (252).

During complement activation, an excessive amount of anaphylatoxins (C3a, C5a) is released that may lead to several negative effects, such as systematic oedema, tissue damage, lipid peroxidation and exuberant release of HNE, ROS and pro-inflammatory mediators (IL-6, IL-8, TNF- $\alpha$ , INF- $\gamma$ ) from activated neutrophils. Thus, the OS and inflammation, already present in HD patients, would be even more pronounced (253). Furthermore, it is observed that patients treated with low biocompatible membranes have higher  $\beta$ 2-microglobulin levels, due to increased synthesis by leukocytes after their contact with C5a. This systemic complement activation in HD patients, accompanied by a pro-inflammatory and pro-thrombotic response, may contribute to the high risk of CVD events observed in HD patients (176, 254).

Unfortunately, even the synthetic membranes with improved biocompatibility compared to cellulose-based membrane, are still able to activate the complement system. During a single HD session, the plasma levels of the terminal complex increase up to 70%. To evaluate the actual complement activation, it is recommended to measure the plasma levels of C3a, C5a and even the membrane attack complex, because they reflect the activation of the complement system at different levels of the cascade, with potential different effects (251, 253). Therefore, the evaluation of the plasma levels of C3a and C5a is very important for a better knowledge about membrane biocompatibility. Lower levels of these markers of complement system activation after HD treatment, will reflect good biocompatibility of the membrane.

## Membrane-induced haemolysis

Increased lysis of circulating RBCs may occur in case of an underlying RBC disorder or when RBCs are damaged. In the assessment of blood-material interactions, haemolysis may result from a direct contact of the RBCs with the material surface; indirect contact, when RBCs are exposed to extractable chemicals from the material; or due to the elevated shear stress caused by the material surface (mechanically-induced haemolysis) (251). The formation of the membrane attacking complex, as a result of the activation of the complement system, may also contribute to haemolysis, since this complex causes destruction of the RBC membranes, leading to the cell lysis.

Haemolysis is a function of time exposure to the material and properties of the material, such as surface energy, surface morphology and surface chemistry. Haemolysis may be assessed by using a direct *in vitro* test. To evaluate membrane induced haemolysis, highly diluted suspensions of erythrocytes are exposed to the test material. After incubation for an adequate period of time and temperature, the level of free Hb is measured; the value of haemolysis is usually reported as the percentage of haemoglobin released, considering the assay conditions. An increased level of Hb manifest increased haemolysis. According to the ISO, the material is considered non-haemolytic if the observed haemolysis of whole blood is < 2% or when the free Hb level is < 10 mg dL<sup>-1</sup> (251).

## Membrane-induced platelet activation

During HD treatment, activation of PLTs may occur, due to their contact with the membrane surface. As the PLT activity is primarily associated with the initiation of coagulation cascades, the level of PLT activation is used to define the material thrombogenicity, therefore ability of to promote or induce the formation of a blood thrombus. The low biocompatible material is more prone to bound the PLTs. The PLT adheres to the surface by specific glycoproteins and when this binding take place that the actual platelet activation process is triggered. After activation, a flip-flop mechanism causes a trans-bilayer movement of cytoskeletal proteins from the inside of the cell membrane to the outside. The expression of these specific proteins (e.g. P-selectin) can be evaluated by using specific fluorescently labelled antibodies and therefore can they serve as markers of cell activation. The amount of activated PLTs can be measured by flow cytometry, using two antibodies: one specific for PLT (e.g. IG Ib) and one specific for PLT activation (P-selectin) (255). An assessment of the various stages of PLT activation can be performed by SEM (256).

Since there is not a general agreement on the limits defining the materials thrombogenicity, the tested material should be compared to a biocompatible surface in order to evaluate the level of PLTs activation.

## **Blood coagulation**

The process of blood coagulation can be activated by the contact of blood with medical devices and materials, as HD membranes. Various standard coagulation tests are designed to detect clinical coagulation disorders. These tests can also be used to detect activation of the blood coagulation process. According to ISO 10993-4-Haemocompatibility, that evaluation should be performed and involves three different tests: activated partial thromboplastin time (APTT), prothrombin time (PT) and thrombin time (TT). These tests are carried out using automatic analysers (251) and, when altered, after contact with the studied material, it may reflect the activation of the blood coagulation process. Therefore, the alteration of the coagulation cascade can be associated with increased risk for thrombotic events. Since the blood composition and reactivity differs between the donors, the obtained results should be compared to a reference material to evaluate the test alteration (257).

### **3.10.4. Mechanical properties**

To meet the demands for the membranes to be used for HD, the polymeric membranes require good mechanical durability, chemical and fouling resistances. Thus, analysis of membranes stress loading conditions and examining their mechanical properties are very important. Furthermore, understanding the mechanical behaviour of polymeric membranes, together with deformation mechanisms, is critical not only for membranes structure improvement, but also for prediction of their reliability and lifetime in HD application (258).

Mechanical characterization of a material requires measuring of how material responds to an applied force. These methods determine the elastic, plastic, viscoelastic, hardness, as well as fracture and toughness properties of the membrane.

#### **Tensile tests**

Tensile testing is one of the most fundamental and the most used testing methods to evaluate the mechanical behaviour of materials. These tests are used to measure the strength of a material, by providing the burden of opposite forces in a straight direction. A sample of the membrane is placed in a machine and is subjected to controlled traction and constant speed until it breaks. Other important mechanical parameters such as Young's modulus, elongation at break, and tensile strength of materials can be obtained from the tensile tests (258).

The elastic properties of a material undergoing tension or compression in one direction is characterized by Young's modulus, or tensile modulus. This numerical constant, measuring material's stiffness or resistance to elastic deformation under load, is defined as the ratio between stress (force applied per unit area) and strain (proportional deformation) in a material during the uniaxial deformation. The tensile strength of a material is the maximum amount of tensile stress that material can endure before rupture. The tensile strength can be described as yield strength, defined as the maximal stress that the material can withstand, without permanent deformation; maximal strength; breaking strength is defined as the stress applied to the material at the point of rupture. The elongation at break is the ratio between changed length at the maximal material elongation and initial length. It expresses the capability of the material to resist to changes of shape, without permanent deformation or rupture (258).

## **4. EXPERIMENTAL PART**

The presented experimental work in this doctoral thesis was carried out at three laboratories - Laboratory of Applied Chemistry and Laboratory of Biochemistry, Faculty of Pharmacy, University of Porto and Laboratory of flow techniques, Faculty of Pharmacy in Hradec Králové, Charles University. All the used methodologies, that led to the obtaining experimental results, and the respective outcomes, are summarized and presented below.

### **4.1. Development and characterization of flat sheet polysulfone membrane.**

#### **4.1.1. Introduction and main objective of the experimental work**

As already mentioned, currently the most often used polymer for the manufacturing of HD membranes is polysulfone (PSf), given by their excellent characteristics, such as thermal and chemical stability and lower ability for the activation of patient's immune system. A membrane is suitable for HD treatment, when it meets certain criteria of permeability and biocompatibility. In particular, the membrane must be permeable for a broad range of uremic toxins, in particular  $\beta$ 2-microglobulin. On the other hand, it should effectively retain albumin, and especially should not activate complement cascade, immune system cells, and induce haemolysis.

Despite the availability of commercial PSf hollow-fibre HD membranes, their large effective area exceeds the scale of testing conditions in our laboratory. For that reason, the downscaled model of PSf membrane, as well as testing equipment, had to be developed,

The main objective of this work was to optimize the polysulfone membrane composition, based on the data available in the literature, and to establish its preparation process involving spin coating and immersion precipitation.

To fulfil this aim, the PSf membranes prepared with different compositions were evaluated in terms of their separation ability, to select the ideal composition of the membrane, showing great separation ability suitable for HD treatment. For this purpose, a lab-made microfluidic cell was constructed, to test the membranes in flow conditions. After selecting the membrane whose composition met the separation requirements for HD, further tests were carried out for its complete characterization.

#### 4.1.2. Chemicals and Instrumentation

##### 4.1.2.1. Chemicals

Water used through the experimental work was distilled ion-exchanged water. Ultrapure water was obtained from the Milli-Q, Millipore purification system, France. All the used reagents were in quality of analytical grade. PSf in pellets with average MW 35 000 g mol<sup>-1</sup>; organic solvent NMP 99.5%; PEG with MW 6 000 g mol<sup>-1</sup>, 20 000 g mol<sup>-1</sup> and 30 000 g mol<sup>-1</sup>; PVP K30 with average MW 40 000 g mol<sup>-1</sup>; bovine serum albumin (BSA) with MW 66 000 Da; human lysozyme with MW 14 300 Da, urea with MW 60 Da, and elastomer Sylgard® 184 were all purchased from Sigma-Aldrich Co. Sodium dodecyl sulphate (SDS) was purchased from Fluka™. Micro BCA™ Protein Assay Kit and monoclonal antibodies for CD42a PE and CD62P APC, were obtained from Thermo Fisher Scientific, MA, USA. Kits required for coagulation tests, partial thromboplastin time (APTT) and prothrombin time (PT), were bought from TECO, Diagnostica Stago, Almada, Portugal. Phosphate buffered saline solution (PBS; 125 mM NaCl and 10 mM sodium phosphate buffer, pH 7.4) was prepared in-house. Bradford reagent was also prepared in-house, by dissolution of 100 mg of Coomassie brilliant blue G-250 in 50 mL of ethanol 95% (v/v), then 100 mL of phosphoric acid 85% was added and the volume was completed till 1 L with deionised water. The solution was filtered prior to use. Erlich's reagent was prepared by dissolving *p*-dimethylaminobenzaldehyde in hydrochloric acid 32% and the final volume was completed by adding deionised water.

##### 4.1.2.2. Instrumentation

Plasma cleaner equipped with oxygen gas supply (Zepto, Diener Electronic GmbH + Co, Germany) was used for the silicon channel mould surface modification. To fabricate the flat sheet membranes, a spin coater (WS-650HZZB-23, Laurell Technologies Co., USA) was used. High-performance dispersion system (Turrax X40, Ystral, GMBH, Germany) and a probe sonicator (VCX130, Sonics and Material Vibra-Cell™, USA), were used to disperse the polymer solution. The experiments involving absorbance measurement were carried out using a microplate reader (Synergy™ HT, BioTek Instruments, USA or Cytation 5, BioTek Instruments, USA). NanoDrop 1000 spectrophotometer (Thermo Scientific, Waltham MA, USA) was used to quantify human lysozyme. To perform the flux experiments, peristaltic pumps (Minipuls 2 and Minipuls 3, Gilson, USA) were used. Flow cytometer (BD Accuri C6, BD Pharmingen) was used for platelet analysis. Optical microscope (Nikon Eclipse Ci) was

used to study cell morphology. Automated blood cell counter (Sysmex K1000; Sysmex, Hamburg, Germany) was used to provide cell counts.

#### 4.1.3. Microfluidic system development to study membrane separation ability

To evaluate the separation ability of newly developed membranes, a microfluidic system was designed and developed to mimic the flow conditions in HD procedure. The miniaturized flow system is composed of two microchannel platforms, peristaltic pump, peristaltic PVC and Teflon tubing. The peristaltic 2 Stop PVC tubes, with internal diameter (ID) 1.3 mm grey/grey Tygon LMT-55, were purchased from Saint-Gobain, France. Teflon tubes with ID 0.8 mm were acquired from Bola, Germany.

The system of microchannels was engraved by a laser cutting machine into an acrylic plate, serving as a pouring form. Further, a silicone elastomer (polydimethylsiloxane) was poured into the form, which was placed into vacuum, for 30 min, to remove air bubbles and then was cured for 1 h at 90 °C. Since the silicon is naturally hydrophobic, and the testing solution passing through the system is aqueous, the microfluidic platform was treated with oxygenated plasma, to reduce hydrophobicity of the material, prior to use (Figure 21). The platform has two inputs and outputs through needles, into a tubing system. The design and dimensions of the silicon microchannel platform is shown at Figure 22. The dimensions of the platform were 4 x 1.5 cm. The total length of the microchannels was 46 cm with an area of 9.2 cm<sup>2</sup>.



Figure 21: Oxygen plasma cleaner used to treat silicon platform in off and on state.

To set up a microfluidic system, two microchannel platforms, separated from each other by the (evaluated) membrane, with an area of 16 cm<sup>2</sup>, were tight together by a set of screws, to prevent leakage of the circulating liquid, and connected to the tubing system and peristaltic pump. The membrane creates a semipermeable barrier between the two closed circuits. One circuit contained the solutes of interest, in PBS pH 7.4, representing the blood circuit, and the other contained circulating pure PBS, to represent the dialysate. The solution flux in both circuits was set up at 20  $\mu\text{L s}^{-1}$  and were in countercurrent to mimic the flow of

blood and dialysis liquid, as occurs in HD systems. The volume of the entire microfluidic system was 4 mL, 2 mL in each circuit, respectively.

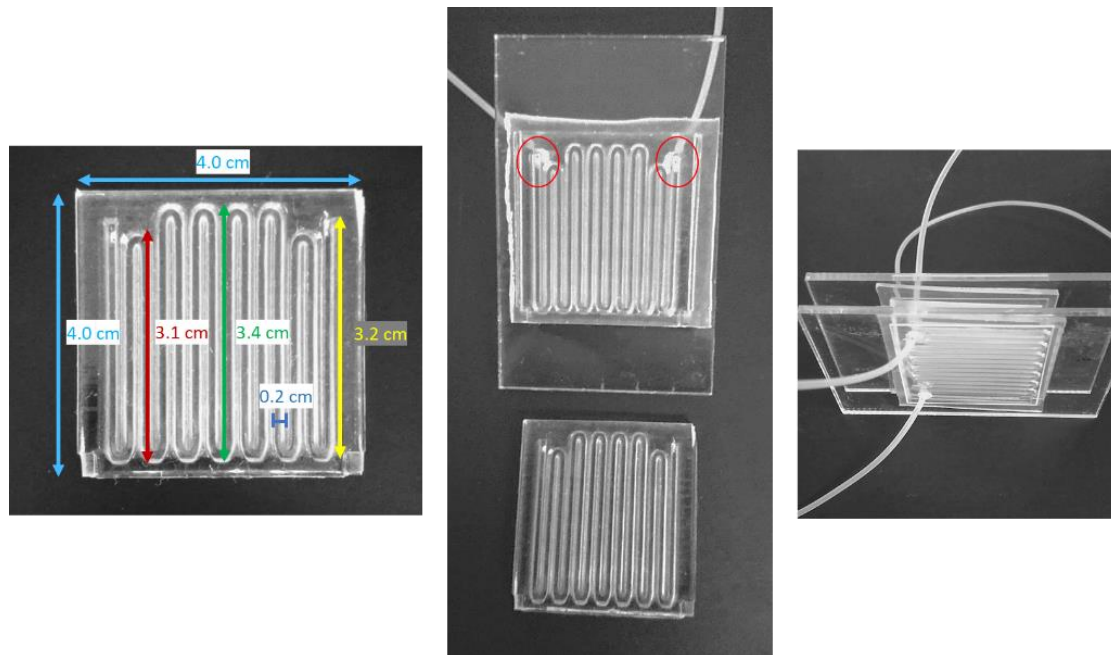


Figure 22: Silicon microchannel platform. The lengths of the channels are showed in colours. The platform was mounted into an acrylic support, with inlet and outlet (circled in red) opened onto teflon tubes. The silicon platform is connected to the tube through an adjusted syringe.

#### 4.1.4. Composition and preparation of the casting solution

The casting solution is the polymeric solution casted on the mechanical support, right before the spinning process. The casting solution is commonly composed of the main polymer (PSf), hydrophilic additive, and solvent. Once the casting solution composition has a significant effect on several membrane characteristics, such as morphology, pore size, porosity and on hydrophilicity, the initial composition had to be optimized, in order to prepare membranes with specific separation characteristics and good biocompatibility. The properties that an ideal membrane should have, are as follows:

- the pore size should be uniform throughout the membrane and uniformly distributed
- the porosity should be high to provide high flux
- the MWCO of the membrane should be sharp
- the diffusion coefficient of middle size solutes should be high
- the membrane dense top layer should be as thin as possible, to provide high permeability of solutes
- the mechanical strength should be high, to withstand the required pressure limits



- the protein adsorption on the membrane surface should be low
- the interaction of the membrane surface with protein and blood cells should be minimal (259).

Therefore, the composition and ratio of single components of the casting solution was tuned to obtain a final membrane meeting the best above-mentioned characteristics. The membrane casting solution was prepared by dissolving PSf in NMP solvent, adding PEG or PVP as hydrophilic additives.

### **Main polymer**

PSf with an average MW 35 000 g mol<sup>-1</sup> was used as a main polymer. The initial tested weight percentage (wt%) in the casting solution was 15 wt%, selected according to preliminary studies and literature survey. Before using the PSf pellets ( $\pm$  0.2 g per pellet), they were dried at 100 °C for 1 h, to remove residual humidity. Then, PSf pellets were rigorously weighed into the glass vessel.

### **Additives**

To improve membrane hydrophilicity, two different hydrophilic additives of different MWs at different weight percentages, were tested. To evaluate the effects of these two variables (MW and wt%) of the additives, on membrane characteristics, a univariate optimization was used. PEG with MW of 6 000, 20 000, 30 000 g mol<sup>-1</sup> was added into the casting solution, with a fixed wt%. Then, the specific WM was fixed, and PEG was added to the casting solution in a range from 2.5 to 10.0 wt%. A similar set of experiments was carried out with PVP; however, only one MW of 40 000 g mol<sup>-1</sup> was tested, that was added to the casting solution in the mass range 2.5 - 8.0 wt%. High molar masses were selected for both additives, because, according to literature, high MW of PEG/PVP promotes an increment in pore size and membrane porosity (260-262).

### **Solvent**

The preliminary tests were carried out using tetrahydrofuran as the solvent. However, due to its low boiling point (66 °C), it proved to be an unsuitable solvent since the dissolution of the casting solution had to be carried out at higher temperatures. Thus, it was replaced by NMP, which has a significantly higher boiling point (202 °C). The NMP solvent was added to the polymer and additive, in such a mass fraction, that the three components reached a total 100% in the casting solution.

The set of prepared membranes with varying composition, with the designations M1 – M9, are shown in Table 8. The exact final compositions of the membranes are summarized in Table 9.

All the above-mentioned components of the casting solutions were weighted, added into a glass vessel, and dissolved overnight under constant stirring, at 60 °C, until the complete dissolution. To assure homogeneity of the dissolved solution, a high-performance dispersing instrument at the velocity of 12 000 rpm for 2 min, was used. The air bubbles formed during the dispersion process were removed by probe-type sonicator. The solution was kept on ice, during the dispersion and sonication, to avoid evaporation of the solvent. However, before the membrane casting, the solution was equilibrated until room temperature ( $\approx 22$  °C).

It is important to notice that the casting solution solidifies in contact with water (a phase inversion process starts to take place immediately after its contact with nonsolvent – water); therefore the casting solution had to be well protected during all the steps from the intrusion of the air humidity into the glass vessel. Besides that, all the used instruments were heat dried prior the contact with casting solution.

To select the ideal casting solution composition, all the membranes (M1 – M9) whose composition is shown in Table 9 were tested concerning to their separation abilities for small, middle-sized, and large solutes. These tests were carried out in the microchannel flow system (described in Section 4.1.6). This evaluation process will be described in detail in Section 4.1.7 “Membrane characterization”.

Table 8: Summary of tested variations of casting solution composition. The fixed parameter of the PSf membrane composition is marked as black crosses, while the variable one is marked as coloured crosses.

Membrane	PSf (wt%)	PEG MW [g mol <sup>-1</sup> ]			PEG wt%				PVP wt% (MW = 40 000 g mol <sup>-1</sup> )		
		6 000	20 000	30 000	2.5	5.0	7.5	10.0	2.5	5.0	8.0
M1	X	X				X					
M2	X		X			X					
M3	X			X		X					
M4	X		X		X						
M2	X		X			X					
M5	X		X				X				
M6	X		X					X			
M7	X								X		
M8	X									X	
M9	X										X

PSf: polysulfone; PEG: polyethylene glycol; PVP: polyvinylpyrrolidone

Table 9: The exact composition of the prepared PSf membranes.

Membrane designation	Membrane composition (wt%)					NMP
	PSf	PEG 6 000	PEG 20 000	PEG 30 000	PVP 40 000	
<b>M1</b>	15.0	5.0	-	-	-	80.0
<b>M2</b>	15.0	-	10	-	-	75.0
<b>M3</b>	15.0	-	7.5	-	-	77.5
<b>M4</b>	15.0	-	5.0	-	-	80.0
<b>M5</b>	15.0	-	2.5	-	-	82.5
<b>M6</b>	15.0	-	-	5.0	-	80.0
<b>M7</b>	15.0	-	-	-	8.0	77.0
<b>M8</b>	15.0	-	-	-	5.0	80.0
<b>M9</b>	15.0	-	-	-	2.5	82.5

#### 4.1.5. Statistical data analysis

Statistical analysis was carried out using the Statistical Package for Social Sciences (SPSS, version 25.0, Chicago, IL, USA) for Windows. Shapiro–Wilk test was used to assess the normality of data distribution. Data were presented as mean  $\pm$  SD (standard deviation) or as mean  $\pm$  SEM (standard error of the mean). As all the variables showed a Gaussian distribution, one-way ANOVA and Student’s unpaired t test were used to compare sets of data. A  $p < 0.05$  was considered statistically significant. Dixon’s Q test was used to identify outliers from the obtained data.

#### 4.1.6. Membrane preparation

The membranes were prepared by spin coating method, followed by a phase inversion process. The casting solution (1.0 mL) was applied using a micropipette, to a mechanical support, single-side polished N-type silicon wafer (purchased by Sigma-Aldrich Co). The polished silicon wafer was placed in the spin coater (Figure 23) and the solution was then casted and spun for 20 s. The silicon wafer, with a thin film on its surface, was instantly placed into the coagulation bath, composed of ultrapure water. After the phase inversion process, the solidified opaque membrane, was readily peeled off from the silicon

wafer, and placed in a fresh deionized water bath. The prepared membranes were washed for at least 24 h in deionised water, in order to remove residual solvent and additive. Thereafter, the membranes were dried on air and stored in dry conditions. The final dried PSf membrane is showed in Figure 24.

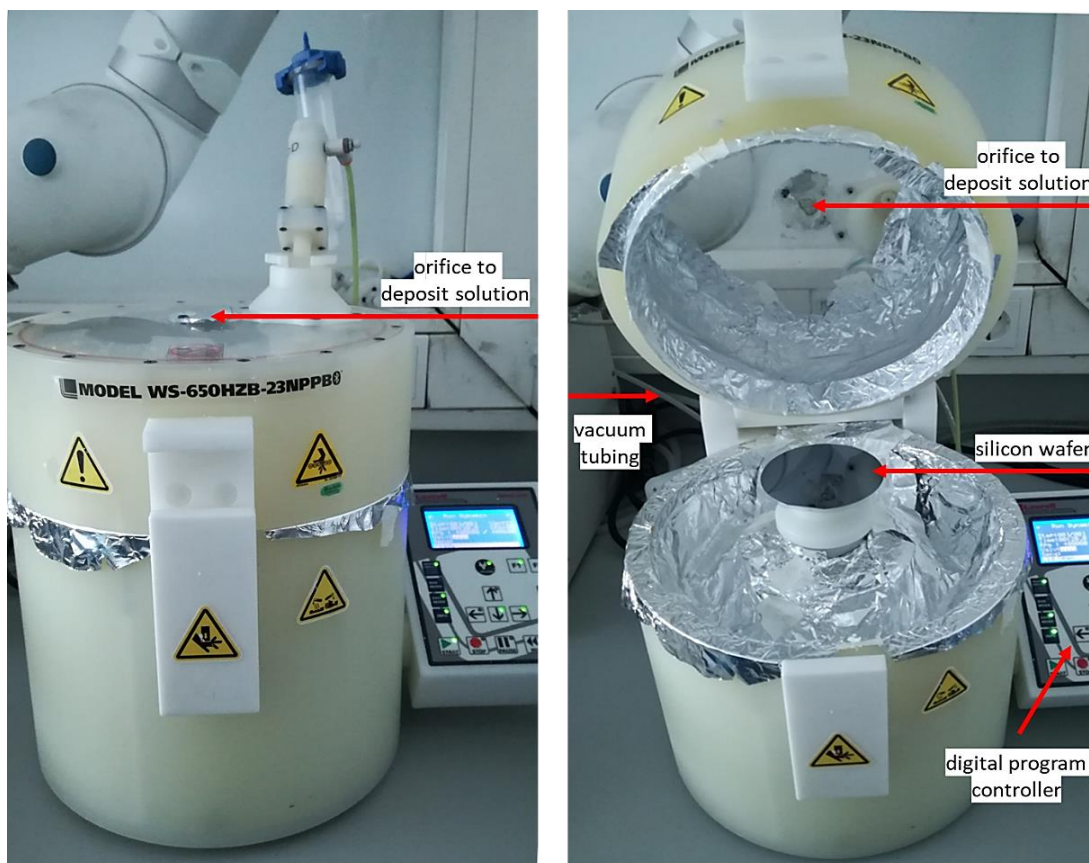


Figure 23: Image of the spin coater in closed and open positions. Silicon wafer is on holding system fixed in stable position by vacuum.



Figure 24: Image of dried PSf membrane.

After optimization of the casting solution composition, the membrane preparation process also underwent several adjustments, namely, time and velocity of the spinning, degree of humidity and temperature of the coagulation bath, to further tailor the membrane characteristics.

Several steps in the membrane preparation process were optimized. Firstly, different spinning angular velocities (1 600, 1 400, 600 ad 200 rpm) were used. When high speeds were used (1 600 and 1 400 rpm) the membranes obtained were very thin, what could be advantageous, since the flow of the membrane is influenced by its thickness. However, these membranes had poor mechanical resistance and were prone to rupture, when the pressure induced by the flow under analysis, was applied. Due to this drawback, the angular velocity was decreased, in order to produce thicker membranes. Membranes casted at lower speed had mechanical stability, although those obtained at 200 rpm, compared to the membranes prepared at 600 rpm, were more rigid, with less elasticity to resist to TMP during the flow process. Therefore, the spinning speed of 600 rpm was kept constant along the preparation process, for all the type of membranes. Indeed, the membranes prepared at this velocity, showed sufficient mechanical stability and elasticity, facilitating their manipulation, and overall, also showed good separation ability.

Another studied parameter during the preparation process was the degree of humidity. As above mentioned, the casting solution solidifies immediately after the contact with the nonsolvent; therefore, a brief test was carried out to evaluate the effect of the ambiental humidity on the final membrane structure. Shortly, following spin coating, the membrane in the wafer was transferred into a chamber with controlled humidity (42% humidity) and incubated in this environment, for 2 and 5 min. Then, the membrane on the wafer was immersed in the coagulation bath, where the additional phase inversion takes place, until the solidified membrane freely peels from the support. The effect of humidity on pore formation can be seen on Figure 25. Regardless of the incubation time, the pore formation starts from membrane edges, advancing to the membrane centre. After 5 min of incubation, the large pores occurred throughout the entire membrane area; while, after 2 mins of incubation, the membrane showed a clear interface between pore formation, in the humid environment, and without pore formation, due to membrane precipitation in the coagulation bath. Thanks to this observation, the standard laboratory humidity was recorded daily and was kept at 27% throughout the fabrication of all the tested membranes.

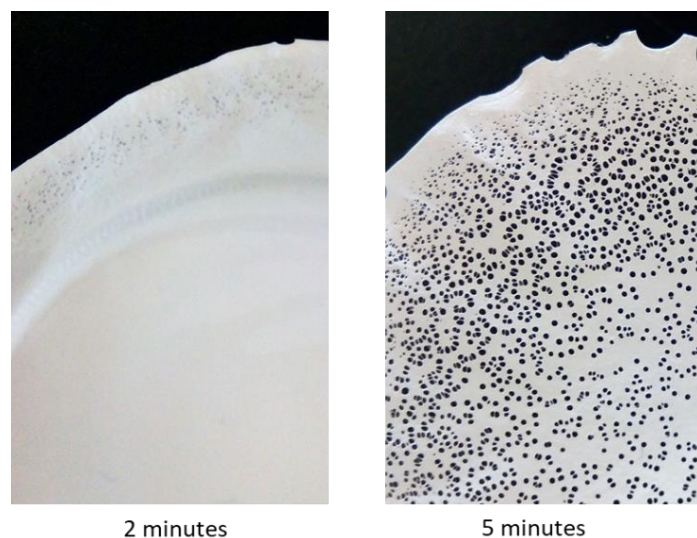


Figure 25: Image of PSf membranes incubated in an environment with high humidity, prior phase inversion in a coagulation bath. Membranes incubated in humid environment (approximately 42% humidity) for 2 and 5 min.

Different temperatures of the coagulation bath were also tested, as the nonsolvent temperature can influence the demixing rate and, therefore, plays an important role in the pore size of the forming membrane (263). The membrane phase inversion was carried out in a coagulation bath at three different temperatures: 37 °C, 22 °C and 15 °C. The separation abilities of the membranes prepared at those temperatures were evaluated in the flow system; membranes precipitated at 15 °C showed improved protein rejection, when compared to those prepared at higher temperatures. Thanks to this protein rejection improvement, all the prepared membranes, along the entire experiments, were immersed in the coagulation bath at a controlled temperature of 15 °C. In summary, the optimal conditions to be used during the membrane preparation process are described in Table 10.

Table 10 : Summarized conditions for PSf membranes preparation.

Parameters	Values
Angular velocity	600 rpm
Time of spinning	20 s
Ambient temperature	≈ 24 °C
Relative spin coater humidity	≈ 22%
Coagulation bath temperature	15 ± 1 °C
Coagulation bath	ultrapure water

#### 4.1.7. Membrane characterization

##### 4.1.7.1. Dialysis experiment

This dialysis experiments were performed by using the aforementioned microfluidic system, simulating the process of HD treatment. The evaluation of all the membranes, with different compositions, were carried out to choose the ideal one, with potential for future real HD procedure. Since one of the requirements for the HD membranes is their semipermeability (separation of solutes according to their mass). Therefore, all the tested membranes were evaluated in terms of permeability for urea, ability to remove around 70% of middle-sized molecules (represented by human lysozyme) and their negligible permeability for albumin (high protein rejection). The membrane that met these requirements was selected for further characterization, namely, for the evaluation of their biocompatibility.

In the dialysis experiments, PBS (acceptor solution) was propelled through one side of the circuit, while PBS with dissolved testing solutes (donor solution) circulated through the other side of the circuit. These circuits, were separated by the membrane under study, as shown in Figure 26.

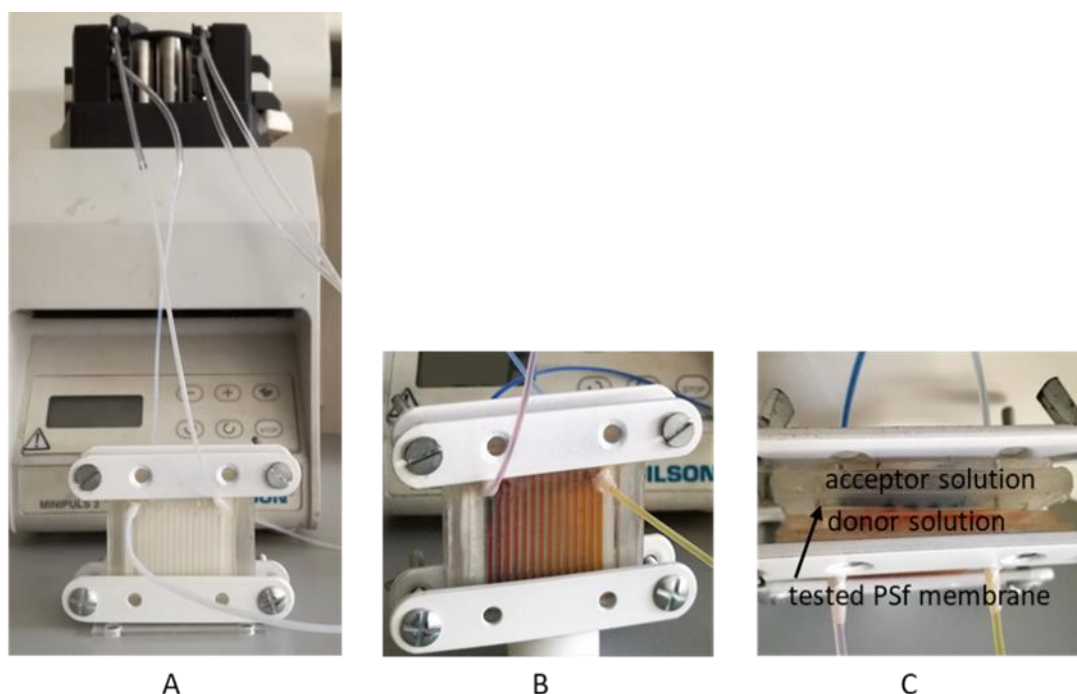


Figure 26: Fluidic system to evaluate membrane separation ability, composed of two closed circuits, separated by the semipermeable membrane under study; (A) the entire fluidic system, microfluidic cell with testing membrane separating two microchannels platforms; (B) microfluidic cell front view; (C) microfluidic cell top view. Modified from (264).



Since the membrane is asymmetric, its orientation is important and, thus, was consistently kept the same orientation throughout all the carried-out experiments. The membrane was orientated with the selective thin top layer, with the small pores, towards the circuit with the testing molecules, representing the blood circuit. Such orientation prevents pore plugging, as the large proteins do not enter into the inner membrane structure, as shown in Figure 27. Moreover, the proteins accumulated on the membrane surface might be removed by shear forces. Each microfluidic platform, therefore, represented a closed loop of donor or of acceptor solution, with a total volume of 2 mL (Figure 26). Urea, human lysozyme and BSA, with different MW, were chosen as modelling solutes, representing three groups of solutes differently separated by the HD membrane during the treatment. In this study, due to its low availability,  $\beta$ 2-microglobulin (MW 11.8 kDa) was replaced by human lysozyme (MW 14.3 kDa), that belongs to the same group of globular proteins and have similar MW and molecule charge. The same type of similarities and easy availability also led to replacement of human serum albumin by BSA.

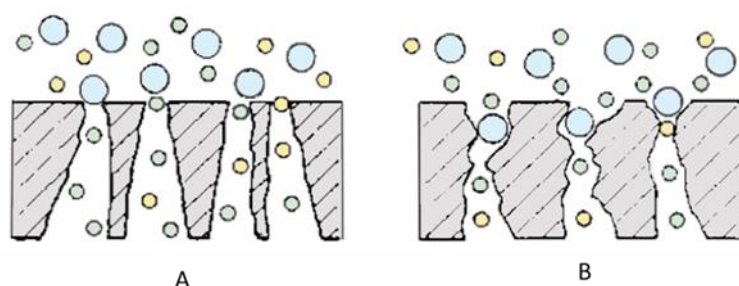


Figure 27: Schematic diagram of solutes filtration by symmetric (A) and asymmetric (B) membrane, showing the importance of membrane orientation to prevent pores plugging by large solutes. Modified from (211).

The testing solutions with the aforementioned solutes were prepared by dissolving urea, lysozyme and BSA in PBS, at pH 7.4, in the concentrations of  $1 \text{ mg mL}^{-1}$ ,  $0.5 \text{ mg mL}^{-1}$ , and  $1 \text{ mg mL}^{-1}$ , respectively. In the microfluidic system, the solutions were propelled in counter current, with a flow rate of  $20 \text{ } \mu\text{L s}^{-1}$ . The samples were collected from each circuit after 4 h of circulation, corresponding to the average duration of an HD treatment. At the end of the dialysis experiment, the solutions were collected from both circuits and their concentration was measured. BSA concentration was quantified spectrophotometrically, measuring the absorbance at 595 nm, according to Bradford protein assay, when the light brown colour of the reagent turns blue in the presence of protein (265). The rejection of BSA was calculated according to the Equation 9, where  $c_1$  represents the concentration of BSA ( $\text{mg mL}^{-1}$ ) in the feed solution, and  $c_2$  corresponds to the concentration in the

permeate, on the opposite site of the membrane, after 4 h of experiment. The results are expressed as percentage of BSA retained, at the end of experiment.

The concentration of lysozyme was determined by direct measurement of the absorbance at 280 nm, by using NanoDrop system. The concentration of lysozyme in the solution was directly provided by the equipment software, using the mass extinction coefficient  $\epsilon_{(\text{lysozyme})} = 26.4 \text{ L g}^{-1} \text{ cm}^{-1}$ . Lysozyme rejection was calculated according to the same equation used for BSA (Equation 9). The concentration of urea was determined spectrophotometrically, measuring the absorbance at 420 nm, according to Levine et al., as the Erlich's reagent in presence of urea forms yellow complexes (266). The percentage of removed urea from donor solution through the membrane, was calculated as the urea reduction ratio (URR), according to the Equation 14:

$$URR [\%] = \frac{U_{pre} - U_{post}}{U_{pre}} \times 100 \quad (\text{Equation 14})$$

Where  $U_{pre}$  represents the concentration of urea ( $\text{mg mL}^{-1}$ ) in the feed solution before dialysis experiments, while  $U_{post}$  is the concentration of urea after 4 h of the experiment.

Firstly, the effect of the MW of the additive on membrane permeation characteristics was evaluated. The casting solutions with the additive PEG (5.0 wt%), with three different MW (6 000, 20 000, 30 000  $\text{g mol}^{-1}$ ) were prepared (Table 9; membranes M1, M4 and M6). The first parameter evaluated was URR, as the urea is the smallest molecule and it should pass freely through the membrane, into the acceptor solution. The membranes M1 (with PEG 6 000  $\text{g mol}^{-1}$ ) showed low permeation of urea; M6 (PEG 30 000  $\text{g mol}^{-1}$ ) showed poor repeatability of the results; the slightly improved URR results, were observed for the membranes M4, prepared with PEG 20 000  $\text{g mol}^{-1}$  in the casting solution. Nevertheless, the measured URR of M4 was still insufficient for HD membranes. For this reason, in an attempt to increase the URR, the MW of PEG in the casting solution was changed to 20 000  $\text{g mol}^{-1}$ . Based on the literature (261, 262), the tested mass of PEG 20 000  $\text{g mol}^{-1}$  were 10.0; 7.5; 5.0 and 2.5 wt%. To these compositions correspond the membranes with the designations of M2, M3, M4, and M5 (Table 9). The lowest URR (13.85%) was showed by the M2 membrane, prepared with 10.0 wt% of the additive, while the highest URR (34.75%) was presented by the M4 membrane with 5 wt% of PEG 20 000  $\text{g mol}^{-1}$ . Besides the low values of URR found for the membranes prepared with PEG, the results also showed very high standard deviations, with irreproducibility in the formation of the membranes, irregular pore size and/or other deficiencies in their structure. This fact could be attributed to the

higher viscosity of the casting solution that favors the formation of thicker membranes, with a thick spongy top layer that is likely to negatively affect membrane flux (267).

To overcome this reduced urea permeability of the membranes prepared with PEG, the next optimisation step in membrane composition led to exchange PEG for another commonly used additive, PVP K30, in the casting solution. The new membranes, with the designations M7-M9, (Table 9) were prepared with three different masses of PVP K30, namely 2.5, 5.0 and 8.0 wt%. These membranes underwent urea permeability, BSA and lysozyme rejection evaluation. Contrary to the previous results obtained with the membranes prepared with PEG, all the membranes prepared with PVP K30 reached a maximum of URR (considering that the system has two closed circuits, the maximal URR is 50%, when urea reaches an equilibrium at both sides of the system), according to the values presented in Figure 28A.

The protein rejection of the membrane strongly depends on the structure and size of the pores in the skin top layer, where the solutes separation takes place. The effect of different wt% of PVP K30 on BSA rejection is shown in Figure 28B. The values of BSA rejection for all the three types of membranes (M7, M8 and M9) are in the range from 90 – 100%, indicating that the membranes prepared with PVP K30 are almost impermeable for BSA. The residual value, corresponding to the passage of albumin, may be considered negligible, in view of what is acceptable for membranes used for HD.

A rejection capacity of the membranes with PVP K30 as the additive, for middle-sized molecules, was evaluated using the lysozyme. The membrane M9 with the PVP 2.5 wt% exhibited a lysozyme rejection of  $50.2\% \pm 2.8\%$ , while the M8, with PVP 5.0 wt%, only showed a lysozyme rejection of  $12.2\% \pm 2.0\%$  (Figure 28C); thus, a significant difference ( $p < 0.05$ ) between these two types of membranes was observed. Due to the decreased lysozyme rejection with the increase of PVP content in membrane structure (M8), the M7 membrane, containing a greater amount of additive, was not evaluated. The lysozyme rejection presented by M9 showed to be more adequate for HD purposes, once it proved to be able to remove middle MW uremic toxins, such as  $\beta$ 2-microglobulin.

Based on the obtained results, it can be concluded that the addition of PVP K30 into the polymer solution plays a very important role in pore formation and in pore size. The presence of a higher concentration of PVP increases pore size and membrane porosity, as was shown by the decreased lysozyme rejection of M8 membrane. The pore size is also associated with membrane MWCO and, according to the results for BSA rejection, for all three types of membranes, the MWCO can be assessed as  $\approx 66\ 000$  Da.

In conclusion, data from the dialysis experiments, suggest that the membrane containing 2.5 wt% of PVP K30 (M9) in casting solution, should be selected for further

characterization (morphology, porosity, density, equilibrium water content, contact angle, protein fouling, mechanical properties, material-induced haemolysis and platelet and complement activation), since it was this membrane composition that gave rise to the membrane with the most suitable characteristics for HD processes. The other prepared membranes, whose composition did not result into characteristics corresponding to a separation ability close to HD membranes, were not further characterized.

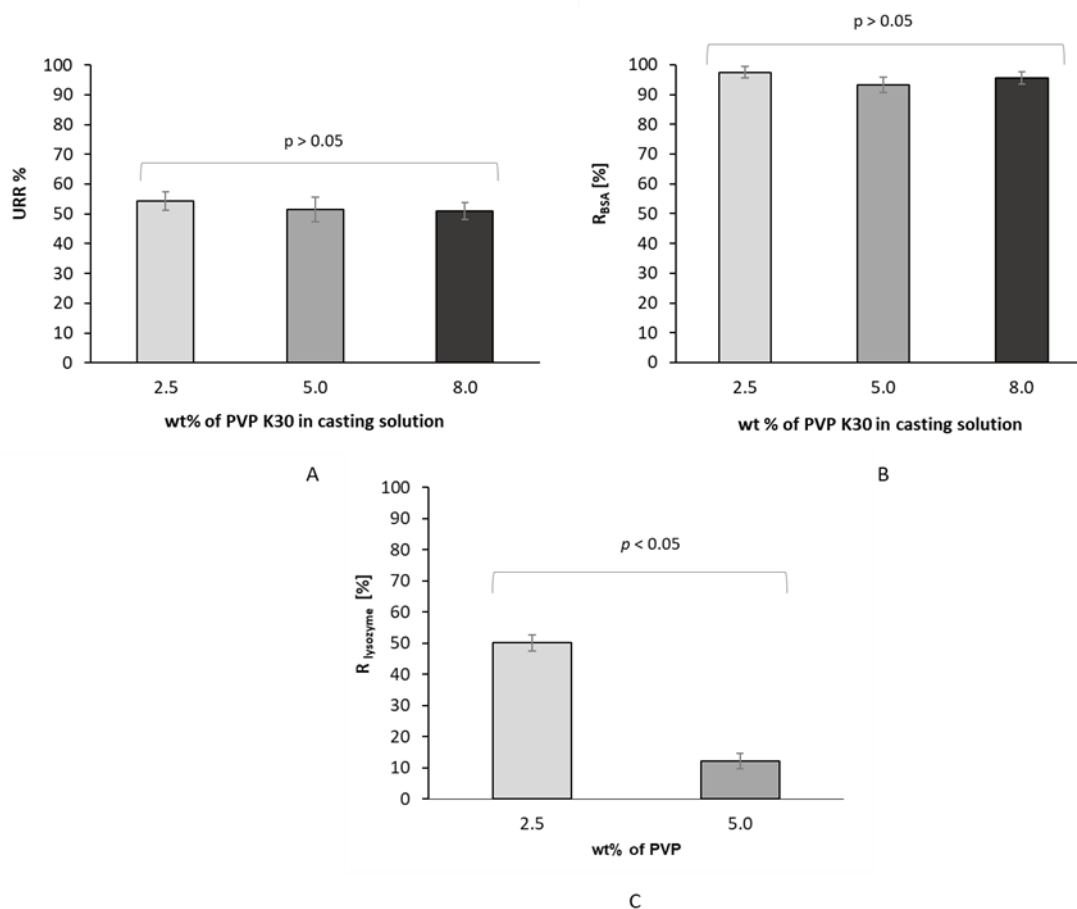


Figure 28: Effect of different masses (wt%) of PVP K30 on membranes (M7-M9) dialysis performance: (A) on URR; the results are expressed as mean URR [%] ( $n = 5$ ) and SD; (B) on BSA rejection; the results are expressed as mean  $R_{BSA}$  [%] ( $n = 5$ ) and SD; (C) on lysozyme rejection by membranes M9 and M8; the results are expressed as mean  $R_{lysozyme}$  [%] ( $n = 5$ ) and SD. The lysozyme rejection values of membranes prepared with 2.5 or 5.0 wt% of PVP showed statistical difference ( $p < 0.05$ ).

PVP: polyvinylpyrrolidone

#### 4.1.7.2. Membrane morphology

The PSf membrane morphology structure was studied by SEM (JSM-6010 LV, JEOL, Japan), an important technique, which directly provides information about membrane morphology and about the pore size and thickness of the membrane. For this evaluation we

had the collaboration of 3B's Research Group (Biomaterials, Biodegradables and Biomimetics), from University of Minho. The membrane was firstly frozen by liquid nitrogen and then cut into suitably sized specimen, which were coated with gold, prior to the analysis. The cross-section images were captured at 1 000x and 4 000x magnitude. Membrane thickness and pore size were measured during SEM analysis and are presented as the average of the values obtained from the captured images.

A microscopic cross-section image of membrane M9 is shown in Figure 29. As can be seen, the M9 membrane has asymmetric structure, consisting of a dense skin layer and a porous sub-layer. This sub-layer is formed by both, finger-like cavities and macrovoid structures. This asymmetric membrane was described by Chakrabarty et al. (260) for PSf membrane with NMP and PVP as solvent and additive, respectively. Also, the formation of the finger-like structure during the instantaneous demixing, due to the high mutual affinity between solvent (NMP) and nonsolvent (water) during the phase inversion process, was described and deeply explained by several authors (201, 205, 234, 235).

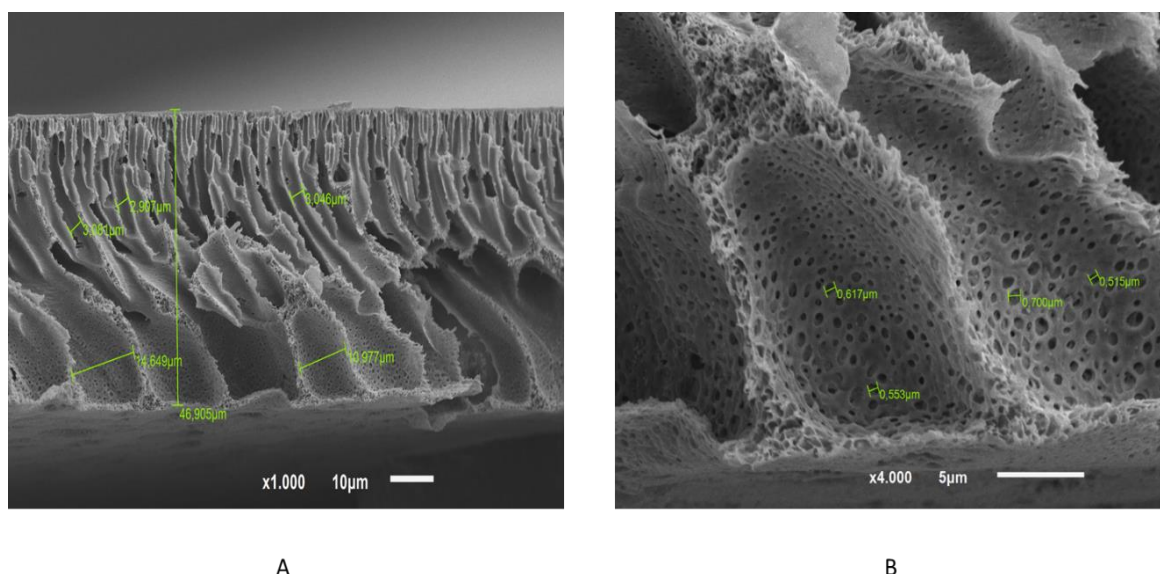


Figure 29: The SEM cross-section images of membrane M9. Magnification 1 000x (A), has depicted with green colour membrane thickness and size of finger-like voids; picture magnified 4 000x (B), with depicted diameters of pores. Accepted from (264).

Quantitative information about the membrane thickness can be also obtained from the cross-sectional SEM image. The membrane thickness was measured in five different membranes and the average values obtained were (mean  $\pm$  SD)  $53.98 \pm 5.32 \mu\text{m}$ . These results with a variation coefficient less than 10%, point to reproducibility of the membrane preparation procedure, particularly of the spin coating process.

#### 4.1.7.3. Mechanical properties

The tensile tests carried out to measure the strength of the material were kindly provided by Department of Nonwovens and Nanofibrous Materials, Technical University of Liberec. The tensile tests of the prepared membranes were conducted by Testometric M350-5 CT equipment. The membranes were cut in 2 cm wide stripes and eight samples from each were tested for maximum elongation at break, maximal force and Young's modulus.

The mechanical properties of M9 (15 wt% PSf, 2.5 wt% PVP K30, and 82.5 wt% of NMP) are summarized in Table 11. The obtained values from tensile tests could be compared to data showed in the work reported by Ravishankar et al. (268), where they carried out the tensile tests with PSf membrane without any additive. Comparing to these results, membrane M9 with 2.5 wt% of additive PVP presented reduced maximal elongation at break. This fact could be caused by increased porosity, induced by different aggregation of polymer chains after addition of PVP into the casting solution. Although the use of PVP in the casting solution did not improve the mechanical strength, the membranes without additive already showed good mechanical stability and sufficient elasticity to be incorporated into the microfluidic cell and used in flux.

Table 11 : Mechanical properties of membrane M9. The results ( $n = 8$ ) are expresses as mean  $\pm$  respective SD.

Parameters	mean $\pm$ SD
Maximal elongation at break [mm]	3.30 $\pm$ 0.62
Tensile strength [MPa]	2.76 $\pm$ 0.63
Young's modulus [MPa]	53.98 $\pm$ 4.63

#### 4.1.7.4. Porosity, density, and equilibrium water content

To evaluate the porosity ( $\epsilon$ ) and equilibrium water content (EWC) of the membrane, its void volume was determined by gravimetric measurement of entrapped water in the void pores. This evaluation procedure, as well as the used calculations, have been already described (269). A piece of membrane with an area of 16 cm<sup>2</sup> was soaked in deionized water for 1 h; the excess water was wiped off with paper tissue help and the membrane was

weighed ( $W_w$ ). Then, it was dried at 60 °C, for 24 h, and again weighed ( $W_d$ ). The EWC was calculated as the difference between these weights, according to Equation 15.

$$\% EWC = \frac{W_w - W_d}{W_w} \times 100 \quad (\text{Equation 15})$$

For density determination, the pycnometer method was used. To determine the volume ( $V$ ) of the membrane, the water mass variation given by the pycnometer with and without the membrane inside was registered, after correcting the values for the working temperature. The membrane porosity was calculated on the basis of the measurement of liquid content in the membrane pores, according to the Equation 13, which was already described.

According to the aforementioned equations, EWC is directly related to the membrane porosity, since the pores and the macrovoids in the sublayer are responsible for the retention of water inside the membrane structure. Thus, the higher the membrane porosity, the higher the EWC value. In addition, higher values of membrane porosity contribute to a better membrane flux; therefore, the increase of membrane porosity by using hydrophilic additives, is a very common approach. According to Ma et al. (270) the porosity of PSf membrane without any additive is about 18%. The results obtained for the membrane M9 with PVP K30 addition showed a porosity around 65% (Table 12). The EWC value of this membrane was  $66.86\% \pm 2.64\%$  (Table 12). These observed values were in accordance with literature (260), and therefore, the use of PVP K30 contributed to increase the membrane porosity and, thus, to enhance membrane permeability.

#### 4.1.7.5. Contact angle

The evaluation of the contact angle of the membrane had the collaboration of Innovation Center of Competence in Polymers, Science and Technology Park of University of Porto. The measurement was carried out with an OCA20 contact meter from DataPhysics equipment. Briefly, a drop of distilled water with an approximate volume of 4  $\mu\text{L}$  was placed on the membrane surface by a Hamilton® syringe, while the objective connected to the computer captured the image of the water drop deposited on the top of the membrane. The contact angle was calculated by the equipment software, as an average of the three drops measurements.

The contact angle ( $\theta$ ) is a membrane characteristic which relates its hydrophilicity/hydrophobicity and, thereby, is also related with protein fouling and, consequently, with membrane biocompatibility. The smaller the contact angle, the greater the hydrophilicity of the material. When the material has  $\theta < 90^\circ$ , it is already considered hydrophilic. The contact angle measured for membrane M9 was approximately  $62^\circ$  (Table

12). This result highlights the hydrophilic character of the membrane, due to the addition of PVP, and also supports the value obtained for the EWC, which translates the water's ability to penetrate the pores of the membrane structure.

#### **4.1.7.6. Protein adsorption**

Protein adsorption is a phenomenon that may occur during intradialytic blood circulation, when blood proteins are gradually deposited on the membrane surface, which leads to a decline in the flux and in membrane permeability. Protein adsorption experiment on the membrane's surface was carried out according to a procedure already described by Mahlicli et al. (220), with BSA dissolved in PBS pH 7.4. The amount of BSA in the solution corresponded to the physiological concentration of total plasma proteins. The membranes with an area of about 1 cm<sup>2</sup> were incubated in this BSA solution for 1 h, under moderate agitation. After the incubation, the membranes were washed with the buffer solution to remove unbounded proteins and the excess liquid was gently wiped off. Then, the membranes were placed into 1 mL of 1% SDS solution, which detached the bonded proteins from the membrane surface. Commercial Micro BCA™ Protein Assay Kit was used to determine the concentration of proteins, desorbed from the membrane, in SDS solution. This assay was used thanks to its sensitivity (lower limit of quantification = 0.5 µg mL<sup>-1</sup>) and compatibility with ionic detergents, as SDS. The absorbance of the solution was measured at 562 nm and the concentration was calculate based on a standard calibration curve.

As already noticed, the susceptibility of the membranes to adsorb proteins is correlated with their hydrophilic character and consequently its biocompatibility. In general, the hydrophilic membranes are considered to be less prone to protein adhesion and more biocompatible. The degree of hydrophilicity can also influence, besides protein adsorption, complement system activation, coagulation process, PLT adhesion and activation, which are known thrombotic risk factors.

The measured amount of adsorbed BSA on the surface of membrane M9 showed the average of 6.8 µg cm<sup>-2</sup> (Table 12). The susceptibility of this membrane to protein's adsorption was lower, when compared with the value found for PSf membrane without any additive (≈ 8 µg cm<sup>-2</sup>) (220). This result shows that by adding even a small amount of hydrophilic PVP the protein adsorption of the membrane was improved, which predicts improved biocompatibility.



Table 12 : Summary of evaluated characteristics of membrane M9. Data ( $n = 5$ ) are expressed as mean  $\pm$  SD.

Parameters	mean $\pm$ SD
Thickness [ $\mu\text{m}$ ]	53.98 $\pm$ 5.32
Porosity [%]	65.13 $\pm$ 7.98
Density [ $\text{g mL}^{-1}$ ]	0.320 $\pm$ 0.03
Equilibrium water content [%]	66.86 $\pm$ 2.64
Contact angle [ $\theta$ ]	62.50 $\pm$ 0.61
Protein adsorption [ $\mu\text{g cm}^{-2}$ ]	6.79 $\pm$ 1.77

#### 4.1.7.7. Biocompatibility

Material biocompatibility is the major requirement for HD membranes, as they are in long-term contact with patients' blood. Actually, the evaluation of biocompatibility is mandatory for every new type of medical device. This characteristic is required and governed by a standard document, in this case the ISO 10993-4: 2017 Biological evaluation of medical devices (251).

The biocompatibility studies included material-induced hemolysis, platelet activation, complement system activation, RBC morphology and blood coagulation tests. These experiments, involving the use of biological samples, were approved by the Ethic Committee of Faculty of Pharmacy, University of Porto, and were performed in compliance with the Declaration of Helsinki (271). All the volunteers gave their informed consent to participate in the study, prior to blood collection. To proceed with these biocompatibility experiments, blood samples were collected from healthy non-smoking volunteers.

The blood samples were collected by venepuncture into collection tubes with the anticoagulant sodium citrate. To standardize experiments, the haemoglobin (Hb) concentration was always adjusted to  $10 \text{ g dL}^{-1}$  with sterile PBS, pH 7.4. To evaluate the material biocompatibility, 1 mL of whole blood ( $10 \text{ g dL}^{-1}$  Hb) was incubated for 3 h at  $37^\circ\text{C}$  with specimens of PSf membranes, each with an area of  $1 \text{ cm}^2$ . Four independent assays were performed with two experimental duplicates including: 1) tested PSf membrane M9, 2) a biocompatible material (polyethylene), as an assay negative control and 3) blank (blood without any material). Afterwards, was performed the microscopic analysis of erythrocyte morphology, the membrane-induced haemolysis test and membrane-induced activation of PLTs.

## Erythrocyte morphology

The evaluation of RBC morphology would help to assess, by a simple and easy way, if the membrane material causes mechanical stress, associated with the roughness of the membrane surface. In such a case, tear cells, cell fragments, and schistocytosis would be observed in the blood smear. After the membrane samples incubation, described above, Wright stained blood smears were prepared and observed by optical microscopy to search for changes in RBC morphology (Figure 30). The observation of the blood smears showed no noteworthy RBCs morphological modifications, when compared to blood incubated without any material (blank). These results showed that the contact of blood with PSf membrane (M9) is safe and does not cause stress-inducing morphological changes of RBCs.

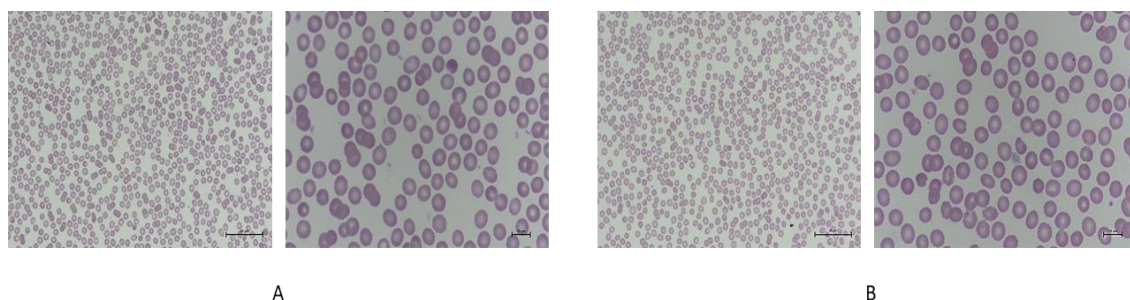


Figure 30: Optical microscopy images of Wright stained blood smears after incubation (3 h at 37 °C) of whole blood only (A) and whole blood incubated with PSf membrane M9. The images were taken with magnification 40x (left image) and 100x (right image).

## Membrane-induced haemolysis

To study the haemolysis induced by the prepared PSf membranes, the test recommended by ISO 10993-4: 2017, was used. According to this, the cut-off level of free Hb in plasma below which the material is considered non-haemolytic is 10 mg dL<sup>-1</sup> (272).

The haemolysis test was proceeded as follow: after the incubation process, described above, an aliquot of the blood sample (800.0 µl) was centrifuged (1 500 g for 10 min, at 4 °C) to obtain platelet-poor plasma. The absorbance of Hb in the plasma samples was measured spectrophotometrically at 540 nm, and the Hb values were obtained from a standard curve (ranging from 1 to 200 mg dL<sup>-1</sup>). Due to naturally occurring certain level of haemolysis, which is cause by the sample handling, the plasma Hb concentration, for each assay, was normalized by subtracting the plasma Hb concentration of the blank.

The plasma Hb concentrations, found after incubation of blood with polyethylene (negative control) and of blood with membrane M9, were 0.9 ± 1.5 and 5.9 ± 1.9 mg dL<sup>-1</sup>

(mean  $\pm$  SEM; n = 4), respectively. The level of Hb measured for M9 with 2.5 wt% PVP was below the recommended haemolysis cut-off value (272), showing that the prepared type of membrane is non-haemolytic, and can be considered as biocompatible.

#### **Material-induced platelets activation**

PLT activation on the membrane surface has been determined, as it is an important biocompatibility factor. To analyse the potential of the membrane to trigger platelet activation, blood samples were incubated with each material, as already described above. After incubation, blood samples were centrifuged for 15 min at 250 g, at 4 °C, to obtain PLT-rich plasma, which was diluted with PBS, in order to obtain suspensions containing about 250 000 PLTs. Then, the platelet suspensions were double-stained (for 15 min, light protected) with monoclonal antibodies for CD42a/GP9 PE and CD62P APC, allowing simultaneous staining of total and activated PLTs, respectively. PLT-specific events were identified by forward and side scatter signals, and 20 000 events were analysed by flow cytometry. Results are presented as percentage of activated PLTs (CD62P positive events) within total platelet count (CD42a positive events).

A negative control presented (mean  $\pm$  SEM)  $32.7 \pm 0.7\%$  of PLT activation, while the membrane M9 sample showed  $33.5 \pm 2.1\%$  of activated PLTs (no statistical difference between membrane sample and negative control was found). Compared to negative control, which was represented by a biocompatible material commonly used for blood-contact equipment, the PLT activation caused by contact with membrane surface was negligible. Therefore, the membrane is not expected to induce PLT activation when the membrane is in contact with blood.

#### **4.1.8. Concluding remarks**

PSf membranes with different casting solution composition were prepared by spin coating and phase inversion method. The membrane composition, as well as the spinning conditions, were optimized. The ideal membrane composition (the type of additive, its MW, and concentration) was optimized and selected, based on the results obtained. Data was collected through experiments performed in the flow system, including the following parameters: URR, lysozyme and BSA rejection. The selected membrane with optimal selective separation ability contained 15 wt% PSf, 2.5 wt% PVP K30, and 82.5 wt% on NMP

in the casting solution (M9). The use of the additive PVP enabled an adequate URR value, partial removal of middle size molecules and BSA rejection near to 100%.

This type of membrane underwent a set of tests to evaluate its most important characteristics, such as morphology, thickness, porosity, hydrophilic character, protein adsorption, mechanical strength, and biocompatibility. The introduction of the hydrophilic polymeric additive PVP K30 to the casting solution ameliorated membrane hydrophilicity and protein fouling, which are properties that have been associated with biocompatibility. The good biocompatibility of the membrane was further stated by material-induced haemolysis test and PLT activation, showing that haemolysis was below the established cut-off value and platelet activation was similar to that from the negative control (biocompatible material). Overall, these findings suggested good biocompatibility and potential of this membrane to be used for future fabrication of HD membranes.

This developed membrane was later used for other experiments and modifications, even beyond the framework of the present dissertation thesis. The experimental procedures and obtained results of the membrane preparation, optimization, and evaluation, have been published in the *Journal of Materials Science*, 2020,55:1292–1307 (Supplement 1).

## **4.2. Development of bioactive membranes by incorporation of antioxidants**

### **4.2.1. Introduction and main objectives of the experimental work**

Patients undergoing regular HD treatment have significantly pronounced OS, which may arise from several causes, namely from activation of leukocytes with release of different activation products into the bloodstream, such as ROS that are able to induce oxidative changes and have a negative impact, as already described. This blood cells activation is caused and related to the by poor biocompatibility of the material used for membrane fabrication. Due to the long-term and recurrent contact of blood with the HD membrane, the leukocytes are stimulated along each treatment session and ROS production may shortly exceed the reduction capacity of the antioxidant system of the patient. Although the improvement of membrane biocompatibility has come a long way, the level of ROS after a single HD treatment is 14 times higher, than before the treatment (103).

To diminish the OS induced during HD treatment, the strategy of using bioactive membranes, enriched with vitamin E, showed a reduction of OS levels in blood. This strategy allows a direct contact of the antioxidant with blood, enabling a rapid scavenging of ROS at the membrane site. It was reported that the use of a dialyser with this bioactive VEM provides more effective antioxidant defence than the oral administration of vitamin E to HD patients. To further increase the antioxidant activity provided by VEM during dialysis, the therapy may be enhanced by complementary administration of other antioxidants, such as vitamin C or lipoic acid. Although data from literature show the advantages of using a combined antioxidant therapy, no bioactive membrane prepared with vitamin E in conjunction with another antioxidant has yet been developed.

The main objective of this experimental work was to enrich the PSf membranes, previously developed, with the antioxidants  $\alpha$ -TCP and ALA, in order to introduce antioxidant capacity to the membranes; and, afterwards, to evaluate whether this change caused major changes in membrane characteristics, such as in the separation ability and biocompatibility. For this purpose,  $\alpha$ -TCP and ALA were incorporated into membranes during the preparation process, either separately or together in a mixture, and their *in vitro* antioxidant capacity, separation ability, and biocompatibility, were evaluated. The properties of the membranes modified with antioxidants were compared with each other and also with the unmodified membranes to determine, whether or not the enrichment was advantageous and, if so, which one was the most suitable and beneficial.

#### 4.2.2. Chemicals and Instrumentation

All the reagents and instruments used for membrane preparation and dialysis tests have been already described in Section 4.1.2. and, therefore, are not further listed. Only the reagents used specifically in the work that gave rise to this chapter will be detailed.

##### 4.2.2.1. Chemicals

Distilled ion-exchanged water, ultrapure water Milli-Q (Millipore water system, Merck, France), and analytical grade chemicals were used without further purification. (±)- $\alpha$ -lipoic acid, (±)- $\alpha$ -tocopherol, ethanol (EtOH) ( $\geq 99.5\%$ ); 2,4,6-Tris(2-pyridyl)-S-triazine (TPTZ), hydrochloric acid 37%, ferrous sulphate heptahydrate ( $\text{FeSO}_4 \cdot 7\text{H}_2\text{O}$ ); ferric chloride hexahydrate ( $\text{FeCl}_3 \cdot 6\text{H}_2\text{O}$ ), phosphoric acid, butanol and 2-thiobarbituric acid were all purchased from Sigma-Aldrich (St. Louis, MO, USA). SDS was purchased from Honeywell Fluka™. Micro BCA™ Protein Assay Kit and monoclonal antibodies for CD42a PE and CD62P APC were obtained from Thermo Fisher Scientific, (MA, USA). Kits required for coagulation tests were bought from TECO (Diagnostica Stago, Almada, Portugal). Plasma levels of components of complement system human C3a and human C5a (two components of an activated complement system) were quantified by commercially available enzyme-linked immunosorbent assays (Affymetrix eBioscience, Thermo Fisher Scientific, IL, USA). Acetate buffer 300 mM pH 3.6 was prepared by dissolving glacial acetic acid anhydrous (Merck, (Darmstadt, Germany) and sodium acetate anhydrous (Sigma Aldrich Co.). Phosphate buffered saline solution pH 7.4, Bradford reagent, and Erlich's reagent were prepared as already described (Section 4.1.2.1)

##### 4.2.2.2. Instrumentation

Ultrasonic cleaner (Thermo Fisher Scientific, MA, USA) was used to degas polymer solution. Absorbance measurements were carried out by a microplate reader (Synergy™ HT, BioTek Instruments, USA) or by UV-VIS double-beam spectrophotometer (Jasco V-660, GmbH, Germany). Fluorescence of  $\alpha$ -TCP was measured by spectrofluorometer (Jasco FP-6500, GmbH, Germany). Flow cytometer (BD Accuri C6, BD Pharmingen) was used for platelet analysis. Optical microscope (Nikon Eclipse Ci) was used to study the morphology of blood cells. Automated blood cell counter (Sysmex K1000; Sysmex, Hamburg, Germany) was used to provide blood cell counts.

#### **4.2.3. Statistical data analysis**

Statistical analysis was carried out using the Statistical Package for Social Sciences (SPSS), version 25.0, (IBM SPSS, Chicago, IL, USA) for Windows. Dixon's Q test was used to identify the outlier values. Shapiro-Wilk test was used to assess the normality of data distribution. Data were presented as mean  $\pm$  SEM, mean  $\pm$  SD (standard deviation) or as median [IQR] (interquartile range), as appropriate. To compare sets of variables that presented Gaussian distribution, the One-Way ANOVA test (coupled with Bonferroni Post Hoc) was used. The Kruskal-Wallis test was chosen to compare sets of data that did not present Gaussian distribution. For the variables studied in biocompatibility evaluation, the non-parametric Friedman's test for repeated measures was used to compare sets of data. A  $p$ -value  $< 0.05$  was considered statistically significant.

#### **4.2.4. Preparation of modified PSf membrane with antioxidants**

For PSf membrane modification with the antioxidants  $\alpha$ -TCP (Figure 5) and ALA (figure 6), two different strategies were followed: direct incorporation (blending) of the antioxidant(s) into the membrane, and surface coating by an adsorption process. The blending method involved incorporation of the antioxidant into the membrane structure, during the preparation process. For this, a fixed amount of antioxidant was dissolved in the NMP solvent and this solution was subsequently used as the casting solution for membrane preparation, as already described in Section 4.1.4. The second method is based on the adsorption of the antioxidant(s) by the membrane surface, after its preparation. The modification, by this later method, was carried out by dissolving the antioxidant(s) in EtOH, in the same concentration which was used in the blending experiment. Samples of PSf membranes with about 16 cm<sup>2</sup> of area were placed in contact with 10 mL of the antioxidant solution and incubated for 10, 30, 60, and 120 min. It was found that after the adsorption experiment, no antioxidant activity was observed in the membranes prepared by this modification process.

Considering the blending method, the enriched membranes were prepared according to the procedure already described above in Sections 4.1.4 and 4.1.6, with minor modifications. Briefly, the casting solution containing the antioxidant(s) was kept cold and light protected during dissolution and casting process, to prevent the degradation of the antioxidant(s) by light or high temperature. For the same reason, the steps of ultra-high dispersion and degassing using probe type ultrasonicator were omitted, to prevent overheating of the solution. The degassing process was replaced by using a bath sonicator,

containing ice, to maintain the temperature low during this process. The prepared membranes were dried and stored in local protected from light, at the temperature of 4 °C.

#### 4.2.5. Optimization of the amount of antioxidant in the casting solution

The amount of antioxidant(s) incorporated in the PSf membranes had to be optimized, since the introduction of a new compound to the casting solution could affect the membrane structure during their preparation process. This optimization was conditioned by two factors: the concentration of  $\alpha$ -TCP and ALA should be sufficient to guarantee the presence of antioxidant activity; the separation and biocompatibility characteristics of the membrane should not be altered. Therefore, membranes with various concentrations of  $\alpha$ -TCP (5, 10, and 20 mg mL<sup>-1</sup>) and ALA (10, 20, 40, 60 mg mL<sup>-1</sup>) in NMP were prepared and their major characteristics were subsequently evaluated by the set of methods already described (Section 4.1.7). The separation ability for small molecules and URR was performed, and the results compared with those from the unmodified PSf membrane, to understand if the introduction of a new compound into the casting solution affected the membrane characteristics. The selected optimal concentrations for  $\alpha$ -TCP and for ALA were then both dissolved in NMP to prepare another type of modified membrane. The properties of this new membrane were then compared with those of the membranes containing only one of the antioxidants. The URR was measured according to the procedure previously described in Section 4.1.7.1. Modified membranes with  $\alpha$ -TCP in the concentrations from 5 to 20 mg mL<sup>-1</sup> dissolved in NMP, were studied and the corresponding URR values are presented in Figure 31A.

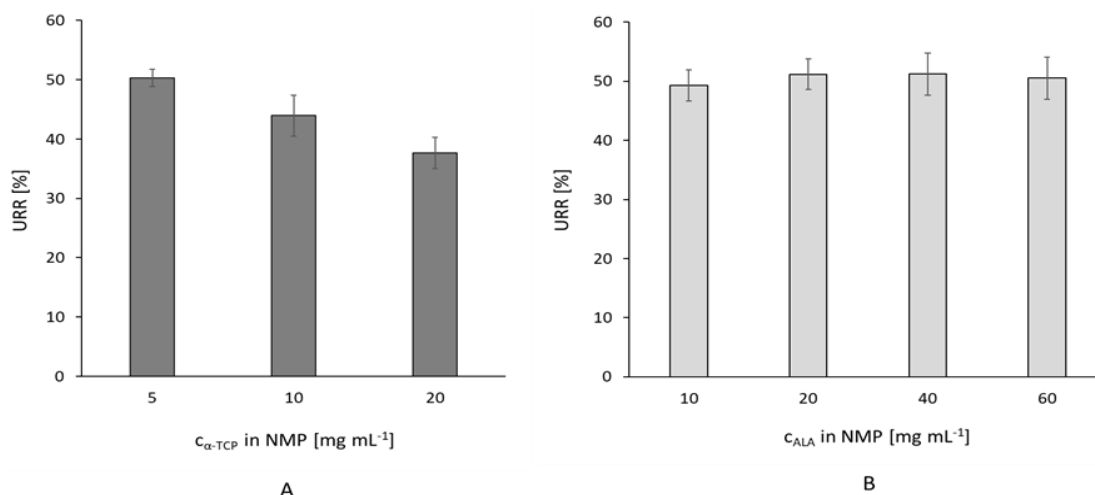


Figure 31: Urea reduction ratio (URR [%]) of PSf membranes modified with different concentrations of  $\alpha$ -TCP (A) and ALA (B). The results from 10 different experiments are presented as mean  $\pm$  SEM



It was observed that increasing the concentration of  $\alpha$ -TCP in PSf membranes, from 5 to 20 mg mL<sup>-1</sup>, the URR value reduced from 57% to 37%, respectively. The decrease of URR may be caused by an alteration in the membrane porosity, due to the lipophilic character of  $\alpha$ -TCP, which may slow down the diffusion rate between solvent and nonsolvent during the phase inversion process. This delayed demixing leads to a denser, spongy membrane, as was already described. Therefore, this structural change may lead to a lower membrane permeability. Considering that the permeability for small molecules is a crucial characteristic for HD membranes, the following studies were carried out with PSf membranes prepared with 5 mg mL<sup>-1</sup>  $\alpha$ -TCP in NMP.

To optimize the concentration of ALA for the modification of PSf membranes, the same procedure of URR experiment was performed. Based on the different lipophilicity and antioxidant capacity of ALA, when compared to  $\alpha$ -TCP, higher concentrations were selected to enrich PSf membranes. The tested concentrations ranged from 10 to 60 mg mL<sup>-1</sup> of ALA, in NMP. The URR results were very similar (approximately 50%) for all tested concentrations (Figure 31B), suggesting that the increase in the concentration of ALA had no influence on the structure of the membranes.

Besides the membrane permeability for small molecules, the antioxidant activity of the prepared membranes must be also evaluated, to select the optimal antioxidant concentration. Therefore, the next step was to assess the antioxidant activity of PSf modified membranes; the concentration of  $\alpha$ -TCP was fixed at 5 mg mL<sup>-1</sup> in NMP, since higher concentrations negatively affected URR values; the concentration of ALA had to be further studied, as any of the tested ALA concentrations did not affect the URR values.

The antioxidant activity of the modified membranes was estimated, based on their redox potential of Fe<sup>3+</sup>. This was measured according to the FRAP assay, previously described by Benzie and Strain (273). As already noticed, FRAP (ferric reducing antioxidant power) method relies on the reduction by the antioxidants, at low pH, of the Fe<sup>3+</sup>-TPTZ complex (colourless) to Fe<sup>2+</sup>-TPTZ (blue coloured complex). The binding of Fe<sup>2+</sup> to the ligand creates a blue colour, which is monitored by the absorbance measured at 593 nm. The FRAP reagent was freshly prepared by mixing acetate buffer, 40 mM TPTZ in HCl, and 20 mM FeCl<sub>3</sub>.6H<sub>2</sub>O in the proportion of 10:1:1 (V/V). In a plastic Petri dish, 4 mL of FRAP reagent was added to the membrane samples with an area of about 16 cm<sup>2</sup>. A membrane prepared without antioxidants was used as a blank. The absorbance of the solution was measured at 593 nm, after 4 h of incubation under constant slow agitation at 37 °C, simulating the duration of HD treatment. The calibration curve was prepared by plotting the absorbance at 593 nm versus the appropriate concentrations of FeSO<sub>4</sub>.7H<sub>2</sub>O. All the measurements were carried out in three independent experiments, run in triplicate.

The PSf membranes enriched with 10, 20, 40, and 60 mg mL<sup>-1</sup> of ALA in NMP did not show a proportional increase of redox capacity with ALA concentration, especially with the highest concentrations (Figure 32). This could be explained by saturation of PSf membrane and/or by removal of the excessive ALA during the phase inversion process. Based on these observations, the concentration of 40 mg mL<sup>-1</sup> of ALA was selected for further experiments, since it appears to correspond to the saturation concentration of ALA at the membrane. Therefore, this concentration seems to be associated with adequate values of URR and antioxidant activity.

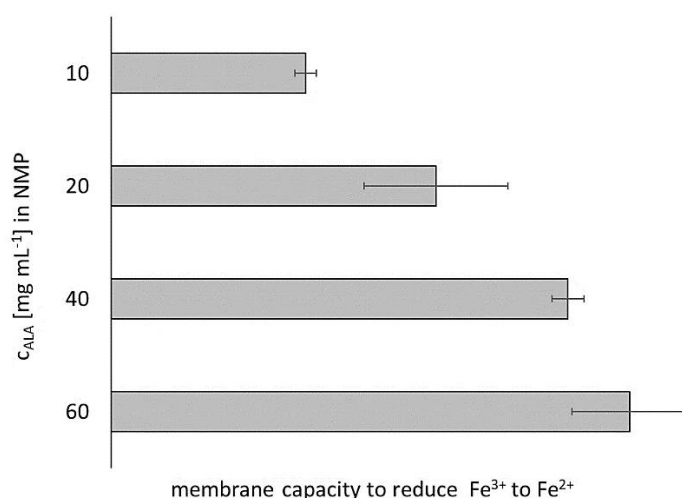


Figure 32: Comparison of the redox capacity of modified membranes prepared with different concentrations of ALA, evaluated by FRAP assay (n = 3).

The selected PSf membrane modified with 5 mg mL<sup>-1</sup> of  $\alpha$ -TCP (referred as PSf -  $\alpha$ -TCP) presented a desirable URR, although its antioxidant capacity was much lower than that showed by the modified PSf membrane with 40 mg mL<sup>-1</sup> ALA (with designation PSf - ALA) (Figure 33). It should be pointed out, that when the membrane is modified with  $\alpha$ -TCP in the same concentration of PSf- ALA (40 mg mL<sup>-1</sup> in NMP), an increase in the antioxidant activity of PSf -  $\alpha$ -TCP was observed. However, it was found that in this concentration of  $\alpha$ -TCP the performance of the membrane is affected, making it unsuitable for HD purposes.

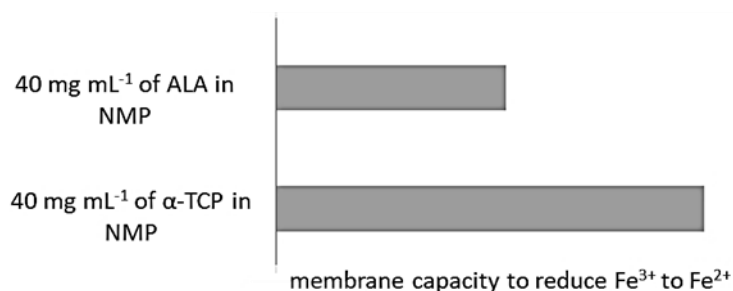


Figure 33: Comparison of the redox capacity of membranes modified with ALA and  $\alpha$ -TCP, evaluated by FRAP assay.

It was already described that when ALA and  $\alpha$ -TCP are used together, the antioxidant capacity is improved, as ALA is able to reduce oxidized  $\alpha$ -TCP (128). Thus, the reduced form of ALA preserves  $\alpha$ -TCP antioxidant activity, improving its antioxidant activity. In order to combine the beneficial effects of both antioxidants and to enhance antioxidant activity, a mixture of  $\alpha$ -TCP and ALA (referred as PSf -  $\alpha$ -TCP/ALA) in the concentrations of 5 mg mL<sup>-1</sup> and 40 mg mL<sup>-1</sup>, respectively, was prepared, in NMP and added to the casting solutions. Both concentrations of  $\alpha$ -TCP and ALA were selected according to the previous results, concerning to membrane separation ability (URR value) and antioxidant capacity (FRAP values) of the membranes containing a single antioxidant. The redox capacity of all three types of enriched membranes (PSf -  $\alpha$ -TCP, PSf - ALA, and PSf -  $\alpha$ -TCP/ALA) were measured by FRAP assay.

Figure 34 shows the antioxidant capacity found for the three type of prepared membranes. As can be seen, the mixture of the two antioxidants helps to increase the antioxidant capacity of the membranes, in accordance with the aforementioned (128). The membrane enriched with the combination of the antioxidants showed the highest redox capacity. Thus, the data show that mixing both antioxidants further contributed to increase the redox potential of the membrane, by combining their antioxidant properties.

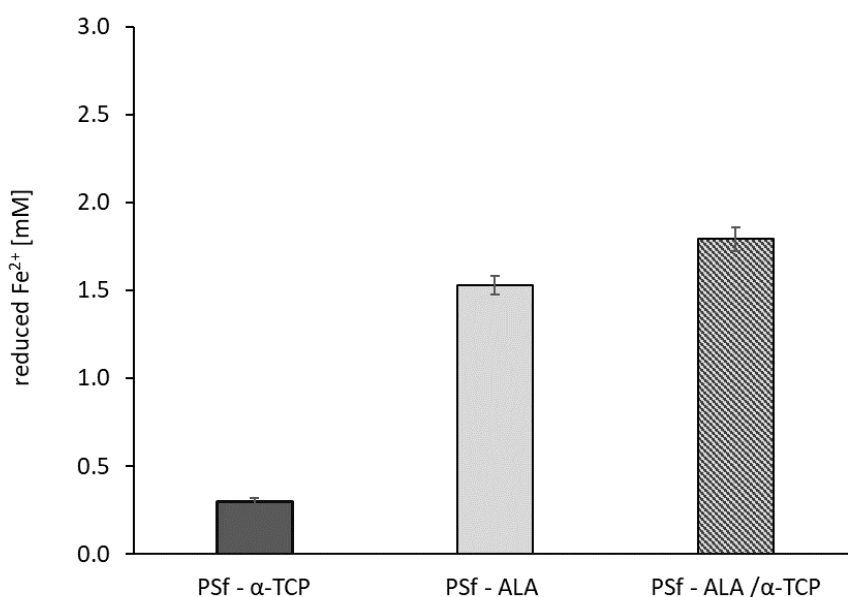


Figure 34: Antioxidant activity of PSf membranes enriched with 5 mg mL<sup>-1</sup>  $\alpha$ -TCP in NMP; with 40 mg mL<sup>-1</sup> ALA in NMP; and, with a combination of both (40 mg mL<sup>-1</sup> ALA/5 mg mL<sup>-1</sup>  $\alpha$ -TCP). Results (n = 3) are expressed as mean  $\pm$  SD.

#### 4.2.6. Dialysis experiment

As already noticed, the selective permeability of solutes is a very important membrane characteristic in haemodialysis. The effect of modifying the membranes with antioxidants caused changes in their separation characteristics and this effect was also studied. After optimizing the  $\alpha$ -TCP and ALA concentration to be incorporated in the casting solution, all the developed membranes were evaluated in flow conditions, to measure their selective permeability. The obtained results were compared with those obtained for unmodified membranes.

The dialysis experiment was carried out with urea, human lysozyme and BSA, according to the procedure already described in Section 4.1.7.1. The URR results, shown on Figure 35, demonstrated that all the modified membranes are fully permeable for small molecules, as the URR% values ( $n = 5$ ) were  $51.2 \pm 3.6$ ;  $50.3 \pm 1.5$ ;  $49.7 \pm 4.2$ , for PSf – ALA, PSf –  $\alpha$ -TCP and PSf – ALA/ $\alpha$ -TCP membranes, respectively, and did not differ ( $p = 0.104$ ) from the URR of the unmodified PSf membrane ( $52.4 \pm 4.6$ ).

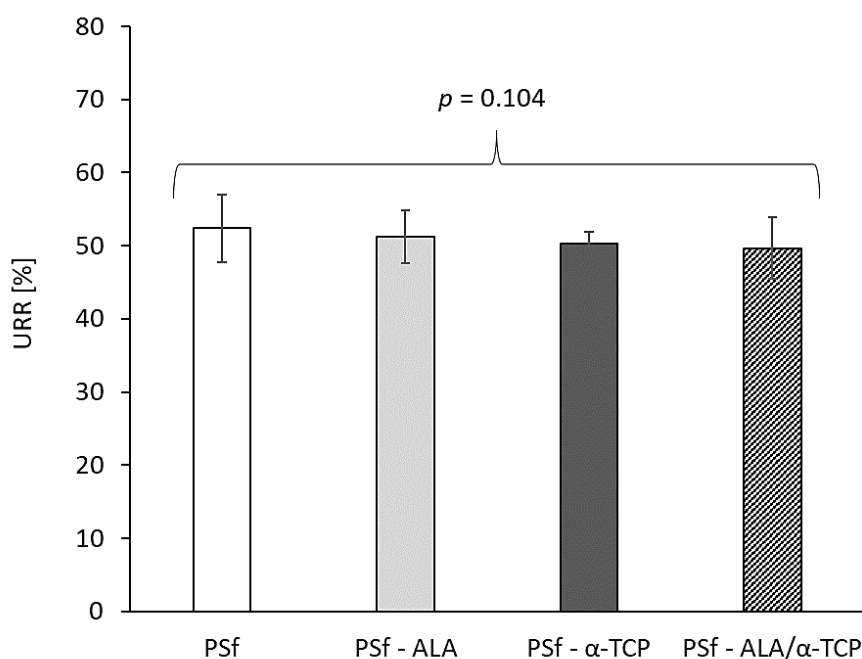


Figure 35: URR values presented by unmodified and modified PSf membranes. Results ( $n = 5$ ) are expressed as mean  $\pm$  SD.

The results of protein rejection, presented in Figure 36, show that the rejection of lysozyme differs significantly between unmodified PSf and enriched membranes. The percentage of lysozyme rejection values were  $50.2 \pm 2.0\%$  for unmodified PSf and  $60.8 \pm 0.5\%$ ,  $57.3 \pm 1.0\%$  and  $57.3 \pm 2.0\%$  for PSf - ALA; PSf -  $\alpha$ -TCP, and PSf - ALA/ $\alpha$ -TCP, respectively. This higher rejection of lysozyme reflects a reduced permeability of the

enriched membranes for middle-sized molecules. On the contrary, the results of BSA rejection did not differ from the unmodified membranes ( $p = 0.422$ ). The BSA rejection reached approximately 95% for all types of membranes, indicating that the membranes are nearly impermeable for large proteins and, therefore, can prevent excessive plasma albumin leakage during the HD process

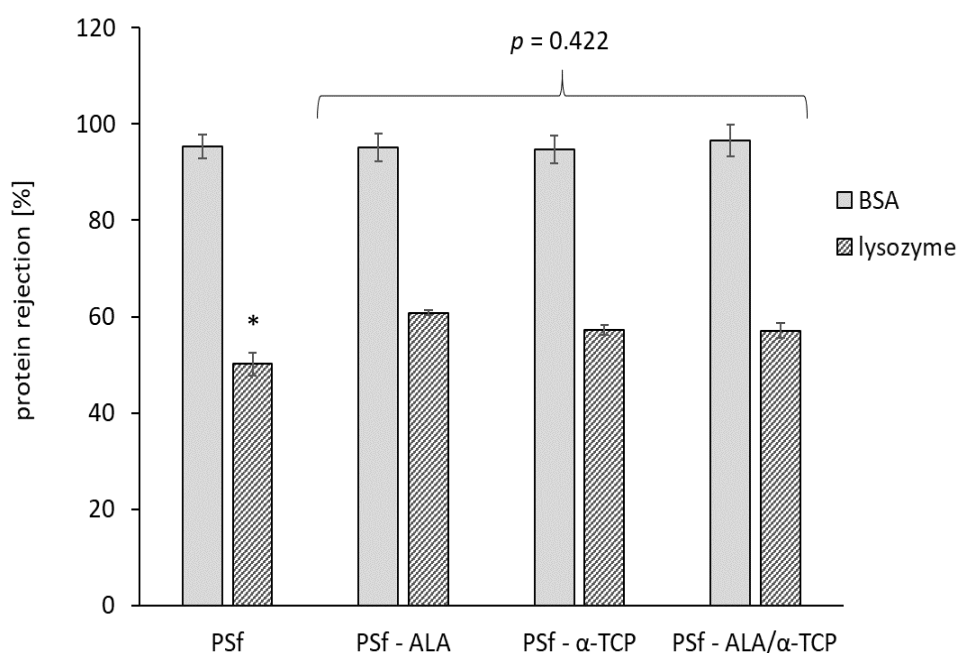


Figure 36: Protein rejection (BSA and human lysozyme) of unmodified and modified PSf membranes, enriched with 5 mg mL<sup>-1</sup> α-TCP in NMP, 40 mg mL<sup>-1</sup> ALA in NMP and with a combination of both (40 mg mL<sup>-1</sup> ALA/5 mg mL<sup>-1</sup> α-TCP). The results (n = 5) are expressed as mean ± SD.

\* Versus all three types of enriched PSf membranes:  $p < 0.05$ .

These results, from the protein rejection experiments, suggest that the presence of lipophilic antioxidants in the casting solution partly affects the membrane formation, namely membrane porosity and/or pores size distribution; further measurements of pore size distribution actually proved that this parameter was not different for modified and unmodified membranes. Nevertheless, these changes observed for the lysozyme rejection are not as relevant, that would prevent the use of the modified membranes for the HD treatment.

#### 4.2.7. Antioxidant stability of the modified membranes over storage time

The antioxidants are known to be unstable molecules, sensitive to light and temperature. Although the modified membranes were stored in a cool place (4 °C) and light protected, it was necessary to evaluate the stability of the antioxidants incorporated into the membrane, over storage time. Three membranes obtained from different batches, enriched

with  $\alpha$ -TCP, ALA, and with their combination, were stored for 8 weeks in the above-mentioned conditions. The stability of their antioxidant activity was assessed weekly. For that, samples with an area of about 1 cm<sup>2</sup> were cut from each membrane and placed into a well of a 24 wells plate. A volume of 1 mL of freshly prepared FRAP reagent was added to each sample and incubated for 4 h, at 37 °C, under gentle agitation. The redox potential was evaluated according to the procedure described before (Section 4.2.5).

During the 8 weeks of storage a decrease in the antioxidant activity, of 27%, 11%, and 19%, was found for PSf -  $\alpha$ -TCP, PSf - ALA, and PSf - ALA/ $\alpha$ -TCP membranes, respectively. The best antioxidant stability, shown by PSf – ALA membrane, could be explained by the fact that its reduced form still possesses antioxidant activity, helping to preserve this activity for a longer time period. In a study published by Mahlicli et al. (220), the authors evaluated the stability off membranes enriched with ALA and reported a decrease of 19% in the antioxidant activity, although the storage conditions were different (4h at 37 °C). This result confirms that storage at 4 °C used for the developed membranes is the most suitable.

Nevertheless, all the modified membranes were used for experiments within one week after their preparation, to diminish the risk of degradation of the incorporated antioxidants.

#### **4.2.8. Antioxidant leaching from the modified membranes**

To evaluate the strength of the antioxidants incorporation into the membrane structure and to assess their release into the blood during the HD conditions, studies to estimate the leaching degree of antioxidants from the modified membranes were performed. For that, membrane samples with an area of about 4 cm<sup>2</sup> were cut, placed into 12 wells plate, and incubated with 1 mL of PBS (pH 7.4). The plates with membrane samples were incubated for 4 h, light protected, under constant orbital shaking (600 rpm). After the incubation time, PBS was collected and the amount of ALA and  $\alpha$ -TCP leached from the membranes into PBS was evaluated spectrophotometrically ( $\lambda$  = 333 nm) and fluorometrically ( $\lambda_{\text{ex}}$  = 290 nm;  $\lambda_{\text{em}}$  = 235 nm), respectively. The concentration of leached ALA from PSf – ALA and from PSf - ALA/ $\alpha$ -TCP membranes, was  $0.18 \pm 0.008$  (n = 4) and  $0.15 \pm 0.007$  (n = 4), respectively. The leached amount of  $\alpha$ -TCP from PSf -  $\alpha$ -TCP and PSf - ALA/ $\alpha$ -TCP membranes, was negligible, since the fluorescence intensity of the blank and the samples, were similar.

The measured levels of released antioxidants were low, despite the rigorous shaking conditions, showing the efficiency of the modification method used, via blending of the

antioxidants in the casting solution, and, therefore, their effective incorporation into the PSf membrane structure. Thus, this modification strategy was proved to be appropriate, and may be also due to the good solubility of both antioxidants in the solvent NMP.

#### **4.2.9. Antioxidant capacity *in vitro*: blood assays**

To establish if the antioxidant effect of modified membranes PSf – ALA, PSf -  $\alpha$ -TCP, and PSf – ALA/ $\alpha$ -TCP could be used *in vivo* for the HD treatment, they were incubated with blood collected from healthy volunteers. The blood collection and further blood processing was already described in Section 4.1.7.7. After the incubation of membrane samples with blood, the levels of lipid peroxidation (LPO) of PLT-poor plasma, total antioxidant status (TAS) and of ascorbic acid (AA), were quantified.

To determine LPO of PLT-poor plasma (to obtain PLT-poor plasma, the blood samples were centrifuged at 1500 g for 10 min, at 4 °C) the method previously described by Mihara et al. (274), with minor modifications, was used. Briefly, 40  $\mu$ L of PLT-poor plasma was mixed with 180.0  $\mu$ L of 1% H<sub>3</sub>PO<sub>4</sub> (v/v) and 60  $\mu$ L of 0.6% thiobarbituric acid (TBA) (w/v), and this mixture was heated in boiling water for 45 min. After cooling down on ice, for 10 min, TBA reactive substances were extracted into butanol, by agitation. The butanol layer was then separated by centrifugation and the absorbance was measured spectrophotometrically, at 535 nm. TAS and AA levels were evaluated by FRAP assay, previously described in Section 4.2.5. Blood samples were also incubated without membranes, to normalize LPO, TAS, and AA plasma levels.

The measured values from LPO, TAS, and AA experiments are listed in Table 13. The results show that the modified membranes were associated with a diminishment of plasma LPO and an increase in TAS median values, when compared with unmodified PSf membranes, although without statistical significance. The highest AA level was found for PSf - ALA membranes, which could reflect the synergistic effect of ALA with other antioxidants. Overall, these results appear to be encouraging, regarding the antioxidant capacity of these modified membranes, when tested with biological samples.

Table 13 : Lipid-peroxidation (LPO), total antioxidant status (TAS) and ascorbic acid (AA) plasma levels after incubation of whole blood with membrane samples. All values were normalised, subtracting the value of the blank samples (whole blood incubated without material). Data are presented as median (IQR). A  $p < 0.05$  value was considered statistically significant.

	PSf	PSf – ALA	PSf - $\alpha$ -TCP	PSf - ALA/ $\alpha$ -TCP	<i>p</i>
<b>LPO</b> [nM]	0.32 (-0.87 – 0.93)	0.19 (-0.64 – 0.74)	0.13 (-0.64 – 0.71)	0.26 (-0.19 – 0.71)	0.892
<b>TAS</b> [ $\mu$ M]	-10.1 (-19.0 – -1.99)	5.13 (-16.4 – 14.7)	0.07 (-12.2 – 20.4)	15.1 (0.46 – 20.4)	0.145
<b>AA</b> [ $\mu$ M]	0.27 (0.04 – 2.28)	2.24 (0.14 – 2.60)	0.70 (-1.30 – 1.79)	-0.07 (-1.33 – 0.62)	0.272

#### 4.2.10. Morphology of the modified membranes

After the selection of antioxidant concentrations, which after incorporation into casting solution preserved the membrane characteristics, adequate for HD, the morphologic evaluation was carried out. The modified membranes were subjected to a morphological study to understand whether the addition of antioxidants influenced their final morphological structure, since changes in the rejection of human lysozyme were observed during the dialysis test. The SEM analysis was kindly provided by Technical University of Liberec, using scanning electron microscope TESCAN Vega 3SB (Czech Republic). Prior the SEM analysis, the sample were frozen in liquid nitrogen and cut into an appropriate size. Then, the samples were sputter coated with gold and analysed. The characterization of the membrane thickness was done by image analysis software. Further image analysis was used to characterize membrane cross-section structure from SEM pictures, using the software NIS Elements (LIM s.r.o., Czech Republic). The average pore size was calculated from 50 measurements of three different membrane batches.

The morphological structure of unmodified PSf and modified membranes containing antioxidants are presented in Figure 37. All the membranes have very similar asymmetric structure, with thin skin layer (approximately 0.7  $\mu$ m) and spongy thick sub-layer (approximately 50  $\mu$ m). No important morphological changes associated to antioxidant incorporation were observed. The similarity of the structure between membranes may be due to good solubility of both antioxidants in NMP, and therefore the diffusion process of solvent into coagulation bath was not disturbed or delayed. Membranes pore size was determined from the SEM images and showed similar values for all membranes, within a range from 0.59 to 0.73  $\mu$ m.



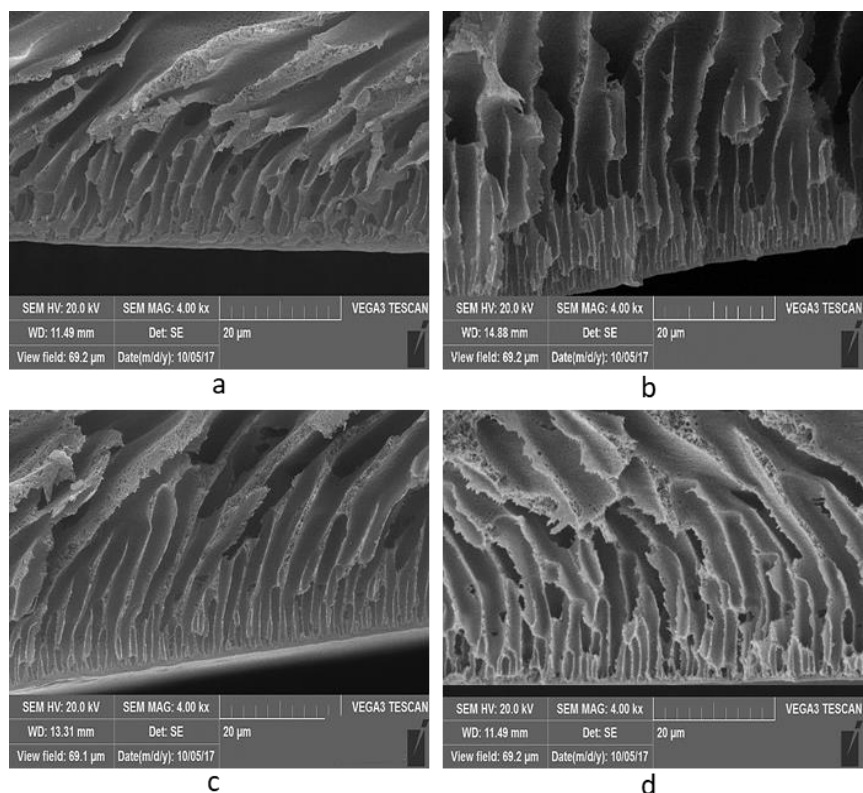


Figure 37: Cross-section images of PSf – ALA (a), PSf -  $\alpha$ -TCP (b), PSf - ALA/ $\alpha$ -TCP (c), and unmodified PSf membranes (d), by scanning electron microscopy (SEM).

#### 4.2.11. Mechanical properties

During the HD process, the membrane undergoes various mechanical burdens. Hence, HD membranes must have mechanical strength and elasticity to resist to the dynamic flow of blood/dialysate, to the hydrostatic pressure across the membrane and to the fluctuation of pressure pump propel. To assess whether the introduction of antioxidants into the membrane structure did not influence its mechanical properties, the tensile tests were carried out, as previously described in Section 4.1.7.3. The results obtained from modified membranes were compared to unmodified ones, and the measured values are summarized in Table 14. The membrane enriched with  $\alpha$ -TCP showed significantly higher Young's modulus and similar tensile strength and elongation at break, suggesting that the introduction of that antioxidant into the membrane structure brings a slight improvement in its mechanical properties, as compared to the others.

Table 14 : Mechanical properties values of unmodified and modified PSf membranes PSf - ALA, PSf -  $\alpha$ -TCP, and PSf - ALA/ $\alpha$ -TCP. The results ( $n = 5$ ) are presented as mean  $\pm$  SD.

Parameters	PSf	PSf - ALA	PSf - $\alpha$ -TCP
Young's modulus [MPa]	53.60 $\pm$ 4.63*	56.07 $\pm$ 3.03**	64.30 $\pm$ 1.78
Maximal tensile strength [MPa]	3.30 $\pm$ 0.62	2.93 $\pm$ 0.63	3.32 $\pm$ 0.61
Maximal elongation at break [mm]	2.76 $\pm$ 0.63	2.96 $\pm$ 0.67	3.56 $\pm$ 0.92

\*  $p < 0.01$  when compared to other types of membranes

\*\*  $p < 0.05$  when compared to other types of membranes

#### 4.2.12. Contact angle

The water contact angle defines the biomaterial hydrophilicity; a low water contact angle signifies hydrophilic character of the material and therefore good biocompatibility. The contact angle measurement was previously described in Section 4.1.7.5. The obtained results for the developed membranes are shown in Table 15. The membranes modified with  $\alpha$ -TCP showed significantly higher water contact angle, when compared to unmodified PSf membrane and to the modified PSf - ALA and PSf - ALA/ $\alpha$ -TCP membranes ( $p < 0.001$ ). This could be explained by the higher lipophilic character of  $\alpha$ -TCP that, after incorporation into membrane structure, increases its hydrophobicity. Nevertheless, according to the literature (275) a borderline value of the water contact angle, dividing material from protein non-adherent to adherent, is 65°. The values of contact angle of and all types of the modified membranes are below this borderline value. Therefore, it can be assumed that even after introducing hydrophobic antioxidant into the membranes structure, they maintain hydrophilic character and present a low tendency to bind proteins, which was confirmed by further biocompatibility evaluation tests.

Table 15: Water contact angle values of unmodified and modified PSf membranes PSf - ALA, PSf -  $\alpha$ -TCP, and PSf - ALA/ $\alpha$ -TCP. The results ( $n = 5$ ) are presented as mean  $\pm$  SD.

Membrane type	Water contact angle [°]
PSf	62.5 $\pm$ 0.61
PSf - ALA	58.3 $\pm$ 0.15
PSf - ALA/ $\alpha$ -TCP	62.7 $\pm$ 0.16
PSf - $\alpha$ -TCP	64.8 $\pm$ 0.20*

\*  $p < 0.05$  when compared to other types of membranes

#### 4.2.13. Protein adsorption

A low protein adsorption is associated with material hydrophilicity, thus with biocompatibility and is strongly associated with membrane separation ability. Membrane protein adhesion may lead to different adverse blood changes, including an inflammatory response and an increase in cardiovascular risk events. As already noticed, the bioactive membranes were reported to present lower protein adsorption, when compared to conventional ones. Therefore, the adsorption of proteins by membranes modified with antioxidants was compared with that of unmodified PSf membranes.

Protein adsorption experiment was carried out according to the procedure described in Section 4.1.7.6. Protein adsorption levels of modified PSf -  $\alpha$ -TCP and the PSf - ALA/ $\alpha$ -TCP presented a significant decrease in the amount of adsorbed proteins, when compared to the unmodified PSf membrane (Figure 38). This shows that the incorporation of antioxidants, especially the combination of ALA with  $\alpha$ -TCP, may positively influence the membrane biocompatibility.

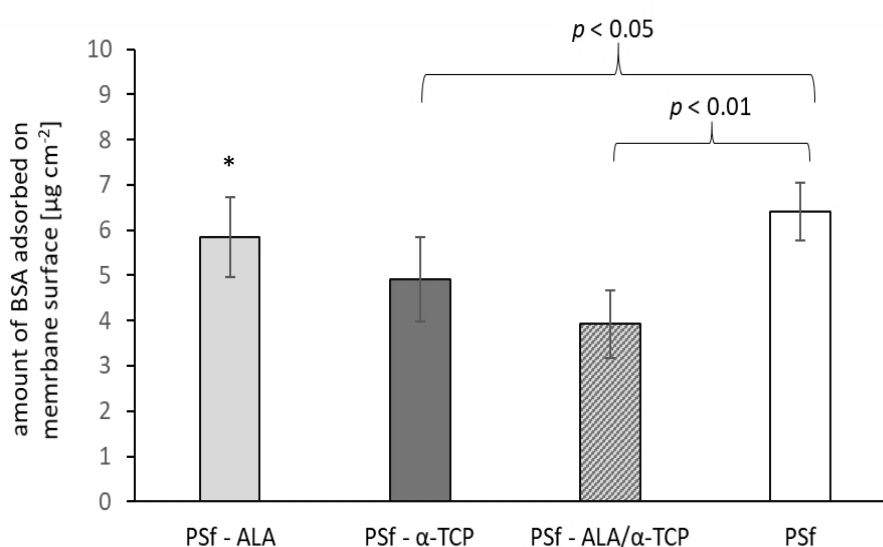


Figure 38: Adsorption of BSA on unmodified and modified PSf membranes.

\* Versus PSf - ALA/ $\alpha$ -TCP:  $p < 0.05$ .

BSA: bovine serum albumin

#### 4.2.14. Biocompatibility

To determine if the introduction of antioxidants into PSf membrane structure can further contribute to improve biocompatibility, a set of tests was performed. The modified membranes were evaluated in terms of morphological changes of RBCs assessment, haemolytic effect, and activation of platelet, coagulation and complement system. These

biocompatibility experiments were carried out according to the ISO 10993-4: 2017 Biological evaluation of medical devices (251) recommendations and the respective procedures were previously described in chapter 4.1.7.7.

### Erythrocyte morphology

The assessment of morphological changes of RBCs caused by contact of blood with modified membranes was performed by using the procedures already described in Section 4.1.7.7. The thorough observation of blood smears (Figure 39) showed no noteworthy RBC morphological modifications, when comparing blood samples incubated with unmodified and modified PSf membranes and with blood alone (blank). This shows that the contact of blood with modified PSf membranes is safe and does not cause stress-inducing morphological changes of RBCs.

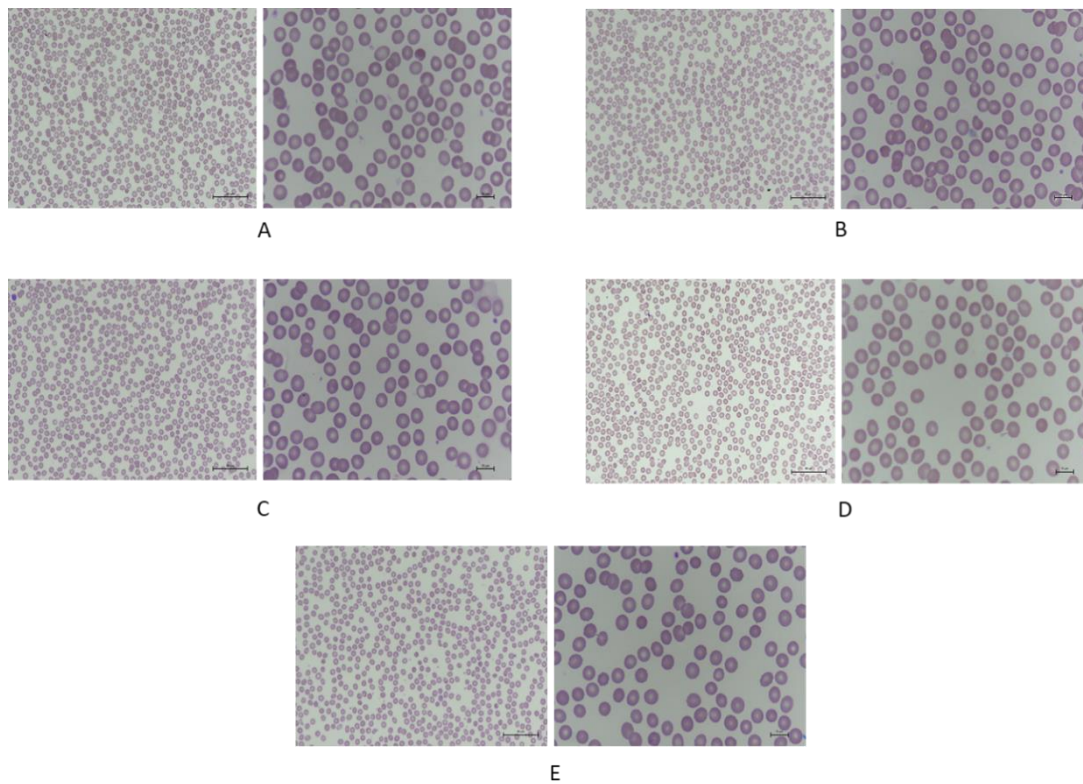


Figure 39: Optical microscopy images of Wright stained blood smears after incubation of whole blood with unmodified and modified PSf membranes: A) blank (only blood), B) PSf, C) PSf -  $\alpha$ -TCP, D) PSf - ALA and E) PSf - ALA/ $\alpha$ -TCP (left side – 40x ampliation; right side – 100x ampliation).

## Membrane-induced haemolysis.

To study the capacity of the modified membranes to induce haemolysis, the procedure described in Section 4.1.7.7 was followed. The results for unmodified and modified PSf membranes were normalised, using the value of free Hb concentration in plasma from blood samples incubated without any membrane. The values of measured free Hb are shown in Figure 40. As can be seen from this figure, all the membranes presented values underneath the cut-off value of plasma free Hb ( $10 \text{ mg dL}^{-1}$ ), showing that they are non-haemolytic. This means that the modification of PSf membrane by incorporation of antioxidants did not affect erythrocyte integrity.

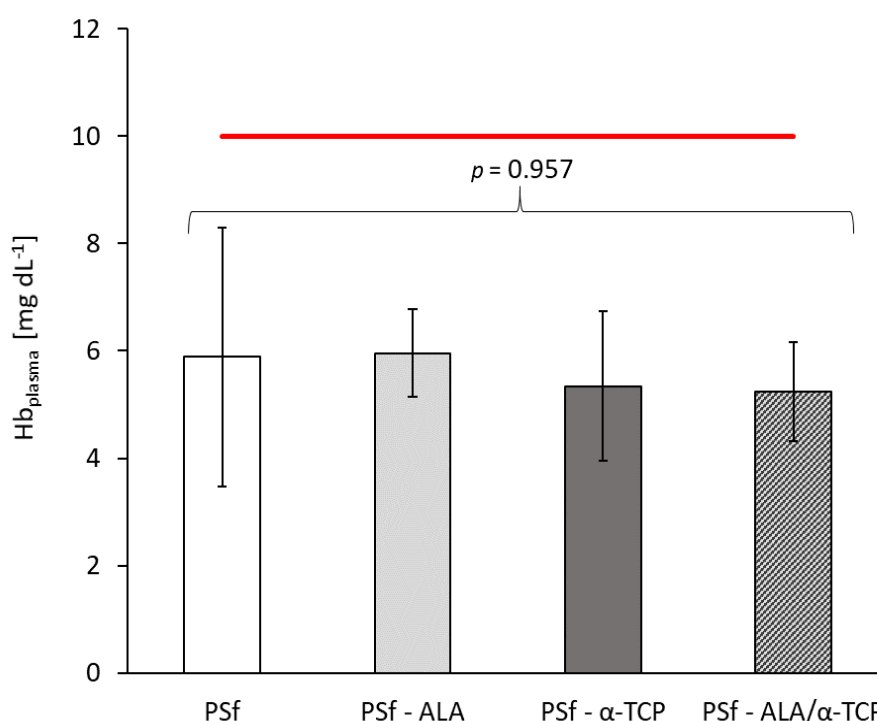


Figure 40: Plasma concentration of free Hb, after incubation of whole blood with unmodified and modified PSf membranes. The results ( $n = 4$ ) are expressed as mean  $\pm$  SEM. Hb plasma values were normalized by subtracting blank value (whole blood incubated without materials). Non-parametric Friedman's Test was used to compare paired samples. The red line determines the non-haemolytic material cut-off value.

## Activation of platelets, coagulation and complement system

Foreign materials can lead to activation of hemostasis and/or complement system activation. Thus, it was crucial to test the modified PSf membranes for activation of PLT, coagulation, and complement system component (namely, C3a and C5a), as important features of biocompatibility.

The evaluation of PLT activation by membrane surface was carried out according to the procedure, described in Section 4.1.7.7. The normalized results that are presented in

Table 16 show that all studied parameters presented similar values after the incubation with membrane samples. The data suggest that the effects of modified PSf membranes on PLT, blood coagulation and complement system, are similar to those induced by unmodified PSf membrane. Thus, considering that PSf membranes are widely used in current HD treatment, this finding indicates that antioxidant enrichment of PSf membranes by direct incorporation is a safe approach for HD membrane fabrication and that the membrane enrichment in antioxidants may reduce the risk for cardiovascular events, the major cause of death in these patients.

Table 16 : Data on coagulation (PLT activation, APTT, PT) and complement activation (C3a, C5a plasma levels), after incubation of blood with unmodified and modified PSf membranes. The results ( $n = 4$ ) were normalised subtracting the value of the blank samples and expressed as median (IQR). Non-parametric Friedman's Test was used to compare paired samples.

	PSf	PSf - ALA	PSf - $\alpha$ -TCP	PSf – ALA/ $\alpha$ -TCP	<i>p</i>
<b>PLT activation</b> [fluorescence units]	104 (-422 – 3102)	81 (-1042 – 1482)	-67 (-297 – 1209)	258 (-1590 – 4946)	0.753
<b>APTT</b> [s]	2.33 (1.16 – 4.34)	4.68 (4.14 – 6.23)	2.65 (1.04 – 5.61)	-0.01 (-2.47 – 6.16)	0.440
<b>PT</b> [s]	0.05 (-0.10 – 0.41)	0.53 (-0.15 – 1.00)	0.11 (-0.60 – 0.18)	0.72 (0.29 – 1.32)	0.127
<b>C3a</b> [ng mL <sup>-1</sup> ]	138 (-93 – 524)	381 (220 – 588)	162 (89 – 329)	184 (-127 – 423)	0.552
<b>C5a</b> [ng mL <sup>-1</sup> ]	2.25 (1.22 – 7.35)	2.44 (1.60 – 4.88)	2.23 (1.32 – 6.24)	1.82 (1.41 – 4.58)	0.753

PLT: platelet; APTT: activated partial thromboplastin time; PT: prothrombin time

To evaluate if the enriched PSf membranes containing antioxidants could alter the coagulation process or the complement system, an incubation with blood samples was performed and afterward PLT-poor plasma was isolated (Section 4.1.7.7). The coagulation tests, partial thromboplastin time (APTT) and prothrombin time (PT), were measured using commercially available kits (TECO, Munich, Germany).

Plasma levels of Human C3a and Human C5a were quantified by commercially available enzyme-linked immunosorbent assays. PLT-poor plasma C3a and C5a concentrations were normalized for each assay, by subtracting the value given by blood incubated without the membranes. The measured values of coagulation test and complement activation assay were normalized by subtracting the values from blood samples incubated without membranes and are listed in Table 16. No significant differences were observed between blood samples incubated with unmodified or modified PSf membranes. The data suggest that modified PSf membranes are associated to similar changes in these biocompatibility tests, as those induced by unmodified PSf membrane. Thus, considering that PSf membranes are widely used in current HD treatment, these findings indicate that modification of PSf membranes by antioxidants does not affect the material biocompatibility and may contribute to reduce the risk for cardiovascular events in these patients.

#### **4.2.15. Concluding remarks**

The modification of PSf membrane with the antioxidants ALA and  $\alpha$ -TCP was successful. Thus, the approach of using direct incorporation (blending) of the compounds into the PSf membrane structure seems to be more effective, when compared with the commonly used method of surface coating. The direct incorporation method also enables to control the amount of antioxidant introduced into the membrane and also allows to reduce the amount of antioxidant required for immobilization.

By using the first enrichment method, the modified membranes proved to have *in vitro* antioxidant activity. The studies of antioxidants leaching from the membrane confirmed a satisfactory strength of their incorporation, as the leaching during the time usually used for an HD treatment was negligible. The stability of the membranes was also shown to be adequate, when the membranes were stored under controlled conditions (dark, 4 °C). Moreover, the presence of both compounds tested did not alter the membrane ability for selective separation of biomolecules, as shown by the results of the dialysis experiments with modified and unmodified PSf membranes. The morphology of the modified membranes was not significantly influenced by the addition of the antioxidants into casting solution. The



modification of PSf membranes with antioxidants  $\alpha$ -TCP and ALA brought certain advantages to the membranes, such as less adsorption of proteins on its surface, which further supports the improvement in the biocompatibility of PSf membranes. The beneficial characteristics of the membranes enriched with one of the antioxidants were even enhanced, when the combination of both antioxidants was used. This type of modified membrane showed less membrane-induced haemolysis and decreased protein adsorption on its surface. Overall, the enrichment of PSf membranes with ALA or  $\alpha$ -TCP and their combination led to the production of haemocompatible biomaterials, with similar characteristics, when compared to the unmodified PSf membrane, commonly used for HD, but with the added benefit of antioxidant activity.

Overall, the modification of PSf membrane by bioactive compounds is a promising area, as it may positively contribute to the reduction of chronic inflammation, common in HD treated patients. Therefore, the modified bioactive membranes may provide a convenient alternative to conventional PSf HD membranes.

The experimental procedures and obtained results of the membrane modified with antioxidants have been published in the *Macromolecular Bioscience* journal, 2020 (Supplement 2).

### **4.3. Development of bioactive membrane enriched with neutrophil elastase inhibitors**

This project task was developed under the cooperation with the group of Medicinal Chemistry, Faculty of Pharmacy, University of Lisbon. The group, under supervision of Prof. Rui Moreira, synthesized, purified and characterized the physicochemical properties of neutrophil elastase inhibitors. The experimental work involving the cytotoxic evaluation of the synthesized compounds was developed in collaboration with the Department of Biological Sciences, Faculty of Pharmacy, University of Porto. This experimental work was an initial part of an interuniversity project with a financial grant “Dial4Life: Design of dialysis membranes targeting neutrophil elastase to reduce inflammation / oxidative stress in end-stage renal disease”.

#### **4.3.1. Introduction and main objective of the experimental work**

The activation of PMNs during HD treatment is associated with the release of different activation products, as already described; HNE is one of the constituents of PMN granules that is released by activated PMNs, increasing its concentration especially at the inflammatory sites. This serine protease is responsible for proteolytic degradation of collagen and elastin of the extracellular matrix and, thus can have a severe impact on organ tissue integrity. Besides that, HNE may also activate and stimulate the inflammatory process of HD treated patients. In physiological conditions, these actions of HNE are regulated by endogenous inhibitors (45). However, in HD treated patients, the levels of released HNE that are further increased after an HD treatment, may far exceed the inhibitory capacity of the endogenous inhibitors. A therapeutic intervention with selective exogenous inhibitors of HNE could bring improvements in the inflammatory status of HD patients, by counteracting the disturbed elastase/inhibitor balance. Thus, it appears that the therapeutic use of HNEI could be a promising treatment strategy. The synthetic HNE inhibitors (HNEI) underwent specific changes in their molecular structure, to improve their pharmacodynamic properties and inhibitory potential, and to enhance their resistance to proteolytic degradation in the presence of excess HNE. The latest generation of the HNE inhibitors have a basic structure of  $\beta$ -lactam ring and present selective and irreversible HNE inhibition (43).

To diminish the negative effects of HNE action, especially the stimulation of the inflammatory reaction, contributing to enhance the chronic inflammation present in HD treated patients, three different inhibitors were newly synthesized. Based on the previous experimental results of the Medicinal Chemistry group (148), the 4-oxo- $\beta$ -lactam derivatives

have emerged as efficient inhibitors, displaying appropriate chemical and metabolic stability, very high selectivity towards HNE but also non-cytotoxicity. Besides that, the 4-oxo- $\beta$ -lactam scaffold is accessible to structural modifications to modulate its selectivity and reactivity. These inhibitors, with 4-oxo- $\beta$ -lactam scaffold as the key structure, were used to modify PSf membrane with the purpose of bringing a new possibility of HNE inactivation in site and time specific manner, during the HD treatment.

The main objective of this work was to enrich the developed PSf membranes with new synthetic elastase inhibitors, presenting different modifications in the 4-oxo- $\beta$ -lactam structure that may have led to changes in the physicochemical properties of the membrane; thus, besides the study of these properties, it was also evaluated *in vitro* their inhibitory capacity at different concentrations.

#### **4.3.2. Chemicals and Instrumentation**

##### **4.3.2.1. Chemicals**

Deionised water, ultrapure water Milli-Q (Millipore water system, Merck, France), and chemicals of analytical grade were used without further purification. Human neutrophil elastase (MW = 29.50 kDa) and fluorogenic elastase substrate V (MW = 627.70 g mol<sup>-1</sup>) were purchased from Merck (Darmstadt, Germany). Dimethyl sulfoxide (DMSO) (MW = 78.13 g mol<sup>-1</sup>), NMP (MW = 99.13 g mol<sup>-1</sup>), sodium salt anhydrous (MW = 82.30 g mol<sup>-1</sup>), and glacial acetic acid (MW = 60.05 g mol<sup>-1</sup>) were all purchased from Sigma-Aldrich Co. Buffering agent HEPES sodium salt 99% (MW = 260.284) was obtained from Acros Organics. Phosphate buffered saline solution pH 7.4, was prepared as already described (Section 4.1.2.1)

##### **4.3.2.2. Instrumentation**

Microplate reader (Synergy™ HT, BioTek Instruments, USA) was used to record fluorescence; automated blood cell counter (Sysmex K1000; Sysmex, Hamburg, Germany) was used to provide cell counts.

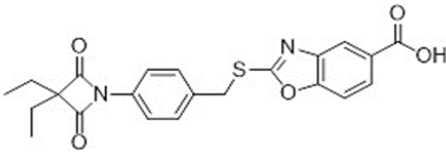
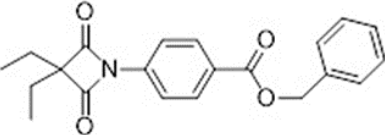
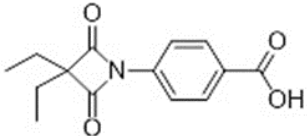
##### **4.3.3. Synthetized elastase inhibitors**

Three newly synthetized HNEI, with the designations of AAN-5, AAN-7, and AAN-8, were provided by the group of Medicinal Chemistry, Faculty of Pharmacy, University of

Lisbon, as a purified powder. Despite the previously described important properties of these HNEI, the disadvantage of the chemical structure containing 4-oxo- $\beta$ -lactam scaffold is low stability in protic solvents and aqueous solutions. The determined half-life ( $t_{1/2}$ ) of the HNEI in buffer solution, pH 7.4, was only 10 h.

The inhibitors were dissolved in the organic solvent DMSO to obtain a final concentration of 1 mg mL<sup>-1</sup>, aliquoted and frozen at -20 °C, until used. The values of MW, inhibitors' partition coefficient and aqueous solubility, together with molecular structure are shown in Table 17.

Table 17 : Summarized characteristics of the newly synthesized elastase inhibitors: AAN-5, AAN-7, and AAN-8.

	MW [g mol <sup>-1</sup> ]	LogP	LogS	Molecular structure
<b>AAN-5</b>	424.47	4.738	-5.157	
<b>AAN-7</b>	351.40	4.499	-5.131	
<b>AAN-8</b>	261.28	2.445	-2.909	

#### 4.3.4. Elastase activity assay

To determine the inhibitory activity presented by the inhibitors, the activity of HNE was evaluated by enzymatic kinetic assay. The inactivation of HNE was quantitatively determined by a fluorogenic substrate, which is highly sensitive and HNE specific. The small amino acids of the substrate for HNE, N-methoxysuccinyl-Ala-Ala-Pro-Val-7-amino-4-methylcoumarin, such as alanine and valine, are preferred by the catalytic site of HNE, releasing 7-amino-4-methylcoumarin, whose fluorescence is evaluated.

Prior to the assay, the commercial HNE was resuspended in 1 mL of 0.05 M acetate buffer, pH 5.5, to obtain a final concentration of 3.39  $\mu$ M. This stock solution was aliquoted and stored at -20 °C. At the time of an assay, an aliquot was diluted with the assay buffer (0.1 M HEPES buffer, pH 5.5), to obtain an elastase concentration of 0.2  $\mu$ M. The fluorogenic HNE substrate was diluted in DMSO to obtain 8 mM stock solution, which was

aliquoted and stored at -20 °C, light protected. Before an assay, an aliquot was freshly diluted 4x with assay buffer, to obtain 2 mM substrate concentration. During the entire handling process, the fluorogenic substrate was kept light protected.

The HNE inactivation assay was carried out in 96 wells plate, using a total volume of 200 µL per well. Each assay well contained 155 µL of assay buffer (0.1 M HEPES buffer, pH 5.5), 20 µL of diluted HNE and 5 µL of tested HNEI solution in DMSO. After plate incubation at 25 °C, for 30 min, 20 µL of the fluorogenic substrate was added. The HNE inhibition assay was carried out at 25 °C, for period of 30 min. The fluorescence was monitored by microplate reader (excitation: 360 nm, emission: 460 nm) in kinetic mode, recording the fluorescence each 60 s. DMSO was used as a negative control.

#### **4.3.5. Elastase activity inhibition by new inhibitors**

To establish the inhibitory potential of the new inhibitors towards HNE and to select the most potent one for the further experiments, the half maximal inhibitory concentration ( $IC_{50}$ ) had to be determined. The inhibition activity of the HNEI is time-dependent, as the initial phase of the reaction is exponential (until initial reaction stabilizes), followed by a linear phase. The linear phase (obtained after 10 min of the kinetic measurement) was then used to calculate  $IC_{50}$ .

Different concentrations of the tested HNEIs were prepared in DMSO, ranging from 4 to 24 000 nM. These solutions were prepared in 40x higher concentrations as in this way it was possible to maintain the final concentration of DMSO in the assay well lower than 5%. This threshold of 5% DMSO was set up, to avoid its cytotoxicity that could interfere in haemolytic tests and in future planned cytotoxicity experiments using experimental animal models. For both types of experiments, the maximal tolerated concentration of DMSO is 5%.

The evaluated concentrations (in the well's reaction mixture) of HNEIs in the inhibitory assay were as follow:

AAN-5 and AAN-7: 0.1; 0.2; 0.5; 1.0; 2.0; 5.0; 10.0; 15.0; 20.0; 40.0; 80.0 and 160.0 nM

AAN-8: 0.05; 0.1; 0.2; 0.5; 1.0; 2.0; 5.0; 10.0; 20.0; 40.0; 80.0; 160.0; 240.0; 300.0; 450.0 and 600.0 nM.

These evaluated concentrations should present 0% to 100% of HNE inhibition. Then, the inhibition activity was determined by the assay described above (Section 4.3.4).

From the obtained results ( $n = 3$ ) of HNE inhibition assay, the  $IC_{50}$  values for all three inhibitors were obtained from the sigmoidal curve of the logarithmical concentration of HNE and the inhibition of HNE activity (Graphpad Prism Version 7 was used to calculate  $IC_{50}$ ).

The example of the curve for  $IC_{50}$  calculation of AAN-5 is shown at Figure 41. The minimal and maximal inhibition was defined and the value of  $IC_{50}$  was obtained from the inflection point of the curve. The obtained  $IC_{50}$  values for AAN-5, AAN-7 and AAN-8 were 11.6 nM, 22.0 nM and 18.1 nM, respectively. The lowest  $IC_{50}$ , and therefore the best inhibitory activity, was observed for inhibitor AAN-5.

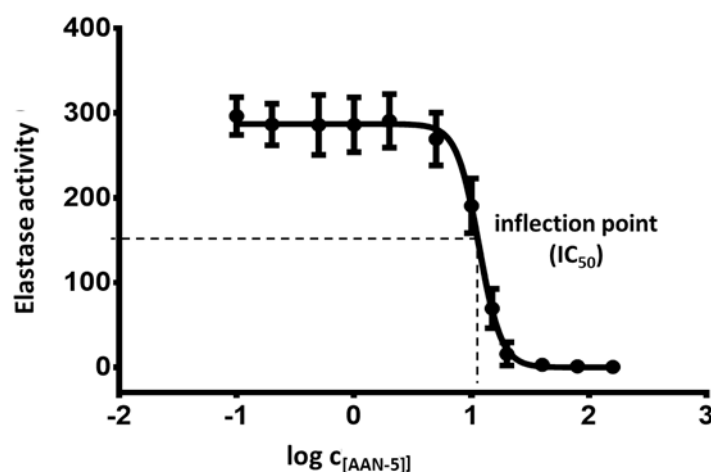


Figure 41: Inhibition curve of AAN-5 used to determine  $IC_{50}$ . The values are expressed as mean (n = 3) and SD.

#### 4.3.6. Elastase activity inhibition by modified PSf membranes with inhibitors

To develop a modified membrane with synthetic HNEI, the approach of membrane surface coating was selected. As already described before, the membrane preparation process involves phase inversion in the ultrapure water, followed by 24 h of constant washing. Due to low stability of the HNE inhibitors in the aqueous solution and, therefore, to avoid their degradation, the inhibitors were immobilized by adsorption on membrane surface.

To evaluate the inhibitory activity of the adsorbed inhibitors, and consequently the membrane adsorption capacity, the adsorption test, followed by the enzymatic elastase assay, were carried out. Firstly, the PSf membranes were prepared as previously described in Section 4.1.6. A small round specimen with a diameter of 2 cm were cut from the membranes, from three different batches, and placed into 12 wells plate (Figure 42). The HNEI solutions were prepared in order to obtain the following concentrations: 10.0; 50.0; 100.0; 250.0; 500.0; 800.0; 1 000 and 2 000 nM, with the maximal DMSO content of 5% in the final solution. The volume of 600  $\mu$ L of each solution concentration was added to the membrane samples and the plate was incubated at a controlled temperature of 25  $^{\circ}$ C, for 3 h, under gentle agitation (50 rpm) to assure the homogeneity of the inhibitor in the solution.

The experiments were run in triplicate for each concentration of the inhibitor. A solution with 5% DMSO without any inhibitor was used as a blank sample.

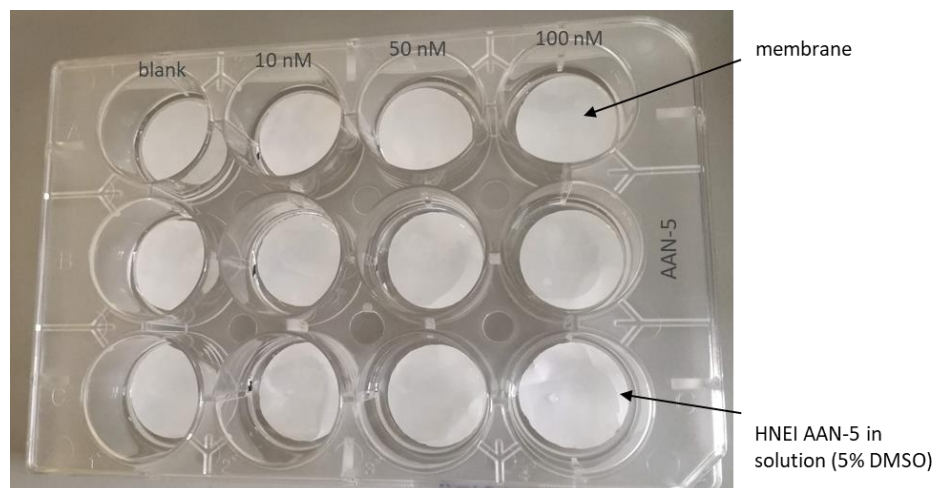


Figure 42: Inhibitor adsorption test on the membranes surface.

After the incubation time, the membranes were removed, and the excess solution was gently wiped off. The membranes with adsorbed inhibitors were placed into 96 wells plate to evaluate the elastase activity inhibition, using the assay described in Section 4.3.4., with small modifications. The volume of added inhibitor (5  $\mu$ L) was replaced by assay buffer. After the incubation time of 30 min, 90  $\mu$ L of elastase solution was placed in a new 96 wells plate and 10  $\mu$ L of fluorogenic substrate was added. The successive elastase quantification corresponded to the described procedure. This intermediate step in the elastase assay enabled to quantify the elastase inhibition, caused by the modified membrane, without interferences in the fluorescence measurement, caused by the presence of a membrane. The inhibitory activities of modified membranes are shown in Figure 43. As can be seen from the figure, the membranes with adsorbed inhibitor AAN-5 show significant HNE inhibition, only when the membrane was incubated with the highest initial concentration of AAN-5 inhibitor (2 000 nM). Better results were observed for membranes incubated with the inhibitor AAN-8, with which a more significant decline in elastase activity was observed, even for the lowest concentrations that were used for membrane adsorption. These observations are in contrary with the results observed in the tests used to calculate  $IC_{50}$ , in which the inhibition activity was measured in the solution, and AAN-5 showed more promising results. This might be explained by different hydrophilic character of AAN-5 and AAN-8; actually, AAN-8 is more hydrophilic ( $\log P = 2.445$ ) and, therefore, can be easier adsorbed, both on the membrane surface and inside the pores structure, which is also

hydrophilic. The membranes with adsorbed inhibitor AAN-7 did not show any HNE inhibition. As it was confirmed by HPLC with MS/MS detection performed by the group of Medicinal Chemistry, Faculty of Pharmacy, University of Lisbon, this compound became degraded during the storage time, and, therefore, was excluded from further experiments.

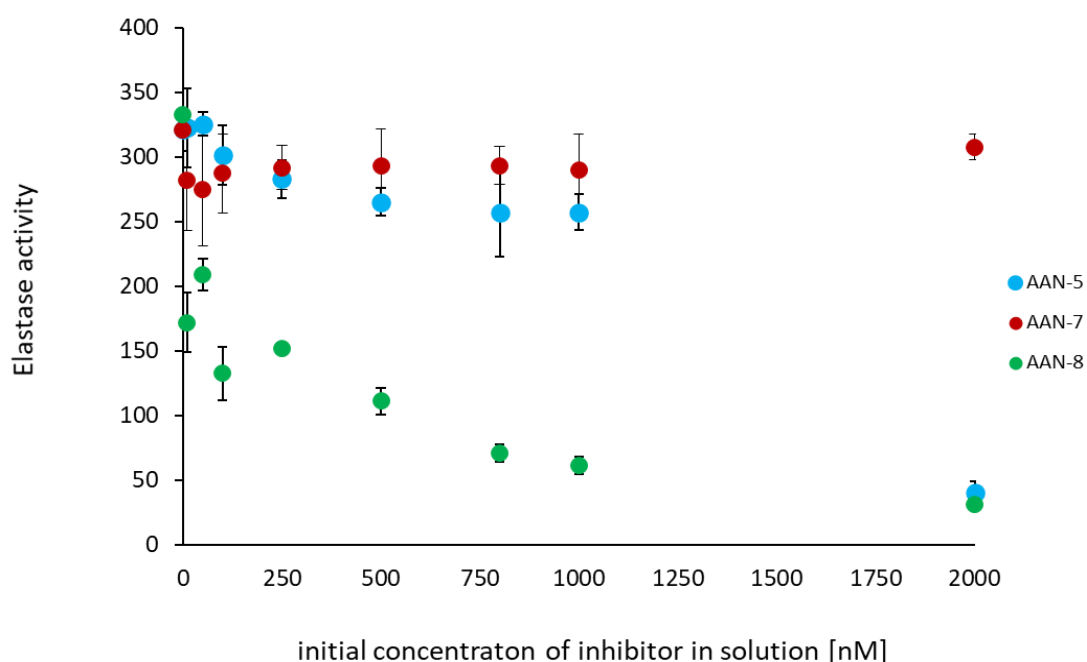


Figure 43: Inhibitory activity of membranes modified with different concentrations inhibitors AAN-5, AAN-7, and AAN-8.

#### 4.3.7. Adsorption of elastase inhibitors on PSf membranes

Adsorption capacity was calculated as the amount of the inhibitor adsorbed by the area of the membrane. To determine the amount of adsorbed inhibitors (AAN-5 and AAN-8) on the membrane surface, membrane round specimens with an area of 3.14 cm<sup>2</sup> cm were cut and placed in the wells of a 12 wells plate. A volume of 700  $\mu$ L of the inhibitors solutions (in the concentrations already listed in Section 4.3.6) were added to the membrane samples. The adsorption was carried out for 3 h at 25 °C, agitated at 50 rpm. After the incubation time, the membranes were removed, and the excess solution was gently wiped off with paper. These membranes were then placed into microcentrifugation tubes and completely dissolved by adding 1.4 mL of NMP and DMSO in the ratio 1:1 (v/v). These solutions of the dissolved membranes were used to quantify the adsorbed inhibitors, using HPLC coupled with MS/MS detection. This measurement was carried out by the group of Pharmaceutical Chemistry, Faculty of Pharmacy, University of Lisbon. The provided results



of inhibitors concentration are listed in Table 18. AAN-8 showed better affinity to the membrane, when compared to AAN-5.

Table 18: Amount of adsorbed HNEI on membrane surface in dependence on the initial concentration.

HNEI	Inhibitor concentration in solution before adsorption test [nM]	Concentration of adsorbed HNEI quantified by HPLC-MS/MS [nM]	Adsorbed HNEI per cm <sup>2</sup> of membrane [nM cm <sup>-2</sup> ]
<b>AAN-5</b>	10	< LOQ	/
	50	< LOQ	/
	100	< LOQ	/
	500	4.0 ± 1.47	1.96
	1 000	5.1 ± 1.88	2.76
	2 000	17.9 ± 5.35	8.77
<b>AAN-8</b>	10	< LOQ	/
	50	2.7 ± 0.72	1.32
	100	4.4 ± 0.62	2.16
	500	7.0 ± 0.82	3.43
	1 000	9.0 ± 1.26	4.46
	2 000	24.1 ± 1.83	11.8

HNEI: human neutrophil elastase inhibitor; LOQ: limit of quantification

#### 4.3.8. Haemolysis test

To evaluate the inhibitors toxicity to RBCs, the haemolysis tests were carried out with inhibitors AAN-5 and AAN-8 in solution. The blood was collected and processed according the procedure described in Section 4.1.7.7. Solution containing 0.125% DMSO without inhibitor was used as a vehicle, Triton X-100 in 0.01% (w/v) was used as haemolytic positive control. Inhibitors were dissolved in DMSO in corresponding concentrations, to reach the final DMSO concentration, in the assay well of 0.125%. The tested concentrations corresponded to their IC<sub>50</sub> multiplied by 0.01, 0.1, 10, 100. Then, 250 mL of diluted blood was placed into 24 wells plate. The same volume of the inhibitor solution was added, and the plate was incubated for 3 h at 37 °C. After the incubation, the plasma free Hb was measures as already described (Section 4.1.7.7). The obtained results are shown in Figure 44. As can be seen from the figure, all the tested inhibitors concentrations were proved to be non-haemolytic, as even the highest tested concentration corresponding to

concentration 100 x higher than corresponding  $IC_{50}$  was found far below the non-haemolytic cut-off value (10 mg dL<sup>-1</sup>) and therefore can be used for future *in vivo* experiments.

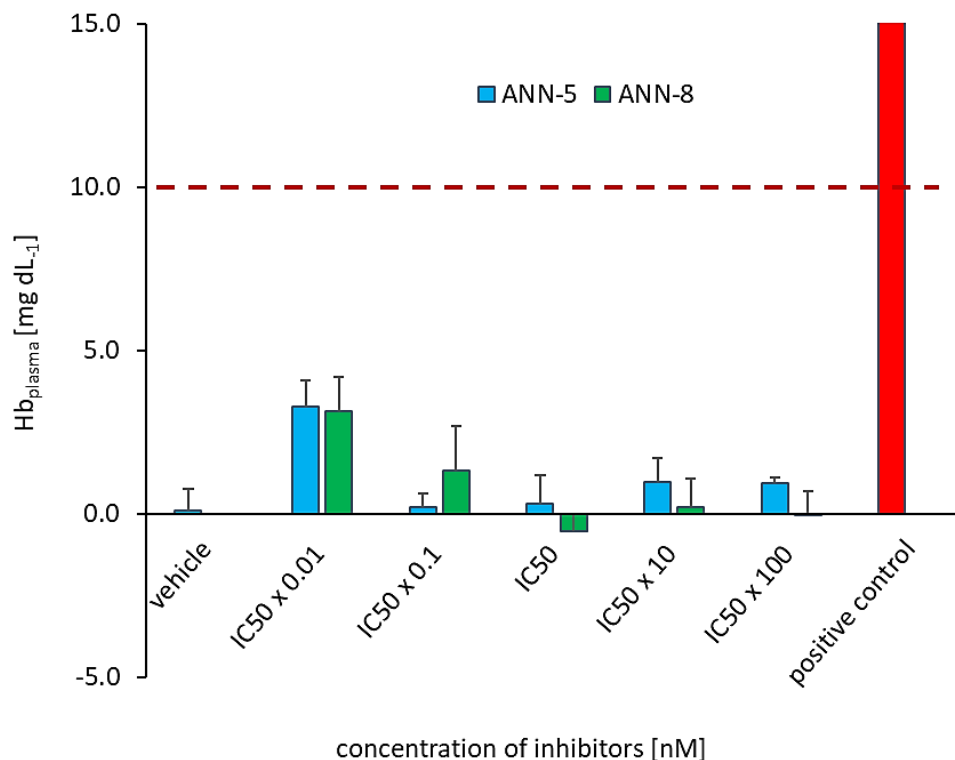


Figure 44: Plasma concentration of free Hb, after incubation of whole blood with HNEI AAN-5 and AAN-8. The results (n = 3) are expressed as mean  $\pm$  SEM. The presented values were normalized by subtracting blank value. 0.125% DMSO was used as a vehicle. The dashed red line determines the non-haemolytic cut-off value.

#### 4.3.9. Concluding remarks

During this experimental work, three different synthetic inhibitors, AAN-5, AAN-7, and AAN-8, were evaluated. Firstly, the inhibitory activity towards HNE was tested in solution. All three inhibitors showed to be very potent, as the  $IC_{50}$  concentrations were in the order of nM. The lowest  $IC_{50}$ , therefore the most potent inhibition, was observed for HNEI AAN-5 ( $IC_{50} = 11.6$  nM). As the main objective of this work was to prepare modified membranes with ability to reduce HNE activity that increases during the HD treatment, the inhibitors were immobilized on the membrane via superficial adsorption. The modification method was further evaluated by measuring the HNE inhibition by these modified membranes. The amount of adsorbed inhibitor on per membrane area was also determined. The results indicated that the AAN-8 with more hydrophilic characteristics had better affinity to the membrane surface, since the membranes with this inhibitor showed the most effective elastase inhibition, as well as the amount of adsorbed inhibitor was higher, when compared

to other tested compounds. The inhibitor with the designation AAN-7 showed insufficient stability, although stored in appropriate conditions, and got degraded

Although the obtained data are preliminary and further biological tests must be carried out, they indicated the optimal physicochemical properties of the inhibitors. Based on these results, the synthesis of new HNEI will be conducted towards more hydrophilic structures, as the compound with this characteristic showed to be more effectively adsorbed on the membrane surface, and, therefore, showed improved HNE inhibition activity, when compared to the less hydrophilic inhibitors.

#### 4.4. Development of membrane incorporating molecularly imprinter polymer

As previously mentioned, uremic toxins are waste products, which, due to insufficient renal filtration, are accumulated in blood and may induce neutrophil activation, resulting in excessive ROS formation and release of other activation products (13). Taking advantage of the experience acquired in the preparation of polysulfone membranes, molecularly imprinting polymers (MIPs) specific for the uremic toxin *p*-cresol were synthesized and incorporated into the membranes. This experimental work is a preliminary study and was developed as a side project to the presented dissertation thesis; despite that the volume of results is limited, they will be important for further experiments that will be carried out by the Sensors and Biosensors group of the Analytical Chemistry Laboratory of Faculty of Pharmacy, University of Porto, in order to be able to take more robust conclusions on this subject.

##### 4.4.1. Introduction and objectives of the experimental work

The retention of uremic toxins in the blood stream of ESRD patients, due to the decline in the GFR, may cause severe adverse effects. *P*-cresol belongs to the group of protein-bound uremic toxins (described in detail in Section 3.3.1) and, due to its ability to bind to albumin, its HD removal is very limited, even when using a high-flux membrane. It is a small molecule that results from the metabolism of the certain amino acids, by the intestinal flora (13). In ESRD patients, the level of *p*-cresol is up to 10 times higher and it has been reported that together with its metabolite, *p*-cresyl sulphate, are correlated with all-cause and CV mortality in ESRD patients. These observations strongly suggest that these uremic toxins may importantly contribute to CVD (276).

MIPs are synthetic polymers with a predetermined selectivity for a given analyte or group of structurally related compounds, obtained using the imprinting technology. Molecular imprinting is a technique that creates recognition sites, which are specific for a target molecule, called a template, within a synthetic polymer. This selectivity is generated during the polymer synthesis, by the interaction of the template with the functional monomers. MIPs have been widely used for different analytical purposes, in particular for the selective adsorption of an analyte presented in a complex matrix.

The preparation of a selective sorbent that was incorporated into the structure of PSf membranes and is selective for *p*-cresol, would be an interesting alternative for the removal of this uremic toxin from the bloodstream, during the HD treatment.

The main objective of this work was to develop a PSf membrane with ability to remove *p*-cresol by entrapping this uremic toxin into specific cavities in the membrane structure. For this purpose, a selective MIP for *p*-cresol was synthesized and embedded in PSf membranes. An optimization process for MIP preparation with structural cavities, specific for *p*-cresol, was carried out and its incorporation into the membranes was made via blending method.

#### **4.4.2. Chemicals and Instrumentation**

##### **4.4.2.1. Chemicals**

Deionised water, ultrapure water Milli-Q (Millipore water system, Merck, France), and chemicals of analytical grade, were used without further purification. *P*-cresol used as template molecule (MW = 108.14 g mol<sup>-1</sup>), monomer methacrylic acid 99% (MAA) (MW = 86.09 g mol<sup>-1</sup>), cross-linker ethylene glycol dimethacrylate 98% (EGDMA) (MW = 198.22), reaction initiator 2,2'-Azobis(2-methylpropionitrile) (AIBN) (MW = 164.21), were all purchased from Sigma-Aldrich Co. (Munich, Germany). All solvents used, such as acetonitrile (ACN) (Merck, Darmstadt, Germany), dichloromethane (DCM) (Sigma-Aldrich Co., Munich, Germany), and methanol (MeOH) (Fisher Chemicals, Thermo Fisher Scientific, MA, USA), were of analytical grade. PBS solution pH 7.4 was prepared as previously described (Section 4.1.2.1).

##### **4.4.2.2. Instrumentation**

Ultrasonic bath (Thermo Fisher Scientific, MA, USA) was used to promote the binding between the template and the monomer. MIP polymerisation took place in an incubator (Indelab, Spain); a centrifuge (Allegra X-15R, Beckman-Coulter) was used during template removal from the MIP. The fluorescence of *p*-cresol was evaluated by using a spectrofluorometer (Jasco FP-6500, GmbH, Germany).

##### **4.4.3. MIP synthesis**

The synthesis of MIP specific for *p*-cresol was as carried out according to the procedures described in the literature, using a template with a molecular structure similar to *p*-cresol (Figure 45) (277, 278).

The template, monomer and cross -linker, were mixed in molar ratios of 1:4:12, 1:4:16, 1:4:20 and 1:2:6, and dissolved in 4.8 mL of porogen (ACN or DCM). To initiate the polymerization, 30 mg of the reaction initiator (AIBN) was added. The glass vessel containing this mixture was sealed and ultrasonicated for 1 h. The mixture was then cooled down on ice and purged with nitrogen, for 10 min, to remove oxygen from the solution. Polymerization took place in an incubator, set up at 60 °C, for 24 h. After the polymerization step, the final solidified polymer was powdered, placed into syringes and the template was removed by successive washing with MetOH : acetic acid 9:1 (v/v), followed by washing with ultrapure water (Figure 46). The complete removal of the template from the polymer was traced by *p*-cresol fluorescence measurement ( $I_{MAX} = 310$  nm). The non-imprinted polymer (NIP) was prepared similarly to MIP, but without the presence of the template in the polymerization media.

After the template removal, the polymers were heat dried and the analytical sieve with mesh size of 40  $\mu\text{m}$  was used to isolate small polymer particles, which could be incorporated into PSf membrane, without altering the integrity of that.

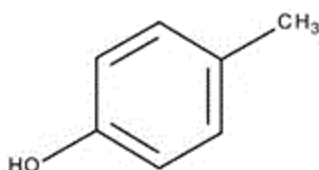


Figure 45: Molecular structure of *p*-cresol.

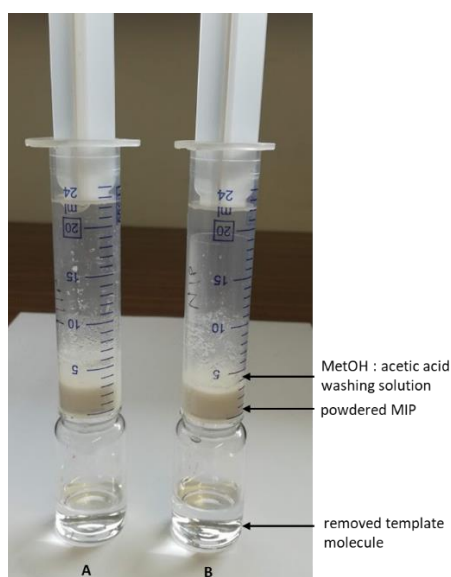


Figure 46: A set up of template molecule removal from powdered MIP.

#### 4.4.4. MIP selectivity evaluation for *p*-cresol

The recognition ability of the MIP and NIP to *p*-cresol was evaluated. For that the powdered polymer (30 mg) and 2 mL of *p*-cresol dissolved in PBS pH 7.4, in a final concentration of 2.0 mg L<sup>-1</sup> were placed into 15 mL centrifugation tubes and shaken for 1 h, at 25 °C; and then centrifugated at 3450 g, during 10 min, to separate the polymer particles from the supernatant containing *p*-cresol. To quantify the *p*-cresol that was bound to MIP, the fluorescence of the supernatant ( $\lambda_{\text{ex}} = 220 \text{ nm}$ ,  $\lambda_{\text{em}} = 310 \text{ nm}$ ) was measured. The concentration of *p*-cresol was quantified by using a calibration curve. The amount of bound *p*-cresol was calculated from the difference between the concentrations of the original solution and its final concentration in the supernatant.

For MIPs selectivity optimization, different amounts of functional monomer and cross-linker were tested, resulting in different formulations. Their adsorption capacities were investigated in comparison to corresponding NIPs. Unfortunately, unspecific binding of *p*-cresol to both types of polymers were observed. Very similar values of solute adsorption were shown for both MIP and NIP in all prepared formulations. Slight improved adsorption was observed for MIP with composition 1:4:12 with ACN as porogen. The MIP with this composition further underwent the pH test, which was carried out to evaluate the effect of different pH of *p*-cresol solution on its adsorption by MIP. No effect of pH on *p*-cresol binding was observed (Figure 47). There was no significant effect of pH on the binding of *p*-cresol to MIP in the studied pH range. Therefore, the use of MIP at physiological pH (7.4), mimicking the patient's blood, is not compromised.

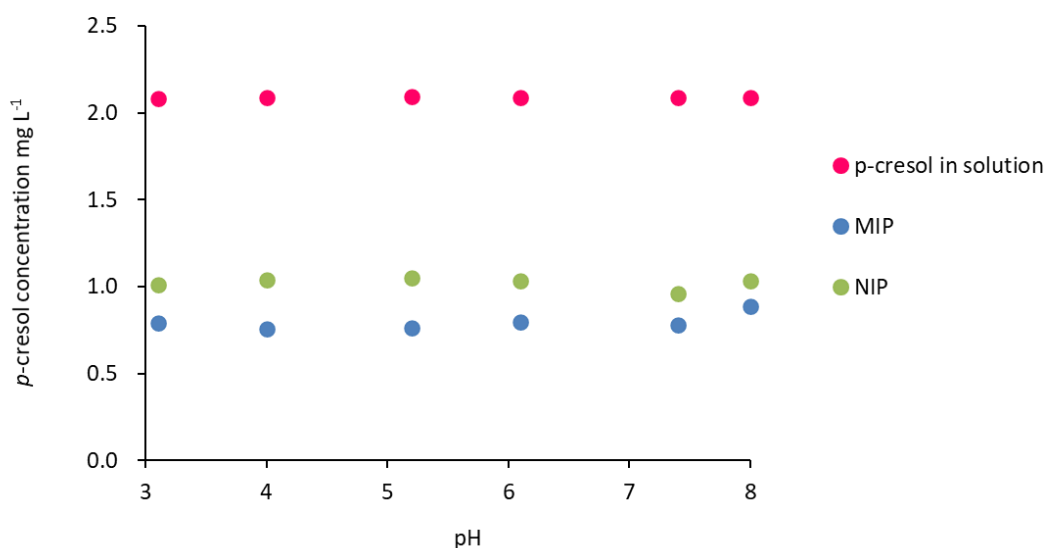


Figure 47: Effect of pH on adsorption of *p*-cresol by MIP.

Although some polymers with different formulations were tested, it was not possible to achieve any satisfactory result regarding the selectivity for the *p*-cresol of these polymers. Despite the lack of selectivity, it was decided to assess whether the incorporation of MIP in the membranes compromised its structure

#### 4.4.5. Modification of PSf membrane with MIP

Regardless of the non-specificity of MIP towards *p*-cresol, the proof of concept of preparation PSf membrane containing MIP able to remove uremic toxin, was performed; polymer particles with size  $\leq 40 \mu\text{m}$  were directly incorporated into PSf membrane, by adding MIP to the casting solution in a final mass of 1.25 wt%.

The membranes were prepared according the procedure described in Section 4.1.6 and underwent morphological evaluation by SEM, as described in Section 4.1.7.2. As can be seen from the cross-section image (Figure 48), MIP gets incorporated along the membrane structure in small clusters, without interfering with the membrane integrity.

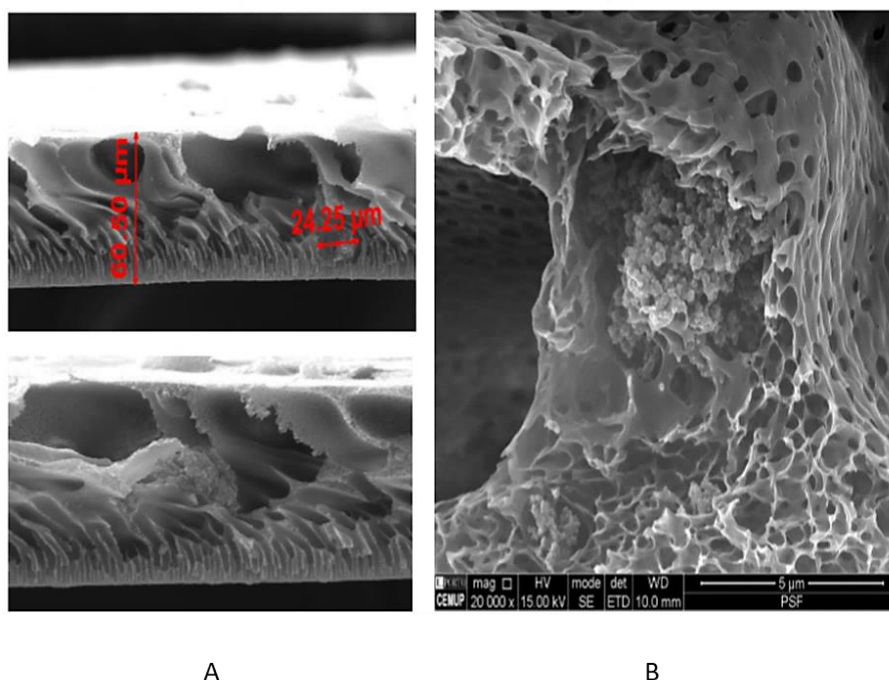


Figure 48: SEM cross-section image of PSf membrane containing MIP incorporated in its structure. Magnification 4 000 x (A), 20 000 x (B).



#### 4.4.6. Concluding remarks

Despite the lack of selectivity of the synthesized MIP towards *p*-cresol, it was decided to assess, whether the direct incorporation of MIP into the PSf membranes compromised its structure. It was proved, that incorporation of the MIP particles of specific size range does not disturb the membrane structure. This concept of membrane modification could be used for removal of other uremic toxins, as far as the synthesis of MIP specific for the toxin of interest would be successful. These preliminary results may be used for further investigation focused on removal of toxins from complex matrices, by using MIP incorporated into polymeric membranes.

## 5. CONCLUSIONS

The main objective of this experimental dissertation thesis was to develop and optimize new types of PSf membranes, with beneficial biological activity and potential to be used for HD treatment. Bioactive membranes enriched with antioxidants or with elastase inhibitors could help to reduce OS and inflammation, commonly high in HD treated patients, and, thereby, reduce their cardiovascular disease risk. Indeed, these patients present high morbidity and mortality rates, mainly due to cardiovascular events. Strategies to minimize associated complications of HD treatments is still an actual topic of high interest. A comprehensive review article addressing this topic was published in an indexed scientific journal.

For the development of the bioactive membrane, we, firstly, prepared flat sheet PSf membranes using the spin coating method and phase inversion via immersion precipitation. The composition of the membrane had to be optimized, in order to obtain suitable separation characteristics, required for HD membranes; namely, to be fully permeable for small molecules, partly permeable for middle sized molecules and have good large protein retention. The final composition of PSf membranes showing this separation characteristics was as following: main polymer PSf 15 wt%, hydrophilic additive PVP K30 2.5 wt% and solvent NMP 82.5 wt%. The suitability of the membrane with this composition was proved by a set of biocompatibility tests, recommended by “ISO 10993-4, Biological evaluation of medical devices — Part 4: Selection of tests for interactions with blood”. The evaluated membrane was not haemolytic, showing a material induced-haemolysis lower than the cut-off haemolytic threshold, did not cause significant PLT and complement activation, nor blood coagulation; when compared to commercially available biocompatible material the results were similar. The data suggest that the prepared and optimized membrane has the appropriated characteristics for possible use for HD procedure. This experimental part, regarding the PSf membrane optimization, preparation, and evaluation was published as a full paper in scientific journal with impact factor.

This developed PSf membrane was used for further modifications, to obtain a bioactive membrane with antioxidant activity, which would be able to scavenge ROS formed during the HD process and, therefore, to reduce oxidative stress. The membrane modification was performed by direct incorporation of the antioxidants  $\alpha$ -TCP and ALA that were dissolved, individually and in a mixture of both, in the casting solution, prior to the membrane preparation process. The redox potential of the membranes containing these antioxidants was evaluated *in vitro*. The effect of the antioxidant incorporation on the membrane separation ability, was also assessed, as well as the membranes

biocompatibility. The obtained results showed redox potential for all three types of modified PSf membranes, although the highest redox potential was presented by the PSf membrane enriched with the mixture of both antioxidants. The separation characteristics of these modified membranes did not significantly differ from the unmodified membrane, confirming that the antioxidants incorporation did not alter membrane structure. Besides, these membranes showed improvements in some biocompatibility parameters. The data showed that the used modification technique preserved the antioxidant activity of the compounds, without altering membrane separation characteristics. Thus, the membrane modification with antioxidants showed to be an effective approach for OS diminishment and seems to have potential to be used in future PSf membrane for HD treatment.

Another approach was the modification of PSf membrane by enrichment with newly synthesized inhibitors of HNE, in order to contribute to diminish inflammation and OS, induced by HD treatment. Three HNE inhibitors, with different physicochemical properties, with the designations AAN-5, AAN-7, and AAN-8, were synthesized by Department of Pharmaceutical Chemistry, Faculty of Pharmacy, University of Lisbon. These HNE inhibitors, from the latest 5<sup>th</sup> generation, contain 4-oxo- $\beta$ -lactam ring. As this structure is not stable in aqueous solutions, the method of superficial adsorption was selected for the membrane modification. The inhibitors activity towards HNE was evaluated *in vitro*, by testing the inhibitors in solution of 5% DMSO. The lowest value of IC<sub>50</sub> (11.6 nM), thus the highest inhibitory activity, was observed for the inhibitor AAN-5. The inhibitors were then adsorbed on the membrane surface and these enriched PSf membranes were tested for their inhibitory activity. Contrary to the results obtained in solutions, the most potent elastase inhibition was shown by the membranes with AAN-8 inhibitor. This inhibitor also showed better affinity to the membrane compare to AAN-5, when the amount of adsorbed compound per area of membrane was determined. This observed difference could be explained by the higher hydrophilicity of this inhibitor, when compared to AAN-5, increasing its affinity for the hydrophilic PSf membranes. The membrane enriched with AAN-7, unfortunately, did not show any inhibition activity of HNE, since this compound did not present sufficient stability, despite the proper storage conditions. As the inhibitors AAN-5 and AAN-8 showed good inhibitory activity, they will be further evaluated by a set of biological tests, to confirm their non-cytotoxicity both *in vitro* and *in vivo*. Moreover, based on the promising results with these HNE inhibitors, others will be synthesized, focusing on improving their hydrophilicity, to have greater adsorption on PSf membrane surface.

The last tested approach of PSf membrane modification was by direct incorporation of MIP, which could effectively entrap the uremic toxin *p*-cresol, which, by binding to plasma proteins becomes difficult to remove by conventional PSf membranes, during HD treatment.

For this purpose, several compositions of polymeric solutions were tested, in order to synthesize MIPs specific for *p*-cresol. Unfortunately, the specific adsorption of *p*-cresol by tested MIPs was not achieved. Despite its non-specificity, the MIP was incorporated into membrane structure, by dissolving in the casting solution. It was verified by SEM analysis, that this incorporation did not disrupt the membrane structure, and, therefore, this approach of membrane modification should be considered in future work; actually, the development of more selective MIP towards *p*-cresol, or towards other kind of uremic toxin, seems to have good potential. To summarize this possibility of using MIPs embedded in PSf membranes, as selective polymers for removing toxins, a review publication is currently being written.

The overall results obtained from the presented work may contribute to future research work on PSf membrane modifications, since membrane preparation and modification processes, using different approaches to improve bioactivity of the membranes, were optimized. Moreover, these approaches, of enrichment of PSf membranes with antioxidants or with newly synthesized HNE inhibitors, proved to have potential for new bioactive HD membranes, deserving further studies. The results also show a wide range of possibilities for membrane modification with other compounds that could diminish OS, inflammation or other HD associated complications. Finally, the data suggest that these new bioactive membranes have potential for future HD membranes that could contribute to decrease the CV risk that has been associated with the high morbidity and mortality rates in end stage renal disease patients on HD treatment.

## 6. REFERENCES

1. Levin A, Tonelli M, Bonventre J, Coresh J, Donner JA, Fogo AB, et al. Global kidney health 2017 and beyond: a roadmap for closing gaps in care, research, and policy. *Lancet*. 2017;390(10105):1888-917.
2. Thomas R, Kanso A, Sedor JR. Chronic kidney disease and its complications. *Prim Care*. 2008;35(2):329-vii.
3. Mortality GBD, Causes of Death C. Global, regional, and national life expectancy, all-cause mortality, and cause-specific mortality for 249 causes of death, 1980-2015: a systematic analysis for the Global Burden of Disease Study 2015. *Lancet*. 2016;388(10053):1459-544.
4. Manjunath G, Tighiouart H, Coresh J, Macleod B, Salem DN, Griffith JL, et al. Level of kidney function as a risk factor for cardiovascular outcomes in the elderly. *Kidney Int*. 2003;63(3):1121-9.
5. van der Velde M, Matsushita K, Coresh J, Astor BC, Woodward M, Levey A, et al. Lower estimated glomerular filtration rate and higher albuminuria are associated with all-cause and cardiovascular mortality. A collaborative meta-analysis of high-risk population cohorts. *Kidney Int*. 2011;79(12):1341-52.
6. Levey AS, Coresh J. Chronic kidney disease. *Lancet*. 2012;379(9811):165-80.
7. National Kidney F. K/DOQI clinical practice guidelines for chronic kidney disease: evaluation, classification, and stratification. *Am J Kidney Dis*. 2002;39(2 Suppl 1):S1-266.
8. Couser WG, Remuzzi G, Mendis S, Tonelli M. The contribution of chronic kidney disease to the global burden of major noncommunicable diseases. *Kidney Int*. 2011;80(12):1258-70.
9. Pippias M, Kramer A, Noordzij M, Afentakis N, Alonso de la Torre R, Ambuhl PM, et al. The European Renal Association - European Dialysis and Transplant Association Registry Annual Report 2014: a summary. *Clin Kidney J*. 2017;10(2):154-69.
10. Cozzolino M, Galassi A, Pivari F, Ciceri P, Conte F. The Cardiovascular Burden in End-Stage Renal Disease. *Contrib Nephrol*. 2017;191:44-57.
11. Sharma S, Sarnak MJ. The global burden of reduced GFR: ESRD, CVD and mortality. *Nature Reviews Nephrology*. 2017;13(8):447-8.
12. Kramer A, Pippias M, Noordzij M, Stel VS, Andrusev AM, Aparicio-Madre MI, et al. The European Renal Association - European Dialysis and Transplant Association (ERA-EDTA) Registry Annual Report 2016: a summary. *Clin Kidney J*. 2019;12(5):702-20.
13. Lisowska-Myjak B. Uremic toxins and their effects on multiple organ systems. *Nephron Clin Pract*. 2014;128(3-4):303-11.
14. Tonelli M, Karumanchi SA, Thadhani R. Epidemiology and Mechanisms of Uremia-Related Cardiovascular Disease. *Circulation*. 2016;133(5):518-36.
15. Chikotas N, Gunderman A, Oman T. Uremic syndrome and end-stage renal disease: physical manifestations and beyond. *J Am Acad Nurse Pract*. 2006;18(5):195-202.

16. Clark WR, Dehghani NL, Narsimhan V, Ronco C. Uremic Toxins and their Relation to Dialysis Efficacy. *Blood Purification*. 2019;48(4):299-314.
17. Vanholder R, Pletinck A, Schepers E, Glorieux G. Biochemical and Clinical Impact of Organic Uremic Retention Solutes: A Comprehensive Update. *Toxins*. 2018;10(1):33.
18. Dhondt A, Vanholder R, Van Biesen W, Lameire N. The removal of uremic toxins. *Kidney Int Suppl*. 2000;76:S47-59.
19. Vanholder R, Gryp T, Glorieux G. Urea and chronic kidney disease: the comeback of the century? (in uraemia research). *Nephrol Dial Transplant*. 2018;33(1):4-12.
20. Oliva-Damaso E, Oliva-Damaso N, Rodriguez-Esparragon F, Payan J, Baamonde-Laborda E, Gonzalez-Cabrera F, et al. Asymmetric (ADMA) and Symmetric (SDMA) Dimethylarginines in Chronic Kidney Disease: A Clinical Approach. *Int J Mol Sci*. 2019;20(15):3668.
21. Salyer WR, Keren D. Oxalosis as a complication of chronic renal failure. *Kidney Int*. 1973;4(1):61-6.
22. Kushner D, Beckman B, Nguyen L, Chen S, Della Santina C, Husserl F, et al. Polyamines in the anemia of end-stage renal disease. *Kidney Int*. 1991;39(4):725-32.
23. Drüeke TB, Massy ZA. Beta2-microglobulin. *Semin Dial*. 2009;22(4):378-80.
24. Vanholder R, Bammens B, de Loor H, Glorieux G, Meijers B, Schepers E, et al. Warning: the unfortunate end of p-cresol as a uraemic toxin. *Nephrol Dial Transplant*. 2011;26(5):1464-7.
25. Motojima M, Hosokawa A, Yamato H, Muraki T, Yoshioka T. Uraemic toxins induce proximal tubular injury via organic anion transporter 1-mediated uptake. *Br J Pharmacol*. 2002;135(2):555-63.
26. Burton GJ, Jauniaux E. Oxidative stress. *Best Pract Res Clin Obstet Gynaecol*. 2011;25(3):287-99.
27. Locatelli F, Canaud B, Eckardt KU, Stenvinkel P, Wanner C, Zoccali C. Oxidative stress in end-stage renal disease: an emerging threat to patient outcome. *Nephrol Dial Transplant*. 2003;18(7):1272-80.
28. Sies H. Oxidative stress: oxidants and antioxidants. *Exp Physiol*. 1997;82(2):291-5.
29. Ling XC, Kuo K-L. Oxidative stress in chronic kidney disease. *Renal Replacement Therapy*. 2018;4(1):53.
30. Canaud B, Cristol J, Morena M, Leray-Moragues H, Bosc J, Vaussenat F. Imbalance of oxidants and antioxidants in haemodialysis patients. *Blood Purif*. 1999;17(2-3):99-106.
31. Yilmaz MI, Saglam M, Caglar K, Cakir E, Sonmez A, Ozgurtas T, et al. The determinants of endothelial dysfunction in CKD: oxidative stress and asymmetric dimethylarginine. *Am J Kidney Dis*. 2006;47(1):42-50.
32. Palleschi S, De Angelis S, Diana L, Rossi B, Papa V, Severini G, et al. Reliability of oxidative stress biomarkers in hemodialysis patients: a comparative study. *Clin Chem Lab Med*. 2007;45(9):1211-8.

33. Frijhoff J, Winyard PG, Zarkovic N, Davies SS, Stocker R, Cheng D, et al. Clinical Relevance of Biomarkers of Oxidative Stress. *Antioxid Redox Signal*. 2015;23(14):1144-70.
34. Spickett CM, Wiswedel I, Siems W, Zarkovic K, Zarkovic N. Advances in methods for the determination of biologically relevant lipid peroxidation products. *Free Radic Res*. 2010;44(10):1172-202.
35. Cobo G, Lindholm B, Stenvinkel P. Chronic inflammation in end-stage renal disease and dialysis. *Nephrology, dialysis, transplantation : official publication of the European Dialysis and Transplant Association - European Renal Association*. 2018;33(suppl\_3):iii35-iii40.
36. Vaziri ND, Pahl MV, Crum A, Norris K. Effect of uremia on structure and function of immune system. *J Ren Nutr*. 2012;22(1):149-56.
37. Yoon JW, Pahl MV, Vaziri ND. Spontaneous leukocyte activation and oxygen-free radical generation in end-stage renal disease. *Kidney Int*. 2007;71(2):167-72.
38. Cohen G, Horl WH. Immune dysfunction in uremia&#8212;an update. *Toxins (Basel)*. 2012;4(11):962-90.
39. Fassett RG, Venuthurupalli SK, Gobe GC, Coombes JS, Cooper MA, Hoy WE. Biomarkers in chronic kidney disease: a review. *Kidney International*. 2011;80(8):806-21.
40. Boehme M, Kaehne F, Kuehne A, Bernhardt W, Schröder M, Pommer W, et al. Pentraxin 3 is elevated in haemodialysis patients and is associated with cardiovascular disease. *Nephrology Dialysis Transplantation*. 2007;22(8):2224-9.
41. Valente MJ, Rocha S, Coimbra S, Catarino C, Rocha-Pereira P, Bronze-da-Rocha E, et al. Long Pentraxin 3 as a Broader Biomarker for Multiple Risk Factors in End-Stage Renal Disease: Association with All-Cause Mortality. *Mediators of Inflammation*. 2019;2019:3295725.
42. Libetta C, Sepe V, Esposito P, Galli F, Dal Canton A. Oxidative stress and inflammation: Implications in uremia and hemodialysis. *Clin Biochem*. 2011;44(14-15):1189-98.
43. Bronze-da-Rocha E, Santos-Silva A. Neutrophil Elastase Inhibitors and Chronic Kidney Disease. *Int J Biol Sci*. 2018;14(10):1343-60.
44. Wiedow O, Meyer-Hoffert U. Neutrophil serine proteases: potential key regulators of cell signalling during inflammation. *Journal of Internal Medicine*. 2005;257(4):319-28.
45. Pham CT. Neutrophil serine proteases: specific regulators of inflammation. *Nat Rev Immunol*. 2006;6(7):541-50.
46. Korkmaz B, Moreau T, Gauthier F. Neutrophil elastase, proteinase 3 and cathepsin G: physicochemical properties, activity and physiopathological functions. *Biochimie*. 2008;90(2):227-42.
47. Sinha S, Watorek W, Karr S, Giles J, Bode W, Travis J. Primary structure of human neutrophil elastase. *Proc Natl Acad Sci U S A*. 1987;84(8):2228-32.
48. Havemann K, Gramse M. Physiology and pathophysiology of neutral proteinases of human granulocytes. *Adv Exp Med Biol*. 1984;167:1-20.

49. Pham CTN. Neutrophil serine proteases fine-tune the inflammatory response. *Int J Biochem Cell Biol.* 2008;40(6-7):1317-33.
50. Dahlen JR, Foster DC, Kisiel W. Inhibition of neutrophil elastase by recombinant human proteinase inhibitor 9. *Biochim Biophys Acta.* 1999;1451(2-3):233-41.
51. Kuzniar J, Kuzniar TJ, Marchewka Z, Lembas-Bogaczyk J, Rabczynski J, Kopec W, et al. Elastase deposits in the kidney and urinary elastase excretion in patients with glomerulonephritis--evidence for neutrophil involvement in renal injury. *Scand J Urol Nephrol.* 2007;41(6):527-34.
52. Costa E, Rocha S, Rocha-Pereira P, Nascimento H, Castro E, Miranda V, et al. Neutrophil activation and resistance to recombinant human erythropoietin therapy in hemodialysis patients. *Am J Nephrol.* 2008;28(6):935-40.
53. Khatib-Massalha E, Michelis R, Trabelcy B, Gerchman Y, Kristal B, Ariel A, et al. Free circulating active elastase contributes to chronic inflammation in patients on hemodialysis. *American Journal of Physiology-Renal Physiology.* 2018;314(2):F203-F9.
54. Locatelli F, Bárány P, Covic A, et al. Kidney Disease: Improving Global Outcomes guidelines on anaemia management in chronic kidney disease: a European Renal Best Practice position statement. *Nephrology Dialysis Transplantation.* 2013;28(6):1346-59.
55. Babitt JL, Lin HY. Mechanisms of anemia in CKD. *J Am Soc Nephrol.* 2012;23(10):1631-1634.
56. Ibrahim FF, Ghannam MM, Ali FM. Effect of dialysis on erythrocyte membrane of chronically hemodialyzed patients. *Ren Fail.* 2002;24(6):779-90.
57. Brzeszczynska J, Luciak M, Gwozdziński K. Alterations of erythrocyte structure and cellular susceptibility in patients with chronic renal failure: effect of haemodialysis and oxidative stress. *Free Radic Res.* 2008;42(1):40-8.
58. Reinhart WH, Chien S. Red cell rheology in stomatocyte-echinocyte transformation: roles of cell geometry and cell shape. *Blood.* 1986;67(4):1110-8.
59. Ganz T, Nemeth E. Iron Balance and the Role of Hepcidin in Chronic Kidney Disease. *Semin Nephrol.* 2016;36(2):87-93.
60. Zaritsky J, Young B, Wang HJ, Westerman M, Olbina G, Nemeth E, et al. Hepcidin--a potential novel biomarker for iron status in chronic kidney disease. *Clin J Am Soc Nephrol.* 2009;4(6):1051-6.
61. Nurko S. Anemia in chronic kidney disease: causes, diagnosis, treatment. *Cleve Clin J Med.* 2006;73(3):289-97.
62. Morceau F, Dicato M, Diederich M. Pro-inflammatory cytokine-mediated anemia: regarding molecular mechanisms of erythropoiesis. *Mediators Inflamm.* 2009;2009:405016.
63. Means RT, Jr., Dessypris EN, Krantz SB. Inhibition of human erythroid colony-forming units by interleukin-1 is mediated by gamma interferon. *J Cell Physiol.* 1992;150(1):59-64.
64. KDOQI Clinical Practice Guidelines and Clinical Practice Recommendations for Anemia in Chronic Kidney Disease. *Am J Kidney Dis.* 2006;47(5 Suppl 3):S11-145.



65. Muzzarelli S, Pfisterer M, Investigators T. Anemia as independent predictor of major events in elderly patients with chronic angina. *Am Heart J*. 2006;152(5):991-6.
66. Johnson DW, Pollock CA, Macdougall IC. Erythropoiesis-stimulating agent hyporesponsiveness. *Nephrology (Carlton)*. 2007;12(4):321-30.
67. Nemeth E, Ganz T. Anemia of inflammation. *Hematol Oncol Clin North Am*. 2014;28(4):671-vi.
68. Kimmel PL, Rosenberg ME. *Chronic Renal Disease*: Elsevier Science; 2019.
69. Himmelfarb J, Ikizler TA. Hemodialysis. *N Engl J Med*. 2010;363(19):1833-45.
70. Sinnakirouchenan R, Holley JL. Peritoneal dialysis versus hemodialysis: risks, benefits, and access issues. *Adv Chronic Kidney Dis*. 2011;18(6):428-32.
71. Alam M, Krause MW. Peritoneal dialysis solutions. *Uptodate*. 2005;13:1.
72. Kaur A, Davenport A. Hemodialysis for infants, children, and adolescents. *Hemodial Int*. 2014;18(3):573-82.
73. Jaar BG, Plantinga LC, Crews DC, Fink NE, Hebah N, Coresh J, et al. Timing, causes, predictors and prognosis of switching from peritoneal dialysis to hemodialysis: a prospective study. *BMC Nephrol*. 2009;10:3-.
74. Kolff WJ, Watschinger B. Further development of a coil kidney; disposable artificial kidney. *J Lab Clin Med*. 1956;47(6):969-77.
75. Kidney Dialysis Information - Inventor of Dialysis [Accessed 12.03.2020]. Available from: <http://www.kidneydialysis.org.uk/inventor-of-dialysis.htm>.
76. Fresenius Medical Care [Accessed 12.03.2020]. Available from: <https://www.freseniusmedicalcare.com/en/healthcare-professionals/hemodialysis/machines/machines-overview/>.
77. Haag-Weber M. Treatment options to intensify hemodialysis. *Kidney Blood Press Res*. 2003;26(2):90-5.
78. Principle of Dialysis Assignment Help [Accessed 14.03.2020]. Available from: <https://www.freeassignmenthelp.com/principle-of-dialysis-assignment-help/>.
79. Misra M. The basics of hemodialysis equipment. *Hemodial Int*. 2005;9(1):30-6.
80. Ahrenholz P, Winkler R, Zendeher-Zartochti D. The Role of the Dialysate Flow Rate in Haemodialysis. 2013.
81. Locatelli F, La Milia V, Violo L, Del Vecchio L, Di Filippo S. Optimizing haemodialysate composition. *Clinical kidney journal*. 2015;8(5):580-9.
82. Vigano SM, Di Filippo S, Manzoni C, Locatelli F. Membrane characteristics. *Contrib Nephrol*. 2008;161:162-7.
83. Ward RA. Do clinical outcomes in chronic hemodialysis depend on the choice of a dialyzer? *Semin Dial*. 2011;24(1):65-71.
84. Karkar A. Modalities of hemodialysis: quality improvement. *Saudi J Kidney Dis Transpl*. 2012;23(6):1145-61.

85. Hootkins R. Lessons in dialysis, dialyzers, and dialysate. *Dialysis & Transplantation*. 2011;40(9):392-6.
86. Ledebro I, Blankestijn PJ. Haemodiafiltration-optimal efficiency and safety. *NDT Plus*. 2010;3(1):8-16.
87. Ronco C, Clark WR. Haemodialysis membranes. *Nature Reviews Nephrology*. 2018;14(6):394-410.
88. Fleming GM. Renal replacement therapy review: past, present and future. *Organogenesis*. 2011;7(1):2-12.
89. Huang Z, Gao D, Letteri JJ, Clark WR. Blood-membrane interactions during dialysis. *Semin Dial*. 2009;22(6):623-8.
90. Aucella F, Gesuete A, Vigilante M, Prencipe M. Adsorption dialysis: from physical principles to clinical applications. *Blood Purif*. 2013;35 Suppl 2:42-7.
91. Gotch FA, Sargent JA. A mechanistic analysis of the National Cooperative Dialysis Study (NCDS). *Kidney Int*. 1985;28(3):526-34.
92. Lowrie EG, Li Z, Ofsthun N. Measurement of dialyzer clearance, dialysis time, and body size: death risk relationships among patients. *Kidney Int*. 2004;66(5):2077-84.
93. Port FK, Ashby VB, Dhingra RK, Roys EC, Wolfe RA. Dialysis dose and body mass index are strongly associated with survival in hemodialysis patients. *J Am Soc Nephrol*. 2002;13(4):1061-6.
94. KDOQI Clinical Practice Guideline for Hemodialysis Adequacy: 2015 update. *Am J Kidney Dis*. 2015;66(5):884-930.
95. Bhimani JP, Ouseph R, Ward RA. Effect of increasing dialysate flow rate on diffusive mass transfer of urea, phosphate and beta2-microglobulin during clinical haemodialysis. *Nephrol Dial Transplant*. 2010;25(12):3990-5.
96. Saha M, Allon M. Diagnosis, Treatment, and Prevention of Hemodialysis Emergencies. *Clinical journal of the American Society of Nephrology : CJASN*. 2017;12(2):357-69.
97. Sars B, van der Sande FM, Kooman JP. Intradialytic Hypotension: Mechanisms and Outcome. *Blood Purification*. 2020;49(1-2):158-67.
98. Morfin JA, Fluck RJ, Weinhandl ED, Kansal S, McCullough PA, Komenda P. Intensive Hemodialysis and Treatment Complications and Tolerability. *Am J Kidney Dis*. 2016;68(5S1):S43-S50.
99. Tharmaraj D, Kerr PG. Haemolysis in haemodialysis. *Nephrology*. 2017;22(11):838-47.
100. Nassar GM, Ayus JC. Infectious complications of the hemodialysis access. *Kidney Int*. 2001;60(1):1-13.
101. Danesh F, Ho LT. Dialysis-related amyloidosis: history and clinical manifestations. *Semin Dial*. 2001;14(2):80-5.
102. Yang CC, Hsu SP, Wu MS, Hsu SM, Chien CT. Effects of vitamin C infusion and vitamin E-coated membrane on hemodialysis-induced oxidative stress. *Kidney Int*. 2006;69(4):706-14.

103. Liakopoulos V, Roumeliotis S, Gorny X, Dounousi E, Mertens PR. Oxidative Stress in Hemodialysis Patients: A Review of the Literature. *Oxid Med Cell Longev*. 2017;2017:3081856.
104. Ratliff BB, Abdulmahdi W, Pawar R, Wolin MS. Oxidant Mechanisms in Renal Injury and Disease. *Antioxid Redox Signal*. 2016;25(3):119-46.
105. Valko M, Leibfritz D, Moncol J, Cronin MT, Mazur M, Telser J. Free radicals and antioxidants in normal physiological functions and human disease. *Int J Biochem Cell Biol*. 2007;39(1):44-84.
106. Rubio CP, Hernández-Ruiz J, Martínez-Subiela S, Tvarijonaviciute A, Ceron JJ. Spectrophotometric assays for total antioxidant capacity (TAC) in dog serum: an update. *BMC Vet Res*. 2016;12(1):166-.
107. Zelko IN, Mariani TJ, Folz RJ. Superoxide dismutase multigene family: a comparison of the CuZn-SOD (SOD1), Mn-SOD (SOD2), and EC-SOD (SOD3) gene structures, evolution, and expression. *Free Radical Biology and Medicine*. 2002;33(3):337-49.
108. Crawford A, Fassett RG, Coombes JS, Kunde DA, Ahuja KDK, Robertson IK, et al. Glutathione peroxidase, superoxide dismutase and catalase genotypes and activities and the progression of chronic kidney disease. *Nephrology Dialysis Transplantation*. 2011;26(9):2806-13.
109. Morena M, Cristol JP, Bosc JY, Tetta C, Forret G, Leger CL, et al. Convective and diffusive losses of vitamin C during haemodiafiltration session: a contributive factor to oxidative stress in haemodialysis patients. *Nephrol Dial Transplant*. 2002;17(3):422-7.
110. Liakopoulos V, Roumeliotis S, Bozikas A, Eleftheriadis T, Dounousi E. Antioxidant Supplementation in Renal Replacement Therapy Patients: Is There Evidence? *Oxid Med Cell Longev*. 2019;2019:9109473.
111. Santangelo F, Witko-Sarsat V, Drüeke T, Descamps-Latscha B. Restoring glutathione as a therapeutic strategy in chronic kidney disease. *Nephrology Dialysis Transplantation*. 2004;19(8):1951-5.
112. Aruoma OI, Halliwell B, Hoey BM, Butler J. The antioxidant action of N-acetylcysteine: its reaction with hydrogen peroxide, hydroxyl radical, superoxide, and hypochlorous acid. *Free Radic Biol Med*. 1989;6(6):593-7.
113. Giannikouris I. The effect of N-acetylcysteine on oxidative serum biomarkers of hemodialysis patients. *Hippokratia*. 2015;19(2):131.
114. Shahbazian H, Shayanpour S, Ghorbani A. Evaluation of administration of oral N-acetylcysteine to reduce oxidative stress in chronic hemodialysis patients: A double-blind, randomized, controlled clinical trial. *Saudi J Kidney Dis Transpl*. 2016;27(1):88-93.
115. Drager LF, Andrade L, Barros de Toledo JF, Laurindo FR, Machado Cesar LA. Renal effects of N-acetylcysteine in patients at risk for contrast nephropathy: decrease in oxidant stress-mediated renal tubular injury. *Nephrol Dial Transplant*. 2004;19(7):1803-7.
116. Taccone-Gallucci M, Lubrano R, Meloni C. Vitamin E as an antioxidant agent. *Contrib Nephrol*. 1999;127:32-43.

117. Traber MG, Atkinson J. Vitamin E, antioxidant and nothing more. *Free Radic Biol Med.* 2007;43(1):4-15.
118. Traber MG. Vitamin E regulatory mechanisms. *Annu Rev Nutr.* 2007;27:347-62.
119. Cristol JP, Bosc JY, Badiou S, Leblanc M, Lorrho R, Descomps B, et al. Erythropoietin and oxidative stress in haemodialysis: beneficial effects of vitamin E supplementation. *Nephrol Dial Transplant.* 1997;12(11):2312-7.
120. Antoniadis G, Eleftheriadis T, Liakopoulos V, Kakasi E, Kartsios C, Passadakis P, et al. Effect of One-year Oral  $\alpha$ -Tocopherol Administration on the Antioxidant Defense System in Hemodialysis Patients. *Therapeutic Apheresis and Dialysis.* 2008;12(3):237-42.
121. Galli F, Varga Z, Balla J, Ferraro B, Canestrari F, Floridi A, et al. Vitamin E, lipid profile, and peroxidation in hemodialysis patients. *Kidney Int Suppl.* 2001;78:S148-54.
122. Boaz M, Smetana S, Weinstein T, Matas Z, Gafer U, Iaina A, et al. Secondary prevention with antioxidants of cardiovascular disease in endstage renal disease (SPACE): randomised placebo-controlled trial. *Lancet.* 2000;356(9237):1213-8.
123. Pearson P, Lewis SA, Britton J, Young IS, Fogarty A. The pro-oxidant activity of high-dose vitamin E supplements in vivo. *BioDrugs.* 2006;20(5):271-3.
124. Duarte TL, Lunec J. Review: When is an antioxidant not an antioxidant? A review of novel actions and reactions of vitamin C. *Free Radic Res.* 2005;39(7):671-86.
125. Ghiadoni L, Cupisti A, Huang Y, Mattei P, Cardinal H, Favilla S, et al. Endothelial dysfunction and oxidative stress in chronic renal failure. *Journal of nephrology.* 2004;17(4):512-9.
126. Abdollahzad H, Egthesadi S, Nourmohammadi I, Khadem-Ansari M, Nejad-Gashti H, Esmailzadeh A. Effect of vitamin C supplementation on oxidative stress and lipid profiles in hemodialysis patients. *International journal for vitamin and nutrition research.* 2009;79(56):281-7.
127. Boudouris G, Verginadis II, Simos YV, Zouridakis A, Ragos V, Karkabounas SC, et al. Oxidative stress in patients treated with continuous ambulatory peritoneal dialysis (CAPD) and the significant role of vitamin C and E supplementation. *International Urology and Nephrology.* 2013;45(4):1137-44.
128. Rochette L, Ghibu S, Muresan A, Vergely C. Alpha-lipoic acid: molecular mechanisms and therapeutic potential in diabetes. *Can J Physiol Pharmacol.* 2015;93(12):1021-7.
129. Packer L. Antioxidant properties of lipoic acid and its therapeutic effects in prevention of diabetes complications and cataracts. *Ann N Y Acad Sci.* 1994;738:257-64.
130. Khabbazi T, Mahdavi R, Safa J, Pour-Abdollahi P. Effects of alpha-lipoic acid supplementation on inflammation, oxidative stress, and serum lipid profile levels in patients with end-stage renal disease on hemodialysis. *Journal of renal nutrition.* 2012;22(2):244-50.
131. El-Nakib GA, Mostafa TM, Abbas TM, El-Shishtawy MM, Mabrouk MM, Sobh MA. Role of alpha-lipoic acid in the management of anemia in patients with chronic renal failure undergoing hemodialysis. *International journal of nephrology and renovascular disease.* 2013;6:161.

132. Ahmadi A, Mazooji N, Roozbeh J, Mazloom Z, Hasanzade J. Effect of alpha-lipoic acid and vitamin E supplementation on oxidative stress, inflammation, and malnutrition in hemodialysis patients. *Iranian Journal of Kidney Diseases*. 2013;7(6):461.
133. Gonzalez-Perez O, Gonzalez-Castaneda RE. Therapeutic Perspectives on the Combination of Alpha-Lipoic Acid and Vitamin E. *Nutr Res*. 2006;26(1):1-5.
134. Wilczynska M, Fa M, Ohlsson PI, Ny T. The inhibition mechanism of serpins. Evidence that the mobile reactive center loop is cleaved in the native protease-inhibitor complex. *J Biol Chem*. 1995;270(50):29652-5.
135. Fitch PM, Roghanian A, Howie SE, Sallenave JM. Human neutrophil elastase inhibitors in innate and adaptive immunity. *Biochem Soc Trans*. 2006;34(Pt 2):279-82.
136. Travis J, Salvesen GS. Human plasma proteinase inhibitors. *Annu Rev Biochem*. 1983;52:655-709.
137. Majewski P, Majchrzak-Gorecka M, Grygier B, Skrzeczynska-Moncznik J, Osiecka O, Cichy J. Inhibitors of Serine Proteases in Regulating the Production and Function of Neutrophil Extracellular Traps. *Front Immunol*. 2016;7:261.
138. Quezada LAL, McKerrow JH. Schistosome serine protease inhibitors: parasite defense or homeostasis? *Anais da Academia Brasileira de Ciências*. 2011;83:663-72.
139. Polanska B, Augustyniak D, Makulska I, Niemczuk M, Zwolinska D, Jankowski A. Elastase, alpha1-proteinase inhibitor, and interleukin-8 in pre-dialyzed and hemodialyzed patients with chronic kidney disease. *Pediatr Int*. 2010;52(5):735-43.
140. Korkmaz B, Horwitz MS, Jenne DE, Gauthier F. Neutrophil elastase, proteinase 3, and cathepsin G as therapeutic targets in human diseases. *Pharmacol Rev*. 2010;62(4):726-59.
141. von Nussbaum F, Li VMJ. Neutrophil elastase inhibitors for the treatment of (cardio)pulmonary diseases: Into clinical testing with pre-adaptive pharmacophores. *Bioorganic & Medicinal Chemistry Letters*. 2015;25(20):4370-81.
142. Yoshimura Y, Hiramatsu Y, Sato Y, Homma S, Enomoto Y, Jikuya T, et al. ONO-6818, a novel, potent neutrophil elastase inhibitor, reduces inflammatory mediators during simulated extracorporeal circulation. *The Annals of thoracic surgery*. 2003;76(4):1234-9.
143. Ohbayashi H. Neutrophil elastase inhibitors as treatment for COPD. *Expert Opinion on Investigational Drugs*. 2002;11(7):965-80.
144. Huang W, Yamamoto Y, Li Y, Dou D, Alliston KR, Hanzlik RP, et al. X-ray Snapshot of the Mechanism of Inactivation of Human Neutrophil Elastase by 1,2,5-Thiadiazolidin-3-one 1,1-Dioxide Derivatives. *Journal of Medicinal Chemistry*. 2008;51(7):2003-8.
145. von Nussbaum F, Li VMJ, Allerheiligen S, Anlauf S, Bärfacker L, Bechem M, et al. Freezing the Bioactive Conformation to Boost Potency: The Identification of BAY 85-8501, a Selective and Potent Inhibitor of Human Neutrophil Elastase for Pulmonary Diseases. *ChemMedChem*. 2015;10(7):1163-73.
146. Stevens T, Ekholm K, Gränse M, Lindahl M, Kozma V, Jungar C, et al. AZD9668: pharmacological characterization of a novel oral inhibitor of neutrophil elastase. *J Pharmacol Exp Ther*. 2011;339(1):313-20.

147. Dell'Aica I, Sartor L, Galletti P, Giacomini D, Quintavalla A, Calabrese F, et al. Inhibition of leukocyte elastase, polymorphonuclear chemoinvasion, and inflammation-triggered pulmonary fibrosis by a 4-alkyliden-beta-lactam with a galloyl moiety. *J Pharmacol Exp Ther*. 2006;316(2):539-46.
148. Mulchande J, Oliveira R, Carrasco M, Gouveia L, Guedes RC, Iley J, et al. 4-Oxo-beta-lactams (azetidine-2,4-diones) are potent and selective inhibitors of human leukocyte elastase. *J Med Chem*. 2010;53(1):241-53.
149. Feng L, Liu X, Zhu W, Guo F, YingchunWu, Wang R, et al. Inhibition of Human Neutrophil Elastase by Pentacyclic Triterpenes. *PLOS ONE*. 2013;8(12):e82794.
150. Melzig MF, Loser B, Ciesielski S. Inhibition of neutrophil elastase activity by phenolic compounds from plants. *Pharmazie*. 2001;56(12):967-70.
151. Braga PC, Dal Sasso M, Culici M, Bianchi T, Bordoni L, Marabini L. Anti-inflammatory activity of thymol: inhibitory effect on the release of human neutrophil elastase. *Pharmacology*. 2006;77(3):130-6.
152. Rennert B, Melzig MF. Free fatty acids inhibit the activity of *Clostridium histolyticum* collagenase and human neutrophil elastase. *Planta Med*. 2002;68(9):767-9.
153. Pochet L, Frederick R, Masereel B. Coumarin and isocoumarin as serine protease inhibitors. *Curr Pharm Des*. 2004;10(30):3781-96.
154. Siedle B, Hrenn A, Merfort I. Natural compounds as inhibitors of human neutrophil elastase. *Planta Med*. 2007;73(5):401-20.
155. Hueso M, Vellido A, Montero N, Barbieri C, Ramos R, Angoso M, et al. Artificial Intelligence for the Artificial Kidney: Pointers to the Future of a Personalized Hemodialysis Therapy. *Kidney Dis (Basel)*. 2018;4(1):1-9.
156. Salani M, Roy S, Fissell WH. Innovations in Wearable and Implantable Artificial Kidneys. *Am J Kidney Dis*. 2018;72(5):745-51.
157. Kim S, Fissell WH, Humes DH, Roy S. Current strategies and challenges in engineering a bioartificial kidney. *Front Biosci (Elite Ed)*. 2015;7:215-28.
158. Figoli A, Marino T, Simone S, Di Nicolò E, Li XM, He T, et al. Towards non-toxic solvents for membrane preparation: a review. *Green Chemistry*. 2014;16(9):4034-59.
159. Abetz V, Brinkmann T, Dijkstra M, Ebert K, Fritsch D, Ohlrogge K, et al. Developments in Membrane Research: from Material via Process Design to Industrial Application. *Advanced Engineering Materials*. 2006;8(5):328-58.
160. Wenten IG, Aryanti PTP, Khoiruddin K, Hakim AN, Himma NF. Advances in Polysulfone-Based Membranes for Hemodialysis. *Journal of Membrane Science and Research*. 2016;2(2):78-89.
161. Cheung AK, Levin NW, Greene T, Agodoa L, Bailey J, Beck G, et al. Effects of High-Flux Hemodialysis on Clinical Outcomes: Results of the HEMO Study. *Journal of the American Society of Nephrology*. 2003;14(12):3251-63.
162. Kim HW, Kim S-H, Kim YO, Jin DC, Song HC, Choi EJ, et al. Comparison of the Impact of High-Flux Dialysis on Mortality in Hemodialysis Patients with and without Residual Renal Function. *PLOS ONE*. 2014;9(6):e97184.

163. Naka T, Haase M, Bellomo R. 'Super high-flux' or 'high cut-off' hemofiltration and hemodialysis. *Contrib Nephrol*. 2010;166:181-9.
164. Girndt M, Fiedler R, Martus P, Pawlak M, Storr M, Bohler T, et al. High cut-off dialysis in chronic haemodialysis patients. *Eur J Clin Invest*. 2015;45(12):1333-40.
165. Clark WR, Hamburger RJ, Lysaght MJ. Effect of membrane composition and structure on solute removal and biocompatibility in hemodialysis. *Kidney Int*. 1999;56(6):2005-15.
166. Pal P. Chapter 5 - Water Treatment by Membrane-Separation Technology. In: Pal P, editor. *Industrial Water Treatment Process Technology*; Butterworth-Heinemann; 2017. p. 173-242.
167. Weber WJ. *Physiochemical processes for water quality control*. 1972.
168. Karkar A. *Advances in Hemodialysis Techniques*; INTECH Open Access Publisher; 2013.
169. Tan X, Rodrigue D. A Review on Porous Polymeric Membrane Preparation. Part I: Production Techniques with Polysulfone and Poly (Vinylidene Fluoride). *Polymers-Basel*. 2019;11(7):1160.
170. MacLeod A, Daly C, Khan I, Vale L, Campbell M, Wallace S, et al. Comparison of cellulose, modified cellulose and synthetic membranes in the haemodialysis of patients with end-stage renal disease. *Cochrane Database Syst Rev*. 2001(3):CD003234.
171. Boure T, Vanholder R. Which dialyser membrane to choose? *Nephrol Dial Transplant*. 2004;19(2):293-6.
172. Horl WH. Hemodialysis membranes: interleukins, biocompatibility, and middle molecules. *J Am Soc Nephrol*. 2002;13 Suppl 1:S62-71.
173. Cheung AK, Parker CJ, Wilcox L, Janatova J. Activation of the alternative pathway of complement by cellulosic hemodialysis membranes. *Kidney Int*. 1989;36(2):257-65.
174. Jaber BL, Cendoroglo M, Balakrishnan VS, Perianayagam MC, Karsou SA, Ruthazer R, et al. Impact of dialyzer membrane selection on cellular responses in acute renal failure: a crossover study. *Kidney Int*. 2000;57(5):2107-16.
175. Girndt M, Heisel O, Kohler H. Influence of dialysis with polyamide vs haemophan haemodialysers on monokines and complement activation during a 4-month long-term study. *Nephrol Dial Transplant*. 1999;14(3):676-82.
176. Hakim RM. Clinical implications of hemodialysis membrane biocompatibility. *Kidney Int*. 1993;44(3):484-94.
177. Subramanian S, Venkataraman R, Kellum JA. Influence of dialysis membranes on outcomes in acute renal failure: a meta-analysis. *Kidney Int*. 2002;62(5):1819-23.
178. Carracedo J, Ramirez R, Madueno JA, Soriano S, Rodriguez-Benot A, et al. Cell apoptosis and hemodialysis-induced inflammation. *Kidney Int Suppl*. 2002(80):89-93.
179. Schaefer RM, Horl WH, Kokot K, Heidland A. Enhanced biocompatibility with a new cellulosic membrane: Cuprophane versus Hemophan. *Blood Purif*. 1987;5(4):262-7.
180. Yamashita AC, Sakurai K. Dialysis membranes—physico-chemical structures and features. *Updates in Hemodialysis*; Suzuki, H, Ed; INTECH: Vienna, Austria. 2015:163-89.

181. Sakai K, Matsuda M. Solute removal efficiency and biocompatibility of the high-performance membrane - from engineering points of view. *Contrib Nephrol.* 2011;173:11-22.
182. Henrich WL. Principles and practice of dialysis 2012.
183. Falca G, Musteata V-E, Behzad AR, Chisca S, Nunes SP. Cellulose hollow fibers for organic resistant nanofiltration. *J Membrane Sci.* 2019;586:151-61.
184. Kajekar A, Dodamani BM, Isloor A, Abdul Karim Z, Ng BC, Ismail A, et al. Preparation and characterization of novel PSf/PVP/PANI-nanofiber nanocomposite hollow fiber ultrafiltration membranes and their possible applications for hazardous dye rejection. *Desalination.* 2015;365.
185. Sakai K. Dialysis membranes for blood purification. *Frontiers of medical and biological engineering : the international journal of the Japan Society of Medical Electronics and Biological Engineering.* 2000;10(2):117-29.
186. Hakim RM, Held PJ, Stannard DC, Wolfe RA, Port FK, Daugirdas JT, et al. Effect of the dialysis membrane on mortality of chronic hemodialysis patients. *Kidney Int.* 1996;50(2):566-70.
187. Jaber BL, Lau J, Schmid CH, Karsou SA, Levey AS, Pereira BJ. Effect of biocompatibility of hemodialysis membranes on mortality in acute renal failure: a meta-analysis. *Clin Nephrol.* 2002;57(4):274-82.
188. Hernandez MR, Galan AM, Cases A, Lopez-Pedret J, Pereira A, Tonda R, et al. Biocompatibility of cellulosic and synthetic membranes assessed by leukocyte activation. *Am J Nephrol.* 2004;24(2):235-41.
189. Linnenweber S, Lonnemann G. Effects of dialyzer membrane on interleukin-1beta (IL-1beta) and IL-1beta-converting enzyme in mononuclear cells. *Kidney Int Suppl.* 2001;78:S282-5.
190. Physical and chemical characteristics of dialysis membranes [Accessed 27.03.2020]. Available from: <https://derangedphysiology.com/main/cicm-primary-exam/required-reading/renal-system/dialysis-and-plasmapheresis/Chapter%201165/physical-and-chemical-characteristics-dialysis-membranes>
191. Wego Healthcare [Accessed 28.03.2020]. Available from: [http://www.wego-healthcare.com/en/product\\_type.html?productId=1&type=1](http://www.wego-healthcare.com/en/product_type.html?productId=1&type=1).
192. Itoh S, Susuki C, Tsuji T. Platelet activation through interaction with hemodialysis membranes induces neutrophils to produce reactive oxygen species. *J Biomed Mater Res A.* 2006;77(2):294-303.
193. Nakano A. Ethylene vinyl alcohol co-polymer as a high-performance membrane: an EVOH membrane with excellent biocompatibility. *Contrib Nephrol.* 2011;173:164-71.
194. Galli F. Protein damage and inflammation in uraemia and dialysis patients. *Nephrol Dial Transplant.* 2007;22 Suppl 5:v20-36.
195. Kohlova M, Amorim CG, Araujo A, Santos-Silva A, Solich P, Montenegro M. The biocompatibility and bioactivity of hemodialysis membranes: their impact in end-stage renal disease. *J Artif Organs.* 2019;22(1):14-28.



196. Streicher E, Schneider H. The development of a polysulfone membrane. A new perspective in dialysis? *Contrib Nephrol.* 1985;46:1-13.
197. Bowry SK, Gatti E, Vienken J. Contribution of polysulfone membranes to the success of convective dialysis therapies. *Contrib Nephrol.* 2011;173:110-8.
198. Walker RJ, Sutherland WH, De Jong SA. Effect of changing from a cellulose acetate to a polysulphone dialysis membrane on protein oxidation and inflammation markers. *Clin Nephrol.* 2004;61(3):198-206.
199. Piroddi M, Pilolli F, Aritomi M, Galli F. Vitamin E as a functional and biocompatibility modifier of synthetic hemodialyzer membranes: an overview of the literature on vitamin E-modified hemodialyzer membranes. *Am J Nephrol.* 2012;35(6):559-72.
200. Liu Y, Koops GH, Strathmann H. Characterization of morphology controlled polyethersulfone hollow fiber membranes by the addition of polyethylene glycol to the dope and bore liquid solution. *J Membrane Sci.* 2003;223(1):187-99.
201. Boom RM, Wienk IM, Vandenboomgaard T, Smolders CA. Microstructures in Phase Inversion Membranes .2. The Role of a Polymeric Additive. *J Membrane Sci.* 1992;73(2-3):277-92.
202. Ji Y, Li X-M, Yin Y, Zhang Y-Y, Wang Z-W, He T. Morphological control and cross-flow filtration of microfiltration membranes prepared via a sacrificial-layer approach. *J Membrane Sci.* 2010;353(1):159-68.
203. Abdelrasoul A, Doan H, Lohi A. Morphology Control of Polysulfone Membranes in Filtration Processes: a Critical Review. *ChemBioEng Reviews.* 2015;2(1):22-43.
204. Chakrabarty B, Ghoshal A, Purkait M. Effect of molecular weight of PEG on membrane morphology and transport properties. *J Membrane Sci.* 2008;309(1-2):209-21.
205. Smolders C, Reuvers A, Boom R, Wienk I. Microstructures in phase-inversion membranes. Part 1. Formation of macrovoids. *J Membrane Sci.* 1992;73(2-3):259-75.
206. Guillen GR, Pan Y, Li M, Hoek EMV. Preparation and Characterization of Membranes Formed by Nonsolvent Induced Phase Separation: A Review. *Ind Eng Chem Res.* 2011;50(7):3798-817.
207. Hilal N, Ismail AF, Wright C. *Membrane Fabrication*: CRC Press; 2015.
208. Mydlik M, Derzsiova K, Racz O, Sipulova A, Lovasova E, Molcanyiova A, et al. Vitamin E-coated dialyzer and antioxidant defense parameters: three-month study. *Semin Nephrol.* 2004;24(5):525-31.
209. Neelakandan C, Chang T, Alexander T, Define L, Evancho-Chapman M, Kyu T. In Vitro Evaluation of Antioxidant and Anti-Inflammatory Properties of Genistein-Modified Hemodialysis Membranes. *Biomacromolecules.* 2011;12(7):2447-55.
210. Yasar Mahlicli F, Şen Y, Mutlu M, Alsoy Altinkaya S. Immobilization of superoxide dismutase/catalase onto polysulfone membranes to suppress hemodialysis-induced oxidative stress: A comparison of two immobilization methods. *J Membrane Sci.* 2015;479:175-89.
211. Sun S, Yue Y, Huang X, Meng D. Protein adsorption on blood-contact membranes. *J Membrane Sci.* 2003;222(1):3-18.

212. Khan M, Hussain A. Haemodialysis Membranes: A Review. *J Membr Sci Technol.* 2019;9:199.
213. Yamamoto K-i, Matsuda M, Okuoka M, Yakushiji T, Fukuda M, Miyasaka T, et al. Antioxidation property of vitamin E-coated polysulfone dialysis membrane and recovery of oxidized vitamin E by vitamin C treatment. *J Membrane Sci.* 2007;302(1):115-8.
214. Girndt M, Lengler S, Kaul H, Sester U, Sester M, Kohler H. Prospective crossover trial of the influence of vitamin E-coated dialyzer membranes on T-cell activation and cytokine induction. *Am J Kidney Dis.* 2000;35(1):95-104.
215. Takouli L, Hadjiyannakos D, Metaxaki P, Sideris V, Filiopoulos V, Anogiati A, et al. Vitamin E-coated cellulose acetate dialysis membrane: long-term effect on inflammation and oxidative stress. *Ren Fail.* 2010;32(3):287-93.
216. Sasaki M, Hosoya N, Saruhashi M. Vitamin E modified cellulose membrane. *Artif Organs.* 2000;24(10):779-89.
217. Panichi V, Rosati A, Paoletti S, Ferrandello P, Migliori M, Beati S, et al. A vitamin E-coated polysulfone membrane reduces serum levels of inflammatory markers and resistance to erythropoietin-stimulating agents in hemodialysis patients: results of a randomized cross-over multicenter trial. *Blood Purif.* 2011;32(1):7-14.
218. Clermont G, Lecour S, Cabanne JF, Motte G, Guillard JC, Chevet D, et al. Vitamin E-coated dialyzer reduces oxidative stress in hemodialysis patients. *Free Radic Biol Med.* 2001;31(2):233-41.
219. D'Arrigo G, Baggetta R, Tripepi G, Galli F, Bolignano D. Effects of Vitamin E-Coated versus Conventional Membranes in Chronic Hemodialysis Patients: A Systematic Review and Meta-Analysis. *Blood Purif.* 2017;43(1-3):101-22.
220. Mahlicli FY, Altinkaya SA. Immobilization of alpha lipoic acid onto polysulfone membranes to suppress hemodialysis induced oxidative stress. *J Membrane Sci.* 2014;449:27-37.
221. Kung FC, Yang MC. Effect of conjugated linoleic acid immobilization on the hemocompatibility of cellulose acetate membrane. *Colloids and Surfaces B: Biointerfaces.* 2006;47(1):36-42.
222. Chang T, DeFine L, Alexander T, Kyu T. In vitro investigation of antioxidant, anti-inflammatory, and antiplatelet adhesion properties of genistein-modified poly(ethersulfone)/poly(vinylpyrrolidone) hemodialysis membranes. *J Biomed Mater Res B Appl Biomater.* 2015;103(3):539-47.
223. Neelakandan C, Chang T, Alexander T, Define L, Evancho-Chapman M, Kyu T. In vitro evaluation of antioxidant and anti-inflammatory properties of genistein-modified hemodialysis membranes. *Biomacromolecules.* 2011;12(7):2447-55.
224. Kohira S, Oka N, Inoue N, Itatani K, Hanayama N, Kitamura T, et al. Effect of the neutrophil elastase inhibitor sivelestat on perioperative inflammatory response after pediatric heart surgery with cardiopulmonary bypass: a prospective randomized study. *Artif Organs.* 2013;37(12):1027-33.

225. Stockley R, De Soyza A, Gunawardena K, Perrett J, Forsman-Semb K, Entwistle N, et al. Phase II study of a neutrophil elastase inhibitor (AZD9668) in patients with bronchiectasis. *Respir Med*. 2013;107(4):524-33.
226. Grano V, Diano N, Portaccio M, De Santo N, Di Martino S, Rossi S, et al. Protease removal by means of antiproteases immobilized on supports as a potential tool for hemodialysis or extracorporeal blood circulation. *The International journal of artificial organs*. 2003;26(1):39-45.
227. Grano V, Tasco G, Casadio R, Diano N, Portaccio M, Rossi S, et al. Reduction of active elastase concentration by means of immobilized inhibitors: a novel therapeutic approach. *Biotechnology progress*. 2004;20(3):968-74.
228. Lalia BS, Kochkodan V, Hashaikeh R, Hilal N. A review on membrane fabrication: Structure, properties and performance relationship. *Desalination*. 2013;326:77-95.
229. Mohamed K. Hollow Fiber Spinning. In: Drioli E, Giorno L, editors. *Encyclopedia of Membranes*. Berlin, Heidelberg: Springer Berlin Heidelberg; 2015. p. 1-3.
230. Peng N, Widjojo N, Sukitpaneemit P, Teoh MM, Lipscomb GG, Chung T-S, et al. Evolution of polymeric hollow fibers as sustainable technologies: Past, present, and future. *Prog Polym Sci*. 2012;37(10):1401-24.
231. Chronakis IS. Novel nanocomposites and nanoceramics based on polymer nanofibers using electrospinning process—A review. *Journal of Materials Processing Technology*. 2005;167(2):283-93.
232. Norrman K, Ghanbari-Siahkali A, Larsen NB. 6 Studies of spin-coated polymer films. *Annual Reports Section "C" (Physical Chemistry)*. 2005;101(0):174-201.
233. Spin Coating: Complete Guide to Theory and Techniques [Accessed 17.12.2019]. Available from: <https://www.ossila.com/pages/spin-coating>.
234. Holda AK, Vankelecom IFJ. Understanding and guiding the phase inversion process for synthesis of solvent resistant nanofiltration membranes. *J Appl Polym Sci*. 2015;132(27).
235. Mulder M. Membrane preparation | Phase Inversion Membranes. 2000. p. 3331-46.
236. Smolders CA, Reuvers AJ, Boom RM, Wienk IM. Microstructures in phase-inversion membranes. Part 1. Formation of macrovoids. *J Membrane Sci*. 1992;73(2):259-75.
237. Figoli A, Marino T, Galiano F. 2 - Polymeric membranes in biorefinery. In: Figoli A, Cassano A, Basile A, editors. *Membrane Technologies for Biorefining*: Woodhead Publishing; 2016. p. 29-59.
238. Wang D-M, Lai J-Y. Recent advances in preparation and morphology control of polymeric membranes formed by nonsolvent induced phase separation. *Current Opinion in Chemical Engineering*. 2013;2(2):229-37.
239. Tan X, Rodrigue D. A Review on Porous Polymeric Membrane Preparation. Part I: Production Techniques with Polysulfone and Poly (Vinylidene Fluoride). *Polymers (Basel)*. 2019;11(7).
240. Kumar TSS. *Characterization of Biomaterials: Chapter 2. Physical and Chemical Characterization of Biomaterials*: Elsevier Science; 2013.

241. Wenzel RN. Surface Roughness and Contact Angle. *The Journal of Physical and Colloid Chemistry*. 1949;53(9):1466-7.
242. Calvo JI, Peinador RI, Prádanos P, Palacio L, Bottino A, Capannelli G, et al. Liquid–liquid displacement porometry to estimate the molecular weight cut-off of ultrafiltration membranes. *Desalination*. 2011;268(1):174-81.
243. Menzies KL, Jones L. The impact of contact angle on the biocompatibility of biomaterials. *Optom Vis Sci*. 2010;87(6):387-99.
244. Xu LC, Siedlecki CA. Effects of surface wettability and contact time on protein adhesion to biomaterial surfaces. *Biomaterials*. 2007;28(22):3273-83.
245. Vogler EA. Structure and reactivity of water at biomaterial surfaces. *Adv Colloid Interface Sci*. 1998;74:69-117.
246. Felgueiras HP, Antunes JC, Martins MCL, Barbosa MA. 1 - Fundamentals of protein and cell interactions in biomaterials. In: Barbosa MA, Martins MCL, editors. *Peptides and Proteins as Biomaterials for Tissue Regeneration and Repair*: Woodhead Publishing; 2018. p. 1-27.
247. Rabe M, Verdes D, Seeger S. Understanding protein adsorption phenomena at solid surfaces. *Adv Colloid Interfac*. 2011;162(1):87-106.
248. Roach P, Eglin D, Rohde K, Perry CC. Modern biomaterials: a review - bulk properties and implications of surface modifications. *J Mater Sci Mater Med*. 2007;18(7):1263-77.
249. Horbett TA. Chapter 13 Principles underlying the role of adsorbed plasma proteins in blood interactions with foreign materials. *Cardiovascular Pathology*. 1993;2(3, Supplement):137-48.
250. Muller TF, Seitz M, Eckle I, Lange H, Kolb G. Biocompatibility differences with respect to the dialyzer sterilization method. *Nephron*. 1998;78(2):139-42.
251. 10993-4 I. Biological evaluation of medical devices — Part 4: Selection of tests for interactions with blood. 2017.
252. Himmelfarb J, McMonagle E, Holbrook D, Hakim R. Increased susceptibility to erythrocyte C5b-9 deposition and complement-mediated lysis in chronic renal failure. *Kidney Int*. 1999;55(2):659-66.
253. Cheung AK. Biocompatibility of hemodialysis membranes. *J Am Soc Nephrol*. 1990;1(2):150-61.
254. Poppelaars F, Faria B, Gaya da Costa M, Franssen CFM, van Son WJ, Berger SP, et al. The Complement System in Dialysis: A Forgotten Story? *Frontiers in immunology*. 2018;9:71-.
255. Gemmell CH. Flow cytometric evaluation of material-induced platelet and complement activation. *Journal of Biomaterials Science, Polymer Edition*. 2000;11(11):1197-210.
256. Fattisson J, Mansouri S, Yacoub D, Merhi Y, Tabrizian M. Determination of surface-induced platelet activation by applying time-dependency dissipation factor versus frequency using quartz crystal microbalance with dissipation. *Journal of The Royal Society Interface*. 2011;8(60):988-97.

257. Sperling C, Maitz MF, Werner C. 4 - Test methods for hemocompatibility of biomaterials. In: Siedlecki CA, editor. Hemocompatibility of Biomaterials for Clinical Applications: Woodhead Publishing; 2018. p. 77-104.
258. Wang K, Abdala A, Hilal N, Khraisheh M. Mechanical Characterization of Membranes. 2016.
259. Deppisch R, Storr M, Buck R, Göhl H. Blood material interactions at the surfaces of membranes in medical applications. Separation and Purification Technology. 1998;14(1):241-54.
260. Chakrabarty B, Ghoshal A, Purkait M. Preparation, characterization and performance studies of polysulfone membranes using PVP as an additive. J Membrane Sci. 2008;315(1-2):36-47.
261. Chakrabarty B, Ghoshal AK, Purkait MK. Effect of molecular weight of PEG on membrane morphology and transport properties. J Membrane Sci. 2008;309(1-2):209-21.
262. Kim IC, Lee KH. Effect of poly(ethylene glycol) 200 on the formation of a polyetherimide asymmetric membrane and its performance in aqueous solvent mixture permeation. J Membrane Sci. 2004;230(1-2):183-8.
263. Zheng Q-Z, Wang P, Yang Y-N, Cui D-J. The relationship between porosity and kinetics parameter of membrane formation in PSF ultrafiltration membrane. J Membrane Sci. 2006;286(1):7-11.
264. Kohlová M, Amorim CG, da Nova Araújo A, Santos-Silva A, Solich P, Montenegro MCBSM. In vitro assessment of polyethylene glycol and polyvinylpyrrolidone as hydrophilic additives on bioseparation by polysulfone membranes. Journal of Materials Science. 2020;55(3):1292-307.
265. Bradford MM. A rapid and sensitive method for the quantitation of microgram quantities of protein utilizing the principle of protein-dye binding. Anal Biochem. 1976;72:248-54.
266. Levine JM, Leon R, Steigmann F. A rapid method for the determination of urea in blood and urine. Clin Chem. 1961;7:488-93.
267. Chen J, Li J, Zhan X, Han X, Chen C. Effect of PEG additives on properties and morphologies of polyetherimide membranes prepared by phase inversion. Frontiers of Chemical Engineering in China. 2010;4(3):300-6.
268. Ravishankar H, Roddick F, Navaratna D, Jegatheesan V. Preparation, characterisation and critical flux determination of graphene oxide blended polysulfone (PSf) membranes in an MBR system. J Environ Manage. 2018;213:168-79.
269. Sinha MK, Purkait MK. Increase in hydrophilicity of polysulfone membrane using polyethylene glycol methyl ether. J Membrane Sci. 2013;437:7-16.
270. Ma YX, Shi FM, Ma J, Wu MN, Zhang J, Gao CJ. Effect of PEG additive on the morphology and performance of polysulfone ultrafiltration membranes. Desalination. 2011;272(1-3):51-8.
271. Association WM. World Medical Association Declaration of Helsinki: Ethical Principles for Medical Research Involving Human Subjects. JAMA. 2013;310(20):2191-4.

272. Standardization IOF. Biological Evaluation of Medical Devices: Selection of Tests for Interactions with Blood: International Organization for Standardization; 2002.
273. Benzie IFF, Strain JJ. The ferric reducing ability of plasma (FRAP) as a measure of "antioxidant power": The FRAP assay. *Anal Biochem.* 1996;239(1):70-6.
274. Mihara M, Uchiyama M. Determination of malonaldehyde precursor in tissues by thiobarbituric acid test. *Anal Biochem.* 1978;86(1):271-8.
275. Vogler EA. Structure and reactivity of water at biomaterial surfaces. *Adv Colloid Interfac.* 1998;74:69-117.
276. Liabeuf S, Drueke TB, Massy ZA. Protein-bound uremic toxins: new insight from clinical studies. *Toxins (Basel).* 2011;3(7):911-9.
277. Garcia D, Gomez-Caballero A, Guerreiro A, Goicolea MA, Barrio RJ. Molecularly imprinted polymers as a tool for the study of the 4-ethylphenol metabolic pathway in red wines. *J Chromatogr A.* 2015;1410:164-72.
278. Zinalibdin MR, Jaafar J, Majid ZA, Sanagi MM. Preparation, characterization and adsorption study of o-cresol molecularly imprinted grafted silica gel sorbent synthesized by sol-gel polymerization. *AIP Conference Proceedings.* 2017;1904(1):020083.

## 7. SUPPLEMENTARY MATERIAL

**Supplement 1:** MICHAELA KOHLOVÁ, CÉLIA GOMES AMORIM, ALBERTO DE NOVA ARAÚJO, ALICE SANTOS-SILVA, PETR SOLICH, MARIA CONCEIÇÃO BRANCO DA SILVA MONTENEGRO

*In vitro* assessment of polyethylene glycol and polyvinylpyrrolidone as hydrophilic additives on bioseparation by polysulfone membranes – Manuscript

*Journal of Materials Science*, 2020, 55(3), 1292-1307. IF<sub>(2019)</sub> 3.553

**Supplement 2:** MICHAELA KOHLOVÁ, SUSANA ROCHA, CÉLIA GOMES AMORIM, ALBERTO DE NOVA ARAÚJO, ALICE SANTOS-SILVA, PETR SOLICH, MARIA CONCEIÇÃO BRANCO DA SILVA MONTENEGRO

Doping Polysulfone Membrane with Alpha-Tocopherol and Alpha-Lipoic Acid for Suppressing Oxidative Stress Induced by Hemodialysis Treatment - Manuscript

*Macromolecular Bioscience*, 2020, e-pub ahead of print, IF<sub>(2019)</sub> 3.416

**Supplement 3:** MICHAELA KOHLOVÁ, CÉLIA AMORIM, ANA DUARTE, ALBERTO ARAÚJO, ALICE SANTOS-SILVA, PETR SOLICH, MARIA CONCEIÇÃO BRANCO DA SILVA MONTENEGRO

The biocompatibility and bioactivity of hemodialysis membranes: their impact in end-stage renal disease - Manuscript

*Journal of Artificial Organs*, 2019, 22(1), 14-28. IF<sub>(2019)</sub> 1.223